THE ROLE OF THE YEAST SEC1/MUNC18 PROTEIN, VPS45P, IN THE ASSEMBLY OF ITS COGNATE SNARE COMPLEX

by

Lindsay Nicole Carpp

DISSERTATION

Presented to the Faculty of Biomedical and Life Sciences
The University of Glasgow

In Partial Fulfilment of the Requirements
For the Degree of

DOCTOR OF PHILOSOPHY

Division of Biochemistry and Molecular Biology
University of Glasgow
October, 2006

Dedicated to my mom and dad

Abstract

The molecular machinery controlling membrane fusion has been strikingly well conserved throughout evolution, and all eukaryotic cells possess a common set of components for its execution. Members of the SNARE (soluble NSF attachment protein receptor) superfamily of proteins are indispensable players in all intracellular transport pathways. Sec1/Munc18 (SM) proteins are also essential for membrane trafficking, but a model encompassing (a) universal function(s) for SM proteins has been difficult to formulate. In part, this difficulty is due to the striking differences that have been observed between the ways that various SM proteins interact with their cognate syntaxins.

The yeast SM protein Vps45p regulates traffic from the *trans*-Golgi network (TGN) to late endosomes and facilitates the assembly of its cognate SNARE proteins (Tlg2p, Tlg1p, Vti1p, and Snc2p) into complexes. The first section of this work addresses the interaction(s) between Vps45p and its cognate SNARE partners. The second area of investigation in this work addresses the functional role(s) of these interactions. Analysis of one mode of interaction between Vps45p and its cognate syntaxin, Tlg2p, reveals that this mode of interaction is dispensable for Vps45p function. A dominant negative version of Vps45p is exploited to uncover an interaction between Vps45p and SNARE complexes that is mediated via a second, distinct mode. An investigation of the ability of Vps45p to interact with each of its individual cognate SNARE proteins also uncovers an interaction between Vps45p and its cognate v-SNARE, Snc2p. Collectively, these results suggest that Vps45p executes its function(s) through multiple modes of interaction with its cognate SNARE proteins, and support a model in which Vps45p undertakes a series of distinct interactions with specific intermediates of the SNARE cycle. Such a model would allow Vps45p to play multiple roles in the SNARE cycle and would also help contribute to a unifying hypothesis to describe SM protein function.

Table of Contents

List of Tables

List of Figures

Acknowledgements

I would like to thank my supervisor, Dr. Nia Bryant, for all of her help and guidance throughout this project (and all of the phases thereof) and also for all of her suggestions and comments during the preparation of this manuscript (and all the preliminary drafts thereof). Also for being a so-called "groovy-kind-of-person". I dedicate the "so-wrong-yet-sooo-right" Figure 4.10 (and all previous versions thereof) to her.
I would also like to thank the Wellcome Trust for providing me with a studentship, and Professor Bill Cushley for his assistance.
Specific thanks go to Fiona Brandie for providing purified GST-Sx4$_{cyto}$, her assistance with the final cloning step in the generation of pCOG022, and her generous supply of technical advice. Specific thanks also go to Scott Shanks for his contributions to the data presented in Figures 3.8 and 4.11, and to Nia Bryant for her contributions to the data presented in Figures 3.8, 4.2, and 4.6. Scott purified the proteins used in Figure 3.8a and generated all of the data presented in Figure 4.11; Nia generated the lovely gel shown in Figure 3.8a and performed all of the work involving S^{35} presented in Figures 4.2 and 4.6.
Thank you to Alan Boyd and Leonora Ciufo for their contributions to the work on the dominant negative and pocket filled versions of Vps45p; in particular, Leonora Ciufo performed the screen generating the dominant negative version and also created many of the constructs to produce these versions of Vps45p in yeast. Thank you to Alan Boyd for ideas regarding possible mechanisms of action of the dominant negative version of Vps45p.
Thank you to Mary Munson for fruitful discussions.
Thank you to Iain Johnstone for his explanation of neomorphs and antimorphs.
Thank you to Rebecca McCann (Rmyi) for the many Tinderbox trips. I wish you lots of luck on that deserted desert island with Danny De Vito and all of his desserts. May you live long and prosper.
Thank you to all the members of the Bryant Lab, past and present. I bequeath "The Dragon" (and mutant versions thereof) to the Bryant Lab (present and future and COGnate members thereof).
Eeehhhhhahaahahhhhhhhhhhhhhhhhhhhhhhhhhhhhhhhhhhhhhhhhhhhhhhhhhhhhhhhhhh (and all variations thereof).

Publications

Derived from this work:

Carpp, L.N., Ciufo, L.F., Shanks, S.G., Boyd, A., Bryant, N.J. 2006. The Sec1p/Munc18 protein Vps45p binds its cognate SNARE proteins via two distinct modes. *J Cell Biol.* 173(6):927-36.

Derived from other work:

Gourlay C.W., Carpp, L.N., Timpson, P., Winder, S.J., Ayscough, K.R. 2004. A role for the actin cytoskeleton in cell death and aging in yeast. *J Cell Biol.* 164(6):803-9.

Malone, R.E., Haring, S.J., Foreman, K.E., Pansegrau, M.L., Smith, S.M., Houdek, D.R., Carpp, L., Shah, B., Lee, K.E. 2004. The signal from the initiation of meiotic recombination to the first division of meiosis. *Eukaryot Cell.* 3(3):598-609

Author's Declaration

The work presented in this thesis was carried out under the supervision of Dr. Nia Bryant in the department of Biochemistry and Molecular Biology at the University of Glasgow between May 2003 and September 2006.

I declare that the work presented in this thesis has been carried out by myself unless otherwise noted or acknowledged. It has not been submitted for any other degree at this or any other university, either in whole or in part. To the best of my knowledge, the ideas presented in this thesis are original and my own, and this manuscript has been composed by myself.

Abbreviations

~	approximately
2μ	2 micron
ADP	adenosine diphosphate
ALP	alkaline phosphatase
API	aminopeptidase I
APNE	*N*-acetyl-DL-phenylalanine β-naphthyl ester
Arf	ADP-ribosylation factor
ATP	adenosine 5'-triphosphate
β-Me	β-mercaptoethanol
CBZ-pheleu	*N*-carbobenzoxy-$_L$-phenylalanyl-$_L$-leucine
CEN	centromeric
CPY	carboxypeptidase Y
cyto	cytosolic
DNA	deoxyribonucleic acid
DTT	dithiothreitol
E. coli	*Escheria coli*
ECL	enhanced chemiluminescence
EDTA	ethylenediaminetetraacetic acid
EE	early endosome
g	gram
g	gravitational force
GDP	guanosine diphosphate
GLUT	glucose transporter
GST	glutathione S-transferase
GTP	guanosine-5'-triphosphate
H_2O_2	hydrogen peroxide
HA	hemagglutinin
HAc	acetic acid
HCl	hydrochloric acid
HEPES	2-[4-(2-Hydroxyethyl)-1-piperazine]ethanesulfonic acid
$His_{(6)}$	six-histidine residue tag
HOPS	homotypic fusion and protein sorting
HRP	horseradish peroxidase
IgG	immunoglobulin G
IP	immunoprecipitation
IPTG	isopropyl-β-D-thiogalactopyranoside
K_2HPO_4	dipotassium hydrogen orthophosphate
KCl	potassium chloride
KH_2PO_4	potassium dihydrogen orthophosphate
KOAc	potassium acetate
KOH	potassium hydroxide
L	litre
LDCV	large dense core vesicle
LE	late endosome
LSB	Laemmli sample buffer
μ	micro
M	molar
mA	milliamp
mg	milligram
$MgCl_2$	magnesium chloride
ml	millilitre

MVB	multivesicular body
Na_2HPO_4	disodium hydrogen orthophosphate
NaCl	sodium chloride
NaN_3	sodium azide
Ni-NTA	nickel-nitrilotriacetic acid
NSF	N-ethylmaleimide-sensitive factor
OD_{600}	optical density at 600 nm
PBS	phosphate-buffered saline
PBS/T	0.1% Tween-20 in PBS
PC12	pheochromocytoma
PCR	polymerase chain reaction
Pfu	*Pyrococcus furiosis*
PI3K	phosphatidylinositol-3-kinase
PrA	protein A
PVC	prevacuolar compartment
S. cerevisiae	*Saccharomyces cerevisiae*
SDS	sodium dodecyl sulfate
SDS-PAGE	sodium dodecyl sulfate polyacrylamide gel electrophoresis
SM	Sec1/Munc18
SNAP	soluble NSF attachment protein
SNAP-25	25 kDa synaptosome-associated protein
SNARE	soluble NSF attachment protein receptor
$t_{½}$	half-life
TAE	Tris-Acetic acid-EDTA
Taq	*Thermus aquaticus*
TBS	tris-buffered saline
TBS/T	0.1% Tween-20 in TBS
TE	tris-EDTA
TEMED	N, N, N', N', - tetramethyl ethylene diamine
Tris	2-Amino-2-(hydroxymethyl)-1,3-propanediol
t-SNARE	target SNARE
TST	tris-saline Tween-20
VAMP-2	vesicle-associated membrane protein 2
v/v	units volume per units volume
VPS	vacuolar protein sorting
v-SNARE	vesicle SNARE
w/v	units weight per units volume
YPD	yeast peptone dextrose

Chapter One: Introduction

Eukaryotic cells are enclosed by a protective phospholipid bilayer, the plasma membrane, and are also compartmentalised into discrete membrane-bound organelles in which a range of metabolic processes are performed. Membranes act as barriers that maintain organelle identity and integrity, but a mechanism is also required by which material can be exchanged across membranes in a specific and regulated manner. In vesicular transport, a vesicle buds from a donor membrane, is targeted to the appropriate target membrane, and delivers its cargo upon fusion of the two membranes (Chen and Scheller, 2001; Jahn and Sudhof, 1999; Ungar and Hughson, 2003). Considering the diverse array of intracellular transport pathways, it is striking that a common core of machinery executes all fusion events (Chen and Scheller, 2001; Ungar and Hughson, 2003). This core machinery has been maintained throughout evolution, and cells as diverse as yeast and neurons share common components of this system (Bennett and Scheller, 1993; Ferro-Novick and Jahn, 1994).

1.1 SNARE proteins

Membrane fusion was first characterised at the molecular level in the late 1980s, beginning with the observation that the ATPase N-ethylmaleimide-sensitive factor (NSF) could restore vesicle trafficking in an cell-free transport assay (developed by Rothman and colleagues) inhibited by the alkylating agent N-ethylmaleimide (NEM) (Block *et al.*, 1988). The membrane association of NSF was next determined to be mediated by its cofactor SNAP (soluble NSF attachment protein; α, β, and γ isoforms), itself essential for fusion (Clary *et al.*, 1990). Recombinant NSF and α-SNAP were then used in affinity chromatography experiments to identify SNARE proteins (soluble NSF attachment protein receptors) as their receptors (Sollner *et al.*, 1993b). Using this approach, syntaxin, SNAP-25 (25 kDa synaptosome-associated protein), and VAMP (vesicle-associated membrane protein or synaptobrevin) were identified as the SNARE proteins involved in exocytosis at the neuronal synapse (Baumert *et al.*, 1989; Bennett *et al.*, 1992; Oyler *et al.*, 1989; Trimble *et al.*, 1988). The original SNARE hypothesis proposed that the pairing of SNAREs on vesicle membranes (v-SNAREs) with specific SNAREs on target membranes (t-SNAREs)

imparts specificity to membrane fusion (Rothman, 1994). A general schematic diagram illustrating SNARE-mediated membrane fusion is shown in Figure 1.1.

A complementary line of investigation, also aimed at identifying components of the molecular machinery of fusion, utilised genetics screens for yeast mutants (*sec*) defective in the secretory pathway (Novick *et al.*, 1981; Novick *et al.*, 1980; Novick and Schekman, 1979). These screens independently identified a number of SNARE proteins and also some of their regulators, foreshadowing the evolutionary conservation of fusion machinery (Novick *et al.*, 1980; Novick *et al.*, 1981). Over a hundred other SNARE proteins have now been identified in a range of organisms (Jahn and Sudhof, 1999). Each SNARE protein has been classified as a homologue of syntaxin, VAMP, or SNAP-25, based on sequence and domain homology (Weimbs *et al.*, 1998). Furthermore, SNARE proteins localise to distinct subcellular compartments in the cell, which helps account for the specificity of vesicle trafficking (Chen and Scheller, 2001; Pelham, 1999).

1.1.1 Characteristics of SNARE proteins

All SNARE proteins contain at least one highly conserved coiled-coil α-helical domain of approximately 60 residues, known as the SNARE motif (Weimbs *et al.*, 1997; Weimbs *et al.*, 1998). Although originally classified as t-SNAREs and v-SNAREs based on their localisation to either target membranes or vesicle membranes (Sollner *et al.*, 1993a), a second system of classification has been developed based on the residue that the SNARE protein contributes to the ionic 0 layer of the assembled complex. This residue is either an arginine (R-SNARE) or a glutamine (Q-SNARE) (Fasshauer *et al.*, 1998b); upon additional sequence homology analysis, Q-SNAREs were further classified as Q_a, Q_b, or Q_c SNAREs (Bock *et al.*, 2001). Most SNARE proteins are type II integral membrane proteins with C-terminal transmembrane domains directly adjacent to their SNARE motifs (Ungar and Hughson, 2003), although some exceptions to this generalisation exist. Notably, SNAP-25 and its relatives possess two SNARE motifs that are separated by a central cysteine-rich region; this region is palmitoylated to facilitate the peripheral membrane attachment of SNAP-25 (Hess *et al.*, 1992). Other SNAREs lacking transmembrane domains include Vam7p (Wada and Anraku, 1992) and syntaxins with cysteine residues in place of transmembrane domains at their C-termini (Jagadish *et al.*, 1997; Tang *et al.*, 1998).

1.1.2 The core complex

The SNARE motif plays an important functional role by participating in the core complex; each core complex contains one α-helix provided by a SNARE protein (v- or R-SNARE) from one membrane and three α-helices contributed by SNARE proteins (t- or Q-SNAREs) present on the opposing membrane. Structural studies of the core complex using a variety of techniques, including quick-freeze/deep-etch electron microscopy (Hanson *et al.*, 1997) and fluorescence resonance energy transfer (Lin and Scheller, 1997), have supported a model in which the α-helical SNARE motifs are arranged in parallel. The crystal structure of the core complex acting at the neuronal synapse, shown in Figure 1.2, reveals that the SNARE motifs assume a twisting cylindrical bundle configuration (Sutton *et al.*, 1998).

Although binary SNARE protein interactions themselves are of moderate affinity (Hayashi *et al.*, 1994; Pevsner *et al.*, 1994a), the neuronal core complex exhibits several noteworthy characteristics, including protease resistance (Poirier *et al.*, 1998), resistance to cleavage by clostridial neurotoxins (Hayashi *et al.*, 1994), resistance to denaturation by SDS (Hayashi *et al.*, 1994), and an extremely high T_m (> 90° C) (Fasshauer *et al.*, 1998a). In addition, unstructured SNARE monomers gain α-helical structure upon their entry into core complexes, providing a thermodynamic explanation of how formation of the core complex could provide the energy required to drive membrane fusion (Canaves and Montal, 1998; Fasshauer *et al.*, 1997; Fiebig *et al.*, 1999).

1.1.3 Minimal machinery for fusion

While mounting evidence suggested that formation of the core complex was thermodynamically favourable, it was unknown whether SNARE proteins alone were sufficient to drive the energetically unfavourable process of fusing two lipid bilayers. Weber and colleagues reasoned that this hypothesis could not be tested *in vivo*, or even in cell-free assays containing biological membranes (Weber *et al.*, 1998). They took advantage of an established biochemical assay that measures the mixing of two populations of artificial liposomes, one population of which contains fluorescent phospholipids at a high concentration such that they are quenched (Struck *et al.*, 1981). The mixing of donor and

acceptor liposomes results in the dilution and subsequent dequenching of the fluorescent phospholipids, which can be measured as a corresponding increase in fluorescence. To test whether SNARE proteins were sufficient for membrane fusion, this assay was adapted by reconstituting recombinantly produced v- and t-SNAREs into the artificial liposomes. The specific fusion of liposomes containing v-SNAREs with those containing t-SNAREs provided strong evidence that SNARE proteins alone constitute the minimal machinery for this process, although the observed rate of this fusion ($t_{½}$ ~ 40 min) was much slower than the rate at which these proteins execute fusion *in vivo* (Nickel *et al.*, 1999; Weber *et al.*, 1998). However, the rate of fusion could be increased through various modifications, including a pre-incubation step to allow docking to occur (resulting $t_{½}$ ~ 7 min), or truncation of a regulatory domain from syntaxin (resulting $t_{½}$ ~ 10 min) (Parlati *et al.*, 1999). It can be inferred from these findings that cells likely possess regulatory mechanisms by which the kinetics of membrane fusion are influenced.

1.1.4 N-terminal domains of syntaxins

The independently folded N-terminal domains possessed by most syntaxins comprise one such regulatory mechanism (Dulubova *et al.*, 2002; Dulubova *et al.*, 2001; Fernandez *et al.*, 1998; Gonzalez *et al.*, 2001; Lerman *et al.*, 2000; Misura *et al.*, 2002; Munson *et al.*, 2000). Detailed structural studies have been performed on a number of these domains; these "H_{abc} domains" are composed of three antiparallel α-helices that assume a twisting bundle configuration (Antonin *et al.*, 2002; Bracher and Weissenhorn, 2004; Dulubova *et al.*, 2001; Fernandez *et al.*, 1998; Lerman *et al.*, 2000; Misura *et al.*, 2002; Munson *et al.*, 2000). Syntaxin 1a exists in two distinct conformations, a closed conformation in which the H_{abc} domain folds back upon the SNARE motif, and an open conformation in which the H_{abc} domain separates from the SNARE motif (Dulubova *et al.*, 1999). As illustrated in Figure 1.3, only the open version of syntaxin 1a can participate in SNARE complexes (Dulubova *et al.*, 1999; Yang *et al.*, 2000).

Other syntaxins have also been demonstrated to adopt closed conformations, notably the yeast syntaxin, Sso1p, and the squid syntaxin, s-syntaxin (Bracher and Weissenhorn, 2004; Munson *et al.*, 2000). Evidence that the H_{abc} domain plays a negative regulatory role has been provided by *in vitro* studies in which

the removal of the H_{abc} domain of syntaxin greatly increases the rate of fusion (Parlati *et al.*, 1999). Furthermore, truncated versions of Sso1p lacking the H_{abc} domain, and constitutively open mutant versions of Sso1p, form complexes three orders of magnitude faster than wild-type Sso1p in gel filtration experiments (Munson *et al.*, 2000; Nicholson *et al.*, 1998).

1.1.5 The SNARE cycle

Membrane fusion consists of a series of distinct stages which progress in a regulated cycle (Figure 1.4) (Chen and Scheller, 2001; Lin and Scheller, 2000; Ungermann and Langosch, 2005). The docking of an incoming vesicle occurs in two sequential steps (Ungermann *et al.*, 1998): In the first step, an incoming vesicle is tethered to its target membrane via members of the Rab family of small GTPases and their effectors (Zerial and McBride, 2001). Other tethering factors such as large, multisubunit complexes and long coiled-coil proteins also contribute to the initial physical link between transport vesicles and target membranes (Whyte and Munro, 2002). The second step of docking is SNARE-mediated; v- and t-SNAREs pair to form transient and irreversible intermediates termed *trans*-complexes, whose members reside in opposing membranes (Ungermann *et al.*, 1998). Formation of *trans*-complexes pulls opposing membranes to be fused in close proximity to one another, presumably helping to overcome the thermodynamic barrier; *trans*-complexes are thusly converted to *cis*-complexes, whose members reside in the same membrane (Sutton *et al.*, 1998; Lin and Scheller, 1997; Hanson *et al.*, 1997). Post fusion *cis*-complexes serve as receptors for NSF and α-SNAP, which disassemble *cis*-complexes in an ATP (adenosine 5'-triphosphate) dependent manner, thereby priming SNARE proteins to participate in additional reactions (Mayer *et al.*, 1996). This priming must occur prior to Rab-mediated docking, in order for the cycle to progress through further rounds (Mayer *et al.*, 1996).

1.1.6 Regulation by other protein families

As discussed above, SNARE proteins clearly play a central role in membrane fusion. However, this process is also regulated by other protein families; namely the Arf (ADP-ribosylation factor) and Rab families of small GTPases, and the Sec1/Munc18 (SM) protein family. Both Arfs and Rabs cycle between GTP- and

GDP- (guanosine-5'-triphosphate and guanosine diphosphate) bound states; Arfs mainly serve to recruit coat proteins (Kawasaki *et al.*, 2005), while Rabs are primarily involved in vesicle tethering (Kawasaki *et al.*, 2005; Zerial and McBride, 2001). In addition to their roles in tethering, however, Rabs also have been implicated in the recruitment of cytoskeletal elements, the regulation of membrane remodelling (via the recruitment of PI3K; phosphatidylinositol-3-kinase), and vesicle formation and budding (Kawasaki *et al.*, 2005; Pfeffer, 1999; Segev *et al.*, 1988). The SM protein family will be discussed in detail in the following section.

1.2 Sec1/Munc18 (SM) proteins

The SM protein family is a relatively small family whose members are essential for membrane fusion; however, the precise role of SM proteins remains unclear despite intense interest in this topic (Jahn, 2000; Toonen and Verhage, 2003). The *Saccharomyces cerevisiae* and *Drosophila menogaster* genomes each contain four SM genes, the *Caenorhabditis elegans* genome possesses six SM genes, and the *Mus musculus* genome contains seven SM genes; similarly, seven SM genes have been identified to date in the *Homo sapiens* genome (Jahn, 2000; Pevsner, 1996; Toonen and Verhage, 2003). Unlike SNARE proteins, which share one highly conserved domain (the SNARE motif), SM proteins do not possess any defined subdomains (Jahn and Sudhof, 1999). Rather, SM proteins share moderate sequence identity that is evenly distributed along their entire sequences (Piper *et al.*, 1994; Halachmi and Lev, 1996; Cowles *et al.*, 1994), suggesting that they might adopt similar structures and perform a common function.

It is clear that SM proteins are indispensable to vesicle trafficking, since each intracellular transport step requires an SM protein (Toonen and Verhage, 2003). Four SM proteins have been identified in *S. cerevisiae*: Sec1p, Sly1p, Vps33p, and Vps45p. Sec1p can be considered the founding member of the SM family, as the *sec1-1* mutant was first identified in Novick and Schekman's classic screen aimed at identifying genes whose products were essential for vesicle transport via the secretory pathway (Novick and Schekman, 1979). At the restrictive temperature, *sec1-1* cells accumulate unfused 50-70 nm secretory vesicles at the plasma membrane, implying that Sec1p is required for their fusion (Aalto *et al.*,

1991; Egerton *et al.*, 1993; Novick and Schekman, 1979). Sly1p mediates ER-to-Golgi transport, and cells depleted of Sly1p accumulate ER membrane and incompletely glycosylated invertase (Dascher *et al.*, 1991; Ossig *et al.*, 1991), two characteristic signs of blocked ER to Golgi transport (Schmitt *et al.*, 1988; Segev *et al.*, 1988), again suggesting an essential role for Sly1p in its transport pathway. Vps33p mediates transport to the vacuole; *vps33Δ* cells accumulate unfused vesicles, lack detectable vacuoles, and exhibit defects in the sorting of vacuolar hydrolases (Banta *et al.*, 1990; Wada *et al.*, 1990). The remaining SM protein identified in yeast, Vps45p, regulates transport in the TGN/endosomal system (Cowles *et al.*, 1994; Piper *et al.*, 1994). Cells lacking Vps45p missort vacuolar hydrolases and accumulate unfused vesicles in the cytoplasm (Cowles *et al.*, 1994; Piper *et al.*, 1994). Taken together, these studies indicate that SM proteins are essential factors for membrane trafficking in yeast.

The necessity for SM proteins in membrane fusion is a universal one, as higher species exhibit a similar requirement (Toonen and Verhage, 2003). The SM protein mediating fusion at the neuronal synapse, Munc18-1, was the first mammalian SM protein to be identified (Hata *et al.*, 1993) (also identified independently in other laboratories; alternatively referred to as n-Sec1 (Pevsner *et al.*, 1994b) and rbSec1A (Garcia *et al.*, 1994)). In *M. musculus*, deletion of Munc18-1 is lethal; unfused synaptic vesicles accumulate and neurotransmission is completely blocked (Verhage *et al.*, 2000). In *C. elegans*, *unc18-1* mutations confer defects in neurotransmission, resulting in an uncoordinated phenotype (Hosono *et al.*, 1992). In *D. melanogaster*, mutants lacking Rop (the *Drosophila* homologue of Munc18) exhibit severe defects in neurotransmission and general secretion, and do not survive past embryonic stages (Harrison *et al.*, 1994). It is clear from these studies that SM proteins are essential factors for fusion *in vivo*.

1.2.1 SM protein/syntaxin interactions

One possible mechanism by which SM proteins couple to the SNARE protein machinery to regulate fusion is through their tight interactions with syntaxins. Most SM proteins interact with one or two syntaxins, and it has generally been assumed that they exert their effect on membrane fusion through this interaction (Toonen and Verhage, 2003). Considering the evenly distributed sequence homology among SM proteins (Jahn and Sudhof, 1999), it was surprising

that many of the SM/syntaxin interactions which have been characterised are strikingly different (Jahn, 2000; Toonen and Verhage, 2003).

1.2.1.1 Interaction with closed syntaxin

A great deal of work has been directed towards understanding the molecular machinery that executes exocytosis at the neuronal synapse. Munc18-1 was originally identified via its binding to syntaxin 1a (Hata *et al.*, 1993); this interaction has since been particularly well-characterised. This interaction is of nanomolar affinity (Pevsner *et al.*, 1994b) and requires almost the entire cytosolic domain of syntaxin 1a (Kee *et al.*, 1995). Munc18-1 only binds the closed conformation of syntaxin 1a (Dulubova *et al.*, 1999), and this interaction prevents syntaxin 1a from binding its cognate SNARE partners VAMP-2 and SNAP-25 (Pevsner *et al.*, 1994a). Syntaxin 1a must adopt the open conformation to enter complexes; consistent with this observation, Munc18-1 does not bind assembled complexes containing syntaxin 1a (Yang *et al.*, 2000). The crystal structure of the Munc18-1/syntaxin 1a complex (shown in Figure 1.5a) reveals that Munc18-1 adopts an arch shape which cradles syntaxin 1a in its closed conformation; domains I and III of Munc18-1 make contacts with syntaxin 1a along its entire cytosolic domain (Misura *et al.*, 2000). Although these biochemical and structural data suggest that Munc18-1 binding to closed syntaxin 1a has an inhibitory effect on SNARE complex assembly, the requirement for Munc18-1 in fusion (Verhage *et al.*, 2000) suggests that Munc18-1 plays a positive role in this process. As one possibility, it has been proposed that when the Munc18-1/syntaxin 1a complex is recognised by the appropriate effector molecule, a conformational change is triggered in Munc18-1; this change could destabilise the closed conformation of syntaxin 1a by changing the environment surrounding important contact points in its linker region (Misura *et al.*, 2000).

1.2.1.2 Interaction via the pocket mode

The yeast SM protein Sly1p interacts with its cognate yeast syntaxin Sed5p with the same nanomolar affinity as syntaxin 1a and Munc18-1 (Grabowski and Gallwitz, 1997). Unlike syntaxin 1a, however, only a short N-terminal region of approximately 40 residues of Sed5p is both necessary and sufficient for Sly1p binding (Yamaguchi *et al.*, 2002). The crystal structure of Sly1p in complex

with a short N-terminal peptide of Sed5p (Sly1p/Sed5p(1-45), shown in Figure 1.5b) reveals that these 45 residues assume an α-helical conformation that inserts into a hydrophobic pocket on the outer surface of domain I of Sly1p (Bracher and Weissenhorn, 2002). Although Sly1p and Munc18-1 have similar overall structures, the hydrophobic pocket of Sly1p that contacts Sed5p is on the opposite face as the inner cavity of Munc18-1 which contacts syntaxin1a. One key feature of this mode of interaction is that the SNARE motif of syntaxin is not shielded from participation in complexes; importantly, Sly1p has been shown to interact with assembled complexes containing Sed5p (Peng and Gallwitz, 2002). This mode of interaction would allow SM proteins to stay associated with syntaxins throughout the SNARE cycle, perhaps exerting late effects in fusion, after complex assembly. Intriguingly, Bracher and Weissenhorn speculated that syntaxin 1a may be able to interact with Munc18-1 via the same mode as that displayed in the Sly1p/Sed5p(1-45) crystal structure (i.e. with the N-terminal region of syntaxin 1a inserting into a hydrophobic pocket in the outer surface of domain I of Munc18-1), based on an analysis of the unliganded ssec-1 crystal structure (Bracher and Weissenhorn, 2001) and the conservation of key contact residues in the N-terminal regions of Sed5p and syntaxin 1a (Bracher and Weissenhorn, 2002).

1.2.1.3 Other SM/syntaxin interactions

A direct interaction between the yeast vacuolar syntaxin Vam3p and its cognate SM protein Vps33p has not been demonstrated, but Vam3p does interact with two multi-protein complexes containing Vps33p, the class C-Vps complex (Sato *et al.*, 2000) and the homotypic fusion and protein sorting (HOPS) complex (Price *et al.*, 2000). Furthermore, in contrast to the syntaxins discussed above, the SNARE motif alone of Vam3p has been demonstrated to be sufficient to capture Vps33p from a yeast lysate (Dulubova *et al.*, 2001).

Sec1p, the yeast SM protein regulating exocytosis at the plasma membrane, has been thought to associate with SNARE complexes, rather than its cognate syntaxin (Sso1p) (Carr *et al.*, 1999). However, a weak interaction between Sec1p and Sso1p was recently demonstrated using recombinantly produced proteins, although the mode of this interaction is unknown (Scott *et al.*, 2004).

1.2.2 Role of SM proteins

Considering the striking similarity between the overall structures of Munc18-1 and Sly1p (Bracher and Weissenhorn, 2002; Misura *et al.*, 2000), and the evenly distributed sequence identity between SM proteins (Halachmi and Lev, 1996), it is appealing to hypothesise that SM proteins share (a) common function(s). However, the diverse interactions described above have severely hindered the formulation of hypothesis encompassing a universal mechanism of action for SM proteins.

1.2.2.1 Evidence for early roles

The mode of interaction shown in the Munc18-1/syntaxin 1a crystal structure supports the idea that Munc18-1 acts prior to SNARE complex assembly, since Munc18-1 must dissociate from syntaxin 1a before complexes can be formed (Dulubova *et al.*, 1999; Misura *et al.*, 2000). Upstream roles (i.e. prior to complex assembly) that have been postulated for SM proteins include facilitating syntaxin to adopt its open conformation, regulating vesicle recruitment/docking, and supervising the fidelity of v- and t-SNARE pairing.

SM proteins as openers of syntaxin: The yeast SM protein Vps45p is normally required for its cognate SNARE proteins to form complexes, but this requirement can be overcome by the removal of the H_{abc} domain of its cognate syntaxin (Tlg2p) (Bryant and James, 2001). This finding is consistent with the idea that Vps45p facilitates Tlg2p to adopt an open conformation.

SM proteins in vesicle recruitment/docking: A role for SM proteins in vesicle docking at the neuronal synapse has been supported by studies demonstrating that *C. elegans* unc-18 mutants exhibit a decrease in the amount of docked vesicles, as quantified by electron microscopy (Weimer and Richmond, 2005); the same result was also obtained in studies of munc18-1 chromaffin cells (Voets *et al.*, 2001). It is worth noting that exocytosis at the neuronal synapse may be considered a unique pathway, in the sense that predocked vesicles are required to execute rapid neurotransmitter release; therefore, special mechanisms may have evolved to regulate docking at the neuronal synapse. However, a role for SM proteins in vesicle recruitment in other transport steps is suggested by the

genetic interactions that have been observed in yeast between genes encoding several SM proteins and their cognate Rabs: *SEC1* AND *SEC4* (Finger and Novick, 2000), *SLY1* and *YPT1* (Dascher *et al.*, 1991; Ossig *et al.*, 1991), and *VPS45* and *VPS21* (Tall *et al.*, 1999). Furthermore, expression of the *SLY1-20* allele bypasses the need for Ypt1p, itself an essential protein (Dascher *et al.*, 1991).

SM proteins as regulators of v- and t-SNARE pairing: It has also been postulated that SM proteins regulate the fidelity of v- and t-SNARE pairing (Peng and Gallwitz, 2002). This idea was supported by the finding that Sed5p readily forms complexes with both cognate and noncognate SNARE partners *in vitro*, but only forms complexes with its cognate partners when Sly1p is present (Peng and Gallwitz, 2002).

1.2.2.2 Evidence for later roles

In contrast to the mode of interaction shown in the Munc18-1/syntaxin 1a crystal structure discussed above, the mode of interaction shown in the Sly1p/Sed5p(1-45) crystal structure (Bracher and Weissenhorn, 2002) would allow SM proteins to associate with their cognate syntaxins prior to complex assembly, during formation of *trans*- complexes, during the conversion of *trans*- to *cis*-complexes, and even during the disassembly of *cis*-complexes. Consistent with a late (i.e. post fusion) role, Sly1p is not displaced from SNARE complexes as they are disassembled *in vitro* (Peng and Gallwitz, 2002). In *sec1-1* mutant cells, the levels of SNARE complexes remain the same even after incubation at the restrictive temperature, suggesting that Sec1p acts after SNARE complexes are assembled (Grote *et al.*, 2000). And, as discussed below, mutant versions of Munc18-1 have been identified that affect late stages of fusion (Ciufo *et al.*, 2005).

1.2.2.3 A unifying hypothesis with multiple roles

In order to integrate these proposed roles into a single hypothesis, it has been proposed that SM proteins perform multiple roles in the SNARE cycle, perhaps executed via distinct interactions with SNARE cycle intermediates (Bryant and James, 2003; Ciufo *et al.*, 2005; Schutz *et al.*, 2005; Scott *et al.*, 2004).

The following evidence has supported this idea:

1) The SM protein Vps45p associates *in vivo* with its cognate syntaxin, Tlg2p, at two distinct stages of the SNARE cycle (Bryant and James, 2003). Specifically, Vps45p appears to associate with monomeric Tlg2p and with *cis*-complexes, but not with *trans*-complexes (Bryant and James, 2003).

2) The SM protein Sec1p interacts with multiple intermediates of the SNARE cycle (Scott *et al.*, 2004). Sec1p binds its cognate syntaxin (Sso1p) in its monomeric state, partially assembled t-SNARE complexes, and fully assembled core complexes (Scott *et al.*, 2004).

3) Mutant versions of Munc18-1 exert distinct effects on exocytosis, as measured by carbon fibre amperometry, when overproduced in bovine adrenal chromaffin cells: One mutant stimulates the early stages of fusion (i.e. vesicle recruitment, as exhibited by an increased rate and overall extent of release), while other mutants affect later stages of fusion (exhibited by an increased quantal size and slower release kinetics) (Ciufo *et al.*, 2005).

4) Similarly, two mutant versions of Munc18-1 exert distinct effects on large dense core vesicle (LDCV) exocytosis, as measured by carbon fibre amperometry, when overproduced in rat adrenal pheochromocytoma (PC12) cells: One mutant (unable to bind syntaxin) stimulates fusion, while the other mutant (with a reduced ability to bind syntaxin) inhibits fusion (Schutz *et al.*, 2005).

If SM proteins do act at multiple stages of the SNARE cycle, this may help explain the apparently conflicting data that has been generated by studies in which SM genes are overexpressed; evidence exists to support both a positive and a negative role for SM proteins in fusion. In support of the idea that SM proteins are negative regulators of fusion, overproduction of Rop inhibits neurotransmitter release in *Drosophila* larvae (Schulze *et al.*, 1994). Furthermore, overproduction of Munc18-2 (an SM protein acting at the plasma membrane of epithelial cells) inhibits transport along its respective trafficking pathway, as measured by the delivery of the marker protein influenza virus hemagglutinin (HA) to the cell surface (Riento *et al.*, 2000). In 3T3-L1

adipocytes, increased production of the SM protein Munc18c also inhibits transport in its respective trafficking pathway, as measured by a decrease in insulin-stimulated translocation of a GFP-tagged version of the glucose transporter GLUT4 (Thurmond *et al.*, 1998). Microinjection of Munc18c peptides, again in 3T3-L1 adipocytes, also results in an inhibition in membrane fusion as assessed by the insulin-stimulated translocation of endogenous GLUT4 to the plasma membrane (Thurmond *et al.*, 2000). Using the same technique of microinjection, an increased level of s-Sec1 at the squid giant synapse inhibits neurotransmitter release as measured by electrophysiological studies (Dresbach *et al.*, 1998). In contrast to these data, however, overproduction of Munc18-1 was found to promote calcium-dependent exocytosis in bovine chromaffin cells (Voets *et al.*, 2001). Complementary approaches are likely required in order to understand the varied effects caused by the overexpression of SM genes.

1.2.2.4 Other possibilities

Another possibility is that SM proteins affect fusion indirectly by acting as chaperone proteins for their cognate syntaxins. In yeast, the syntaxin Tlg2p undergoes rapid proteasomal degradation in the absence of its cognate SM protein Vps45p (Bryant and James, 2001). Furthermore, syntaxin 1 levels are reduced to 30% of wild-type in the neuronal cells of munc18-1 knockout mice (Toonen *et al.*, 2005). While this is unlikely to be the main role of SM proteins, this observation must be taken into account when interpreting data obtained using *in vivo* systems devoid of an SM family member.

1.3 Membrane traffic in yeast

The amenability of *S. cerevisiae* to genetic manipulation has made it an invaluable model organism in which to study membrane trafficking. Understanding of the basic principles and machinery involved in membrane trafficking has been tremendously aided through genetic screens in this yeast. Two major membrane trafficking pathways in *S. cerevisiae* are the secretory pathway and the endocytic pathway. These pathways overlap somewhat and share common compartments; nevertheless, it is somewhat useful to delineate overall routes of traffic flow.

1.3.1 The secretory pathway

The secretory pathway, which is essential for cell growth, delivers proteins such as nutrient transporters, signalling receptors, and mating factors to the cell surface, along with membrane to allow growth and expansion of the daughter bud (Finger and Novick, 1998). Proteins destined for the plasma membrane, or for secretion, are co-translationally inserted into the membrane of the ER (or translocated into its lumen) and travel through the Golgi cisternae via *SEC*-dependent vesicular transport. 100 nm secretory vesicles bud from the late Golgi and are transported along actin cables to exocytic zones along the plasma membrane, where the exocyst complex and its effectors mediate vesicle docking (Finger and Novick, 1998; Lipschutz and Mostov, 2002).

1.3.2 The endocytic pathway

The endocytic pathway executes the uptake of extracellular nutrients, the internalisation and degradation of membrane proteins such as mating factors and ion/nutrient transporters, and the regulation of molecules available on the cell surface that respond to signalling pathways (Gruenberg, 2001; Shaw *et al.*, 2001). Signalling receptors and ion/nutrient transporters residing at the plasma membrane are targeted for internalisation via conjugation of ubiquitin, either as a monomer or in a short chain of Lys^{63}-linked molecules (Hicke, 1999). In one of the best characterised endocytic mechanisms, proteins targeted for internalisation are concentrated into clathrin coated pits that invaginate and transport their cargo along actin cables through a series of endocytic compartments, beginning with early endosomes (Schmid, 1997). Although there has been some debate regarding the subtypes of endosomes, most models distinguish at least two kinds; early (EE) and late (LE; also referred to as PVCs, prevacuolar compartments) (Pelham, 2002). After transit through the endosomal system, some proteins are recycled back to the plasma membrane. The chitin synthase Chs3p, which plays a role in cell wall assembly, is one such example (Valdivia *et al.*, 2002). However, the majority of proteins transiting this system are destined for degradation. This is achieved via the actions of the multiprotein ESCRT -0, -I, -II, and -III sorting complexes, which recognise ubiquitinated cargo and direct their entry into the multivesicular body (MVB) via the invagination of its outer membrane into luminar vesicles (Babst *et al.*,

2002a; Babst *et al.*, 2002b; Bowers and Stevens, 2005; Hurley and Emr, 2006; Katzmann *et al.*, 2001; Urbanowski and Piper, 2001). The MVB ultimately matures into, or fuses with, the vacuole, where protein degradation is accomplished by a host of vacuolar proteases (Klionsky *et al.*, 1990).

1.3.3 Other pathways

Other branches of membrane traffic in yeast include the cytoplasm-to-vacuole targeting (Cvt) pathway and the autophagic pathway. In the Cvt pathway, newly synthesised proteins such as the soluble vacuolar hydrolase aminopeptidase I (API) are packaged into vesicles that are constitutively targeted to the vacuole (Abeliovich *et al.*, 1999; Baba *et al.*, 1997). This pathway operates via a route that is independent from the portion of the secretory pathway that reaches the vacuole (Harding *et al.*, 1996). The autophagic pathway uses much of the same machinery as the Cvt pathway, but rather than operating constitutively, it is induced under starvation conditions via a Tor kinase response (Klionsky and Emr, 2000; Noda and Ohsumi, 1998).

1.3.4 Protein transport to the vacuole

The vacuole is a large, acidified organelle, responsible for a diverse array of functions, including protein degradation, storage of amino acids and other small molecules, osmoregulation, and pH regulation (Klionsky *et al.*, 1990). These functions help the vacuole regulate signalling pathways, manage nutrient metabolism, and maintain cellular homeostasis. The many roles performed by the vacuole require a range of proteins for their execution; therefore, multiple routes exist along which proteins can be transported to the vacuole (Figure 1.6). Vacuolar proteins can reach their destination via the endocytic pathway, mother-to-daughter inheritance following cell division, the cytoplasm-to-vacuole targeting pathway, the autophagic pathway, or the early stages of the secretory pathway followed by sorting away into vacuolar trafficking pathways (Bowers and Stevens, 2005; Bryant and Stevens, 1998). The late Golgi marks the point in the secretory pathway at which proteins destined for the vacuole are diverted into alternative pathways to the vacuole. The ALP and CPY pathways are two such pathways; each is named after a representative cargo protein (alkaline phosphatase, a vacuolar membrane protein, and carboxypeptidase Y, a soluble

vacuolar hydrolase, respectively). The ALP pathway to the vacuole bypasses the endosomal system (Cowles *et al.*, 1997; Klionsky and Emr, 1989; Piper *et al.*, 1997), while the CPY pathway to the vacuole traverses through PVCs (Raymond *et al.*, 1992; Vida *et al.*, 1993).

1.3.4.1 The CPY pathway

The trafficking of CPY has been extremely well characterised, making it a model protein to monitor vacuolar trafficking (Johnson *et al.*, 1987; Stevens *et al.*, 1982). After the synthesis of its inactive precursor, prepro-CPY, an N-terminal signal sequence directs its translocation into the ER. A combination of signal peptidase cleavage and N-linked glycosylation next generates p1CPY, a 67 kDa form of the enzyme (Blachly-Dyson and Stevens, 1987; Hasilik and Tanner, 1978; Johnson *et al.*, 1987). p1CPY transits the early stages of the secretory pathway, acquiring oligosaccharide modifications in the Golgi that generate a 69 kDa form of the enzyme, p2CPY (Stevens *et al.*, 1982; Trimble *et al.*, 1983). Upon reaching the late Golgi, p2CPY is diverted away from the secretory pathway via recognition by its receptor, Vps10p (Marcusson *et al.*, 1994). Vps10p/p2CPY complexes are trafficked to PVCs in a clathrin-dependent manner, in concert with the dynamin homologue Vps1p (Bensen *et al.*, 2000; Deloche *et al.*, 2001). At the PVC, p2CPY dissociates from Vps10p, which cycles back to the Golgi; on the other hand, p2CPY is transported on to the vacuole (Deloche and Schekman, 2002; Seaman *et al.*, 1997). Upon delivery to the vacuolar lumen, vacuolar proteases cleave p2CPY to its mature, active form of 61 kDa (mCPY) (Hasilik and Tanner, 1978).

1.3.4.2 Identification of *VPS* genes

Genetic screens have provided a fruitful avenue for the identification of genes whose products execute transport along the *VPS* pathway. In an initial approach, approximately 60 mutants were identified as deficient in vacuolar proteolytic activity, measured by a reduced ability to cleave the CPY substrate *N*-acetyl-DL-phenylalanine β-naphthyl ester (APNE) (Jones, 1977). However, the bulk of the *vps* mutants were identified about 10 years later, in two independent sets of screens. Mutants identified in the first set of screens were designated vacuolar protein targeting (*vpt*) mutants due to their inability to sort CPY-Inv

hybrid proteins to the vacuole (Bankaitis *et al.*, 1986; Robinson *et al.*, 1988). These hybrid proteins consisted of N-terminal regions of CPY, containing its vacuolar targeting signal (Johnson *et al.*, 1987; Valls *et al.*, 1987), fused in frame to a truncated version of invertase. Invertase is normally trafficked via the secretory pathway to the cell surface, where it facilitates sucrose catabolism (Esmon *et al.*, 1987); however, the vacuolar targeting signal contained in the CPY-Inv hybrid proteins diverted them to the vacuole. Screens were then performed in strains lacking invertase activity (and therefore unable to grow on media containing sucrose as the sole fermentable carbon source, unless the CPY-Inv fusion protein was missorted to the cell surface); in this manner, over 600 *vpt* mutants, corresponding to more than 50 gene products, were identified.

The second set of screens were based upon a similar principle; in these screens, mutants identified were designated vacuolar protein localization (*vpl*) mutants by virtue of their inability to sort, and subsequent secretion, of active CPY (Raymond *et al.*, 1992; Rothman *et al.*, 1989; Rothman and Stevens, 1986). Since active CPY can liberate leucine from the "blocked" dipeptide *N*-carbobenzoxy-$_L$-phenylalanyl-$_L$-leucine (CBZ-pheleu), *leu2* strains could only grow on medium containing CBZ-pheleu as the sole leucine supplement if CPY was missorted to the cell surface. This approach led to the identification of approximately 500 *vpl* mutants, corresponding to about 50 gene products. The *vpl* and *vpt* designations were subsequently dropped, and the *v*acuolar *p*rotein *s*orting (*vps)* nomenclature was adopted (Rothman *et al.*, 1989). The *vps* mutants, which constitute over 40 complementation groups, have since been designated into six classes (A through F) based mainly on vacuolar morphology (Banta *et al.*, 1988; Raymond *et al.*, 1992). Since many of the mutants with similar morphologies exhibit blocks at the same step of protein trafficking, this system of classification has helped identify proteins that act in concert with one another.

1.3.4.3 Class D *VPS* genes

Class D *vps* mutants are characterised by large, singular vacuoles, defects in mother-to-daughter vacuolar inheritance, and missorting of vacuolar proteases (Raymond *et al.*, 1992). The products of the class D *VPS* genes are thought to

execute vesicular transport between the late Golgi and late endosomes (Bryant and Stevens, 1998). Several of the class D *VPS* genes encode components of the molecular machinery mediating membrane fusion: the small Rab GTPase Vps21p (Horazdovsky *et al.*, 1994), its guanine nucleotide exchange factor Vps9p (Burd *et al.*, 1996; Hama *et al.*, 1999), the Sec1/Munc18 protein Vps45p (Cowles *et al.*, 1994; Piper *et al.*, 1994), and the syntaxin homologue Pep12p (Becherer *et al.*, 1996). The other products encoded by class D *VPS* genes are Vps34p, a phosphatidylinositol-3-kinase (PI3K) (Herman and Emr, 1990; Schu *et al.*, 1993), Vps15p, a serine/threonine kinase (Herman *et al.*, 1991), Vac1p, which contains a FYVE (Fab1, YOTB/ZK632.12, Vac1, and EEA1) finger domain that may interact with phosphatidylinositol 3-phosphate (Weisman and Wickner, 1992), Vps8p, which contains a RING finger Zn^{2+} binding motif (Horazdovsky *et al.*, 1996) and Vps3p, which plays a role in vacuolar inheritance (Raymond *et al.*, 1990) and has also been suggested to be involved in remodelling of the vacuole during progression of the cell cycle (LaGrassa and Ungermann, 2005). The idea that these proteins work in concert in a common pathway is supported by the abundance of physical and genetic interactions among them (Burd *et al.*, 1997; Hama *et al.*, 1999; Peterson *et al.*, 1999; Tall *et al.*, 1999; Webb *et al.*, 1997).

1.3.4.4 *VPS45*

VPS45 was cloned in two independent studies by its ability to complement the growth defect observed in temperature sensitive alleles of *vps45* (Cowles *et al.*, 1994; Piper *et al.*, 1994). Sequence alignments with other known yeast SM proteins (Sec1p, Sly1p, and Vps33p) identified Vps45p as an additional member of the SM protein family, sharing 22% sequence identity and 46% sequence similarity with Munc18-1 (Piper *et al.*, 1994). Cells lacking Vps45p exhibit phenotypes characteristic of class D *vps* mutants, including the secretion of a significant percentage (70-85%) of their CPY in its p2 (Golgi modified) precursor form, the accumulation of small (40-60 nm) unfused vesicles throughout the cytoplasm, and large, singular vacuoles that do not segregate into daughter buds (Cowles *et al.*, 1994; Piper *et al.*, 1994). Although Vps45p is a hydrophilic protein, fractionation studies reveal that it is present in both cytosolic and membrane bound pools, with its membrane association presumably mediated by a saturable site (Cowles *et al.*, 1994; Piper *et al.*, 1994). Although another one of the class D *VPS* genes, *PEP12*, encodes a syntaxin homologue which has been

shown to mediate transport to late endosomes (Becherer *et al.*, 1996), and genetic interactions have been observed between *PEP12* and *VPS45* (Burd *et al.*, 1997), no direct physical interactions have been reported between Vps45p and Pep12p (Bryant and James, 2001; Dulubova *et al.*, 2002; Nichols *et al.*, 1998).

1.3.4.5 Relationship between Vps45p and Tlg2p

Tlg2p is a syntaxin homologue that localises to the TGN and plays an important role in the endocytic pathway (Nichols *et al.*, 1998). Other cellular processes in which Tlg2p is thought to play a role include endosome biogenesis (Seron *et al.*, 1998), transport along the cytoplasm to vacuole targeting pathway (Abeliovich *et al.*, 1999), the localisation of certain kinases to the plasma membrane (Panek *et al.*, 2000), and homotypic fusion in the TGN (Brickner *et al.*, 2001).

Mounting evidence has suggested that Vps45p is the SM protein that regulates Tlg2p: First, a direct interaction between Vps45p and Tlg2p has been demonstrated with *in vitro* binding experiments (Bryant and James, 2001; Dulubova *et al.*, 2002; Yamaguchi *et al.*, 2002). Second, an *in vivo* interaction between Vps45p and Tlg2p can be inferred from the findings that Vps45p depends on Tlg2p for its membrane association (Bryant and James, 2001; Nichols *et al.*, 1998), and Vps45p and Tlg2p co-precipitate from yeast lysates (Bryant and James, 2001; Coe *et al.*, 1999; Nichols *et al.*, 1998). In addition, the maintenance of wild-type protein levels of Tlg2p requires Vps45p (Bryant and James, 2001; Nichols *et al.*, 1998).

Vps45p and Tlg2p also share a functional relationship *in vivo*. As discussed above, the protein levels ofTlg2p are downregulated in the absence of Vps45p, but they can be stabilised via the abolishment of proteasomal activity (Bryant and James, 2001). However, this population of stabilised Tlg2p is unable to form SNARE complexes with its cognate partners in this situation (i.e. in the absence of Vps45p), despite being targeted correctly (Bryant and James, 2001). These data suggest that Vps45p actively facilitates the entry of Tlg2p into SNARE complexes.

A second important study examining the relationship between Vps45p and Tlg2p demonstrated that Vps45p associates *in vivo* with Tlg2p at two distinct stages of the SNARE cycle; specifically, prior to complex formation (i.e. with monomeric

Tlg2p) and post-fusion (i.e. with *cis*-complexes) (Bryant and James, 2003). Furthermore, Vps45p was not found to be associated with *trans*-complexes (Bryant and James, 2003). These observations suggested that Vps45p may perform multiple functions.

1.4 Aims of this work

With the overall aim of contributing to the current understanding of the function(s) of SM proteins, the work presented in this dissertation endeavored to investigate the role(s) of Vps45p in the assembly of its cognate SNARE complex. Specific objectives of this work included:

1.4.1 Characterisation of the interactions between Vps45p and its cognate SNARE proteins

a) Interaction(s) of Vps45p with monomeric Tlg2p and Tlg2p-containing complexes: As discussed above, Vps45p interacts with both monomeric Tlg2p and Tlg2p-containing complexes (Bryant and James, 2003). One aim of this work was therefore to characterise, through a biochemical approach, both of these interactions. The interaction between Vps45p and monomeric Tlg2p is examined in Chapter Three, while the interaction between Vps45p and its cognate SNARE complex is investigated in Chapter Four.

b) Interaction(s) of Vps45p with non-syntaxin SNAREs: The yeast SM protein Sly1p was recently demonstrated to interact with other (i.e. non-syntaxin) members of its cognate SNARE complex. Therefore, another aim of this work was to investigate whether Vps45p also interacts with other members of its cognate SNARE complex.

1.4.2 Functional analysis of these interactions

a) Functional role(s) of the interaction between Vps45p and Tlg2p: Based on the recent finding that the interaction between the yeast SM protein Sly1p and its cognate syntaxin Sed5p is nonessential for ER-to-Golgi traffic (Peng and Gallwitz, 2004), one aim of the work presented in Chapter Four was to

determine whether the interaction between Vps45p and Tlg2p was similarly dispensable for traffic through the endosomal system.

b) Dominant negative version of Vps45p: In Chapter Four, a dominant negative version of Vps45p is presented. Another aim of the work presented in this chapter was to gain insight into the mechanism of this dysfunctional version of the wild-type protein. Data from both biochemical and genetic approaches directed towards this aim are presented in Chapter Four.

1.4.3 Stabilisation of protein levels of Tlg2p

Vps45p also helps stabilise the protein levels of Tlg2p (Bryant and James, 2001). In Chapter Five, an initial investigation into the molecular mechanism of this stabilisation is presented, and ideas for future work in this area are discussed.

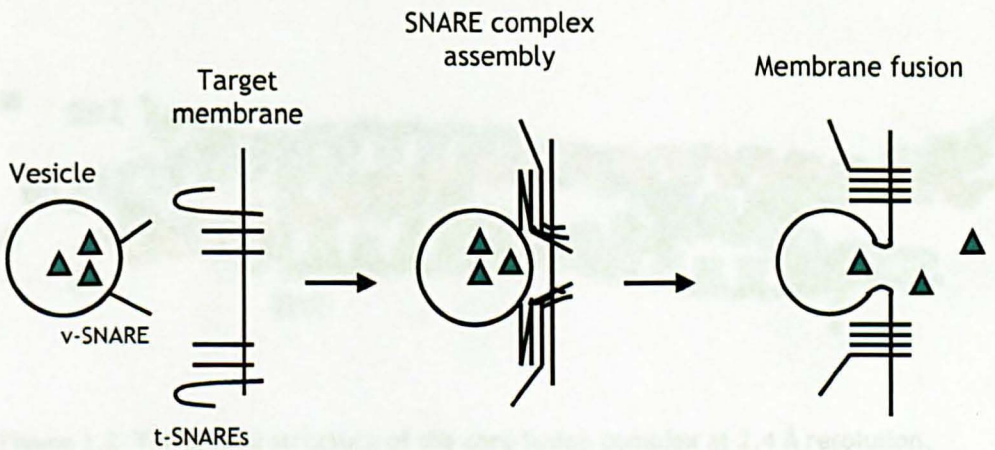

Figure 1.1 General schematic diagram of membrane fusion mediated by SNARE proteins. v-SNAREs residing on an incoming vesicle pair with t-SNAREs at a specific target membrane. As v- and t-SNAREs form SNARE complexes, the two membranes to be fused are brought in close proximity to one another, helping to provide the energy needed to overcome the energetic barrier to this thermodynamically unfavourable process. Membrane fusion and cargo delivery result.

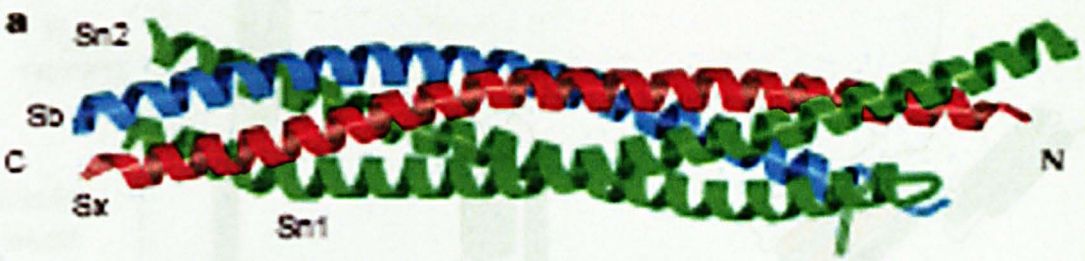

Figure 1.2 The crystal structure of the core fusion complex at 2.4 Å resolution. Reproduced from Sutton *et al.*, 1998. This structure illustrates how the core fusion complex is composed of four parallel α-helices arranged in a twisting cylindrical configuration. Each α-helix corresponds to a SNARE motif; the blue helix (So) represents the SNARE motif of synaptobrevin-II, the red helix (Sx) represents the SNARE motif of syntaxin 1a, and the two green helices (Sn1 and Sn2) represent the N- and C-terminal SNARE motifs of SNAP-25b, respectively. The Sn1, Sn2, and Sx helices each contribute a Gln residue to the buried '0' layer, designating SNAP-25b and syntaxin 1a as "Q-SNARES"; syntaptobrevin-II contributes an Arg residue to the buried '0' layer, designating it as an "R-SNARE" (Fasshauer *et al.*, 1998.). The "Q_a, Q_b, and Q_c" categories into which Q-SNAREs are further classified correspond to the position of the α-helices contributed by the Q-SNAREs in reference to this (i.e. the neuronal) core complex structure. Therefore, a Q-SNARE contributing the α-helix which occupies the same position as the Sx α-helix in this structure is designated a "Q_a-SNARE", whereas Q-SNAREs whose α-helices occupy the positions of the Sn1 and Sn2 helices in this structure are designated Q_b- and Q_c-SNAREs, respectively (Bock *et al.*, 2001).

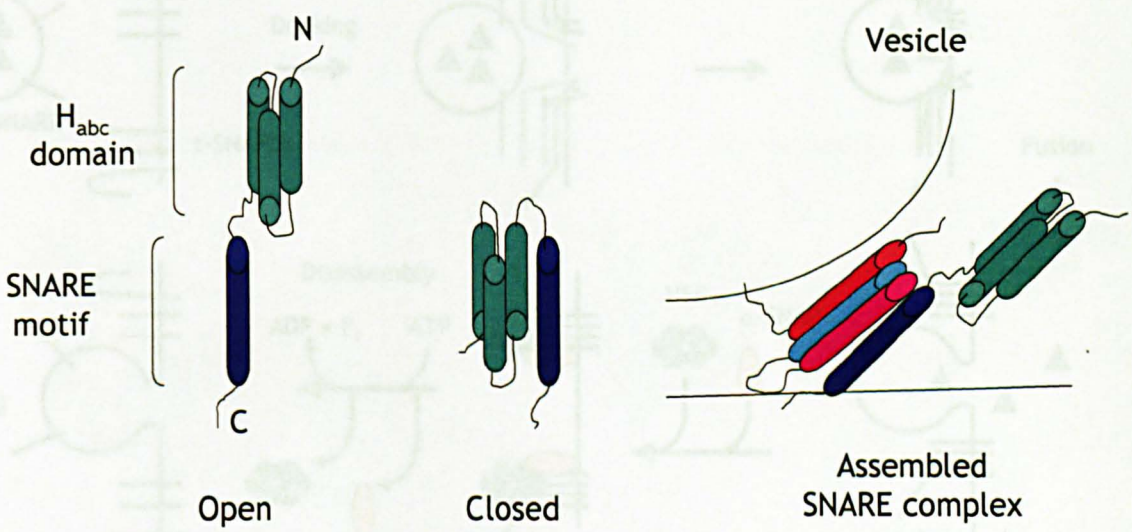

Figure 1.3 The open and closed conformations of syntaxin. The regulatory H_{abc} domain must swing away from the SNARE motif in order for syntaxin to participate in complexes.

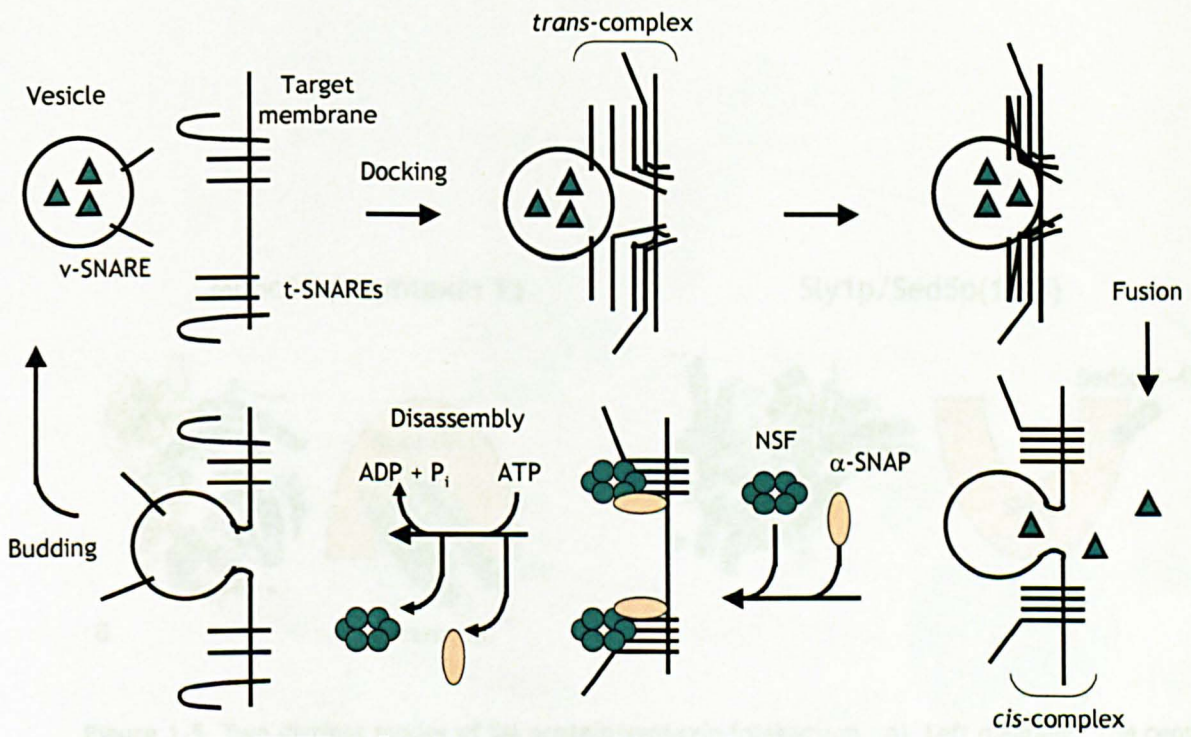

Figure 1.4 Stages of the SNARE cycle. An incoming vesicle is docked at its target membrane in two stages: First, it is tethered (for simplicity, tethering factors are not shown); second, v- and t-SNAREs align to form *trans*-complexes. The formation of *trans*-complexes brings the two membranes in close contact, helping drive the conversion of *trans*- to *cis*-complexes. Membrane fusion occurs, and the vesicle's cargo is delivered. Post-fusion *cis*-complexes are disassembled by NSF and α-SNAP. SNARE proteins are then recycled and used in additional rounds of fusion.

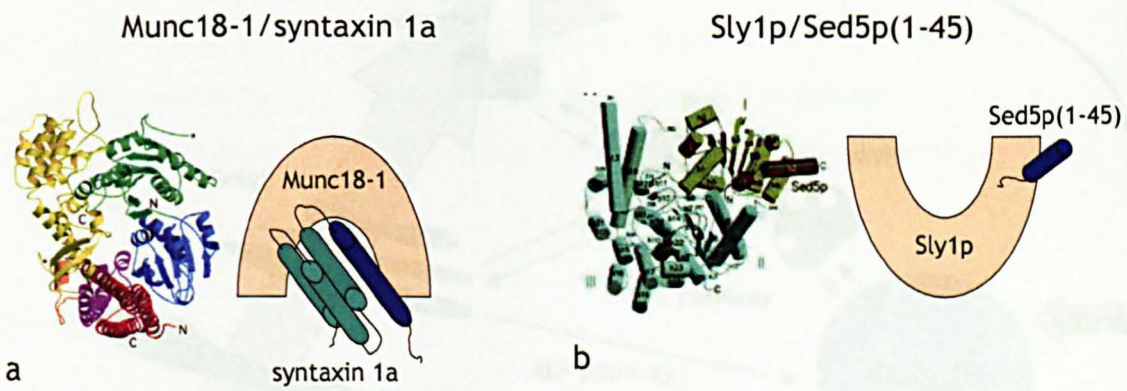

Figure 1.5 Two distinct modes of SM protein/syntaxin interaction. a) Left diagram: The central cavity of the arch-shaped Munc18-1 molecule (with its three domains depicted in yellow, green, and blue) surrounds syntaxin 1a (depicted in red and purple) in its closed conformation (Misura, Scheller *et al.* 2000). Right diagram: A simplified representation of the Munc18-1/syntaxin 1a interaction. The Munc18-1 molecule is depicted as a pink arch, and syntaxin 1a is represented as a blue cylinder (its SNARE motif) and three turquoise cylinders (the three helices of its H_{abc} domain). b) Left diagram: The N-terminal region of Sed5p (depicted in red) inserts into a hydrophobic pocket on the outer surface of domain I of Sly1p (depicted in yellow). The other domains of Sly1p are depicted in light blue. (Bracher and Weissenhorn 2002). Right diagram: A simplified representation of the Sly1p/Sed5p(1-45) interaction. The Sly1p molecule is depicted as a pink arch, and the N-terminal peptide from Sed5p is depicted as a blue cylinder.

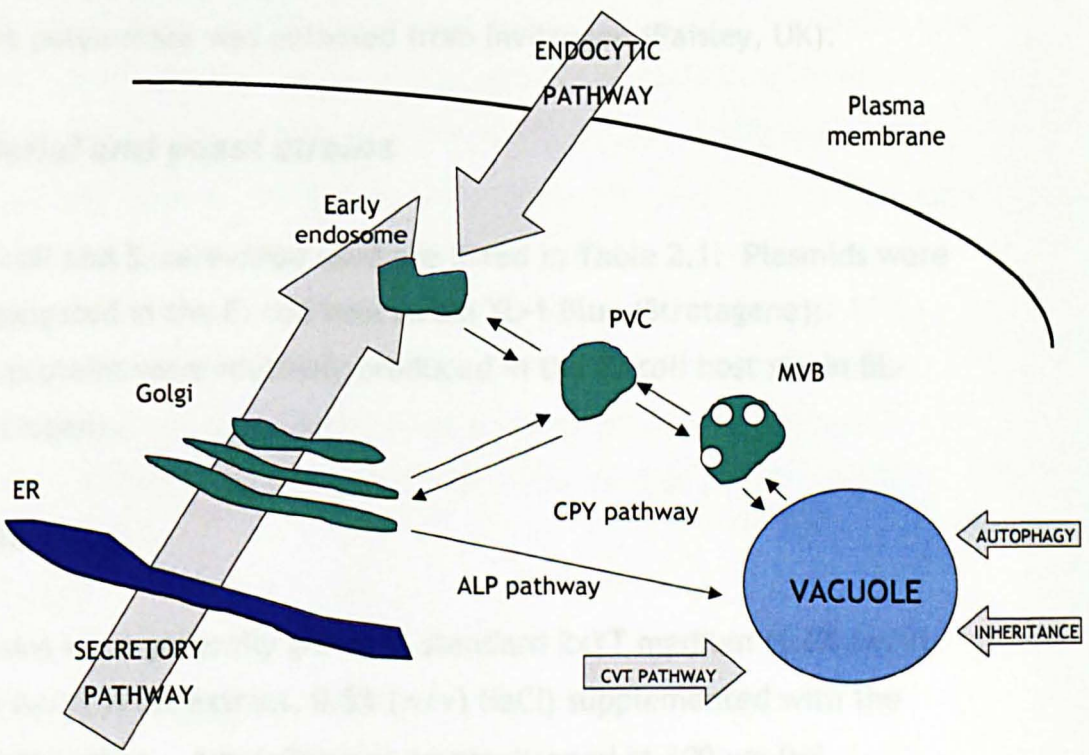

Figure 1.6 Membrane trafficking to the vacuole in yeast. Routes to the vacuole include the endocytic pathway, mother-to-daughter inheritance, the cytoplasm-to-vacuole targeting pathway, the autophagic pathway, and the ALP and CPY pathways.

Chapter Two: Materials and Methods

2.1 Materials

2.1.1 Reagents and enzymes

Chemical reagents were obtained from Sigma (Poole, UK), VWR (Poole, UK), Fisher Scientific (Leicester, UK) or Melford Laboratories Limited (Suffolk, UK). Restriction endonucleases, *Taq* polymerase, and T4 DNA ligase were obtained either from Promega (Southampton, UK) or New England Biolabs (Hitchin, UK). Platinum *Pfx*® polymerase was obtained from Invitrogen (Paisley, UK).

2.1.2 Bacterial and yeast strains

Strains of *E. coli* and *S. cerevisiae* used are listed in Table 2.1. Plasmids were routinely propagated in the *E. coli* host strain XL-1 Blue (Stratagene); recombinant proteins were routinely produced in the *E. coli* host strain BL-21(DE3) (Invitrogen).

2.1.3 Media

Bacterial strains were generally grown in standard 2xYT medium (1.6% (w/v) tryptone, 1% (w/v) yeast extract, 0.5% (w/v) NaCl) supplemented with the appropriate antibiotics. Ampicillin was routinely used at 100 μgs/ml, chloramphenicol at 34 μgs/ml, and kanamycin at 60μgs/ml. For solid plates, micro agar was added to 2% (w/v). For production of recombinant proteins, bacterial strains were grown in nutrient enriched Terrific Broth medium (Melford Labs Ltd; 1.2% (w/v) tryptone, 2.4% (w/v) yeast extract, 0.4% (v/v) glycerol, 0.017 M KH_2PO_4, 0.072 M K_2HPO_4), again supplemented with the appropriate antibiotics.

Yeast cultures were grown in either rich medium (1% (w/v) yeast extract, 1% (w/v) peptone, 2% (w/v) dextrose; YPD) or standard minimal medium containing dextrose as the carbon source (SD), yeast nitrogen base, and the appropriate amino acid drop-out supplement (ForMedium; Norwich, UK) (Sherman *et al.*, 1986). For solid plates, micro agar was added to 2% (w/v).

2.1.4 Antibodies

Rat monoclonal antibodies (clone 3F10) that specifically recognise the epitope YPYDVPDYA (derived from the human influenza hemagglutinin (HA) protein) were purchased from Roche (Mannheim), and were routinely used at a 1:2000 dilution. Mouse monoclonal α-ALP antibodies (clone 1D3A10) raised against a GST-fusion protein containing the luminal domain (residues 155-487) of ALP were used (at a 1:50 dilution) as previously described (Nothwehr *et al.*, 1996). Rabbit polyclonal α-Tlg2p, α-Vps45p, and α-PGK antibodies have been previously described (Bryant and James, 2001; Piper *et al.*, 1994) and were routinely used at 1:1000, 1:1000, and 1:100,000 dilutions, respectively. Rabbit polyclonal α-Vti1p antibodies have been previously described (Coe *et al.*, 1999), and were routinely used at a 1:1000 dilution. Mouse monoclonal α-CPY antibodies (clone 10A5) have been previously described (Roeder and Shaw, 1996), and were used at a 1:50 dilution. Rabbit polyclonal α-Tlg2p antibodies were raised against two peptides from Tlg2p; peptide sequences were obtained from a region just N-terminal to its transmembrane domain (residues 272-287) and the C-terminus (residues 381-396). α-Tlg2p antibodies were affinity purified from serum using protein A-Sepharose (Sigma); affinity purified antibodies were used at a 1:100 dilution.

2.2 Methods

2.2.1 Molecular cloning

Plasmid DNA was routinely obtained from bacterial cultures using the Promega Wizard® Plus SV Miniprep kit. Oligonucleotides used in PCR amplification of DNA sequences are listed in Table 2.2. The high fidelity polymerase Platinum *Pfx*® (Invitrogen) was used for PCR amplification of DNA sequences for TA cloning. Products created by PCR amplification with *Pfx* to be cloned into pCR2.1-TOPO (Invitrogen), which has 3' thymine overhangs, were treated with *Taq* polymerase to generate adenosine overhangs prior to TA cloning. Standard techniques used to manipulate DNA for molecular cloning followed methods outlined by Sambrook (1989). DNA fragments were resolved electrophoretically through agarose gels (0.6-1.0 % (w/v) agarose in tris-acetate (TAE) buffer (0.04M Tris-acetate, 0.001M EDTA)). Plasmids constructed and/or used in this study are listed in Table 2.3.

2.2.2 *Transformation of* E. coli *and* S. cerevisiae

Bacterial DNA transformations followed the method described by Hanahan (Hanahan, 1983). Yeast transformations were performed according to the lithium acetate method (Ito *et al.*, 1983).

2.2.3 *Isolation of yeast chromosomal DNA*

Yeast cells were grown to stationary phase in 10 mls of medium, harvested, and washed in 1.0 M sorbitol, 0.1 M EDTA (pH 7.5). Cells were resuspended in 0.4 mls of the same and transferred to a 1.5 ml Eppendorf tube. Following the addition of 15 µls of 15 mg/ml zymolyase (in 50 mM Tris-HCl pH 7.7, 1 mM EDTA, 50% (v/v) glycerol), cells were converted to spheroplasts in a 30 min incubation, with shaking, at 30°C. Spheroplasts were harvested in a microcentrifuge (5000 rpm, 2 min) and resuspended in 500 µls TE (10 mM Tris-HCl pH 8.0, 1 mM EDTA pH 8.0). Spheroplast lysis was achieved through the addition of 90 µls of lysis solution (0.25 M EDTA pH 8.0, 0.4 M Tris-HCl pH 8.0, 2% SDS), a brief (2 sec) period of vortexing, and a 30 min incubation at 65°C. After spheroplast lysis, 80 µls of 5M KOAc were added to the lysates, and mixtures were left on ice for at least 60 min. Precipitated matter, including insoluble potassium dodecyl sulfate and denatured proteins, was pelleted in a 15 min spin at top speed at 4°C in a microcentrifuge. Following the transfer of the supernatants to fresh 1.5 ml Eppendorf tubes, DNA was precipitated by the addition of an equivalent volume of ice-cold 100% ethanol. Precipitated DNA was harvested in a 15 min spin at top speed at 4°C in a microcentrifuge; pellets were washed with 100% ethanol and recovered in another 15 min spin at top speed at 4°C in a microcentrifuge. Pellets were washed with 1 ml of 70% ethanol, recovered in another 15 min spin at top speed at 4°C in a microcentrifuge, and air-dried at 25 °C for at least 1 hr. DNA was dissolved in 100 µls TE (10 mM Tris-HCl pH 7.5, 1 mM EDTA). 1 µl was routinely used as template for PCR.

2.2.4 *SDS-PAGE*

Electrophoretic separation of proteins was achieved using discontinuous SDS polyacrylamide gels as previously outlined (Laemmli, 1970). Gels were composed of a stacking region (5% acrylamide in stacking buffer; 0.25 M Tris-HCl

pH 6.8, 0.2% (w/v) SDS) and separating region (7.5-14.5% acrylamide in separating buffer; 0.75 M Tris-HCl pH 8.8, 0.2% (w/v) SDS). A 30% acrylamide-bisacrylamide mixture (37.5:1 ratio; Severn Biotech Ltd, Worcestershire) was used. Gels were run in tris-glycine electrophoresis buffer (25 mM Tris-HCl, 250 mM glycine, 0.1% (w/v) SDS). Protein samples analysed by SDS-PAGE were generally denatured by heating for 5 min at 95°C - 100°C in 2xLSB (100 mM Tris-HCl pH 6.8, 4% (w/v) SDS, 20% (v/v) glycerol, 0.2% (w/v) bromophenol blue, 10% (v/v) β-Me).

Resolved proteins were visualised by agitating gels in Coomassie Brilliant Blue solution (0.25 g Coomassie Brilliant Blue R250 in methanol:H_20:glacial acetic acid (4.5:4.5:1 v/v/v)) for one hour, followed by agitation in destain solution (5% (v/v) methanol, 10% (v/v) glacial acetic acid) until bands were clearly visible (generally overnight).

2.2.5 Immunoblot analysis

A Bio-Rad Trans-Blot® SD cell was used to transfer proteins from polyacrylamide gels to nitrocellulose membranes (Protran, 0.45μ pore size). Gels and membranes were sandwiched between 6 pieces of Whatman 3MM paper presoaked in semi-dry transfer buffer (50 mM Tris-HCl, 40 mM glycine, 0.037% (w/v) SDS, 10% (v/v) methanol) prior to the application of constant 180 mA current. Current was routinely applied for 35 min (for one gel) up to 60 min (for four gels). After protein transfer, unfilled sites on the membranes were blocked in 5% (w/v) non-fat dried milk in PBS/T (0.1% Tween-20 (v/v) in phosphate-buffered saline (PBS; 2.7 mM KCl, 1.8 mM KH_2PO_4, 137 mM NaCl, 10.1 mM Na_2HPO_4)) for at least 30 min. Alternatively, membranes probed with α-CPY antibodies were handled in TBS/T (0.1% Tween-20 (v/v) in Tris-buffered saline (20 mM Tris-HCl pH 7.5, 500 mM NaCl). Membranes were exposed to primary antibody in 1% (w/v) non fat dried milk in either PBS/T or TBS/T for 2 hrs. Following 30 min of 5 min washes, membranes were exposed to secondary antibody [α-rabbit (at a 1:5000 dilution), α-rat (at a 1:2000 dilution), or α-mouse (at a 1:2000 dilution) IgG HRP conjugate; Amersham Biosciences, Bucks, UK] in 5% (w/v) non fat dried milk in either PBS/T or TBS/T for 2 hrs. Following another 30 min of 5 min washes, protein bands were visualised using enhanced chemiluminescence (ECL).

2.2.6 Protein expression and purification

Chemically competent BL-21(DE3) cells (Invitrogen) were transformed with plasmids driving the production of the appropriate fusion protein(s). Overnight cultures of transformed cells were diluted 1:100 into Terrific Broth medium (with appropriate antibiotics) and incubated, with shaking, at 37°C until an OD_{600} of ~0.6 was reached. Expression of recombinant proteins was then induced with 1 mM isopropyl-β-D-thiogalactopyranoside (IPTG) for 4 hrs. Cells were routinely harvested by centrifugation in a Beckman Coulter SX4750 rotor at 3,273 *g* for 20 min. Cell pellets were washed in PBS (~1/20 the volume of the original culture) and usually stored at -20°C until cell lysis was performed. To achieve cell lysis, pellets were thawed on ice, resuspended in PBS (cells from ~ 1-2 L of culture/40 mls PBS) and incubated with lysozyme (1 mg/ml) for 30 min on ice. Cells were lysed by immersing the probe of a Sanyo Soniprep 150 in the suspension and sonicating for 6 x 20 sec pulses, with 20 sec cooling periods on ice separating the pulses of sonication. In the purification of $Tlg2p_{cyto}$-PrA, protease inhibitors were added to the lysis buffer (1 tablet complete protease inhibitor cocktail (Roche)/50 mls PBS). Cell lysates were clarified by centrifugation in a Beckman JA-20 rotor for 25 min at 4°C at 48,400 *g*. To recover fusion proteins, the appropriate resin (Ni-NTA agarose (Qiagen, West Sussex), GST-Sepharose (Amersham Biosciences), or IgG-Sepharose (Amersham Bioscience)) was pre-equilibrated (as per the manufacturer's instructions) and made up to a 50% slurry in either 20 mM imidazole in PBS (Ni-NTA agarose), PBS (GST-Sepharose), or TST (IgG-Sepharose). An aliquot of bead slurry was added to cleared bacterial lysate containing either $His_{(6)}$-, GST- (glutathione S-transferase), or PrA- (protein A) tagged fusion proteins. Generally, ~1-2 mls of slurry were used per litre of original culture; as an exception, ~1 ml of IgG-Sepharose slurry was used per 4-6 litres of original culture in the purification of $Tlg2p_{cyto}$-PrA. To recover fusion proteins, lysates and resins were mixed, with rotation, for at least 1 hr at 4°C. Beads loaded with recombinant proteins were routinely harvested in a 2 min spin at 500 *g* at 4°C, followed by at least 3 washes with the appropriate buffer (in a volume at least 5 times the bed volume of resin, generally 1 ml) to remove nonspecifically bound proteins. To elute PrA-tagged fusion proteins, ~1 ml of 0.5 M HAc (pH 3.4) per 500 μls settled IgG-Sepharose beads were mixed, with rotation, for at least 1 min. IgG-Sepharose beads were harvested in a 1 min spin at 500 *g*, and eluates were dialysed against

5 L of ice-cold PBS for ~16 hrs. To elute $His_{(6)}$-tagged fusion proteins, ~1 ml of 250 mM imidazole in PBS per 1 ml settled Ni-NTA resin were mixed, with rotation, for at least 1 min. Ni-NTA agarose beads were harvested in a 2 min spin at 500 *g*, and eluates were dialysed against 5 L of ice-cold PBS for ~16 hrs.

2.2.6.1 Purification of SNARE complexes

Chemically competent BL-21(DE3) cells (Invitrogen) were co-transformed with pCOG038 (driving the co-production of $His_{(6)}$-Snc2p_{cyto} and Tlg1p_{cyto}) and either pCOG032 (driving the co-production of Tlg2p_{cyto}-PrA and Vti1p_{cyto}), pCOG033 (driving the co-production of Tlg2$p_{cyto}\Delta$N36-PrA and Vti1p_{cyto}), or pCOG034 (driving the co-production of Tlg2$p_{cyto}\Delta$N230-PrA and Vti1p_{cyto}). The entire transformation was then added to 5 mls of 2xYT + ampicillin (100 μgs/ml) + chloramphenicol (34 μgs/ml) and incubated overnight, with shaking, at 37°C. The next day, the entire overnight culture was added to 500 mls Terrific Broth medium, again containing the appropriate antibiotics. Protein expression was induced with 1 mM IPTG when cells reached an OD_{600} of ~ 0.7. Cells were grown for an additional 4 hrs at 37°C, then harvested in a Beckman JS-4.2 rotor for 20 min at 3,464 *g*. Pellets were stored at -20°C until purification. To achieve cell lysis, pellets were thawed on ice and resuspended in PBS (~2.5% of the original volume of culture) with lysozyme (Sigma) added to 1 mg/ml. After 30 min on ice, cells were sonicated for 6 x 20 sec periods, interspersed with 20 sec intervals on ice. Cell lysates were clarified by centrifugation in a Beckman JA-20 rotor for 25 min at 4°C at 48,400 *g*. To cleared cell lysates, ~200 μls of 50% IgG-Sepharose slurry (Amersham Pharmacia Biotech, pre-equilibrated as per manufacturer's instructions) were added. Protein complexes containing Tlg2p_{cyto}-PrA were recovered by gently rotating the lysate with IgG-Sepharose beads for ~1 hour at 4°C. To remove non-specifically bound proteins, beads were washed 10 times with TST buffer (50 mM Tris-HCl pH 7.6, 150 mM NaCl, 0.05% (v/v) Tween-20); ~1 ml of TST was used to wash ~100 μls of settled IgG-Sepharose beads. To liberate complexes from IgG-Sepharose beads, thrombin protease was used to cleave the PrA tag from Tlg2p_{cyto}-PrA. 25 U of thrombin protease (Amersham Pharmacia Biotech) in 500 μls PBS (final concentration 50 U/ml) were combined with the IgG-Sepharose beads loaded with proteins in a 1.5 ml Eppendorf tube; thrombin cleavage was allowed to occur during 4 hrs of gentle rotation at 25°C. Following thrombin cleavage, IgG-Sepharose beads were

harvested in a microcentrifuge for 2 min at 500 *g*. The resultant supernatant, containing thrombin-cleaved protein complexes, was transferred to a fresh 1.5 ml Eppendorf tube. Protein complexes containing $His_{(6)}$-$Snc2p_{cyto}$ were recovered via affinity purification onto Ni-NTA agarose; ~ 200 µls of 50% Ni-NTA bead slurry (Qiagen, pre-washed 5 x 1 ml of PBS + 20mM imidazole) were added to the supernatant and allowed to mix, with rotation, at 4°C for ~ 1 hour. To remove non-specifically bound proteins, beads were washed 5 times with 20 mM imidazole in PBS; ~1 ml was used to wash ~100 µls of settled Ni-NTA agarose. Protein complexes bound to Ni-NTA beads were eluted in LSB (~1µl LSB/~1 µl settled Ni-NTA beads), denatured for 5 min at 95°C, and resolved by SDS-PAGE. Proteins were either visualised by staining with Coomassie Brilliant Blue, or transferred to nitrocellulose membrane prior to immunoblot analysis.

2.2.6.2 Co-expression of recombinant fusion proteins with the chaperone proteins GroEL/GroES

For the co-production of fusion proteins with the chaperone proteins GroEL and GroES, induction of recombinant protein expression was achieved using 0.5 mM IPTG. After the addition of IPTG, cells were grown for 16 hrs at 22°C.

2.2.7 Immunoblot analysis of whole cell extracts

To assess the steady-state levels of proteins in yeast whole cell extracts, cells from 10 OD_{600} units were harvested and resuspended in 100 µls TWIRL buffer (5% (w/v) SDS, 8M urea, 10% (v/v) glycerol, 50 mM Tris pH 6.8, 0.2% (w/v) bromophenol blue, 10% (v/v) β-mercaptoethanol); cell extracts were generated by a 10 min incubation at 65°C, followed by vortexing. The proteins contained within 15 µls of cell extract were resolved by SDS-PAGE, transferred to nitrocellulose membrane, and subjected to immunoblot analysis.

2.2.8 Binding experiments with yeast lysates and purified proteins

Yeast strains transformed with the appropriate plasmids were grown to mid-log phase (OD_{600} = 0.6-1.0). Cells were harvested, washed in 1/50 of the original volume of binding buffer (40 mM HEPES-KOH pH 7.4, 150 mM KCl, 1 mM DTT, 1

mM EDTA, 0.5% (v/v) Triton X-100), and concentrated to 1/100 of the original volume in binding buffer. After the addition of glass beads (400-625 μm; Sigma) in a 1:2 (v/v) ratio, cells were lysed with four 30 sec pulses of vortexing, interspersed with 1 min cooling periods on ice. Unlysed cells and glass beads were pelleted in a 5 min clearing spin at 500 *g* at 4°C, and a sample of cell lysate was removed for SDS-PAGE analysis. To set up binding reactions, an aliquot of yeast lysate was added to an aliquot of resin-bound fusion protein (in a 50% slurry in either PBS for $His_{(6)}$- tagged proteins, or TST for PrA-tagged proteins) in a 1.5 ml Eppendorf tube. Reaction volumes were normalised to 1 ml through the addition of the appropriate volume of PBS. Proteins from yeast lysates were allowed to bind to immobilised fusion proteins by rotating tubes for ~16 hrs at 4°C. Following binding reactions, beads loaded with recombinant proteins (and associated proteins) were washed three times with 1 ml of the appropriate buffer (TST for IgG-Sepharose resin or 20 mM imidazole in PBS for Ni-NTA resin) to remove nonspecifically bound proteins. PrA-tagged fusion proteins and associated proteins were eluted from IgG-Sepharose beads with 0.5 M HAc pH 3.4 (generally in a ratio of 15 μls HAc : 25 μls of settled beads); an equivalent volume of 2xLSB, with saturated Tris-HCl added to a final concentration of 5%, was added to the HAc eluate. $His_{(6)}$-tagged fusion proteins and associated proteins were eluted from Ni-NTA beads with LSB (approximately 1 μl LSB/1 μl settled beads). Proteins were denatured for 5 min at 95°C prior to SDS-PAGE analysis and either visualised by staining with Coomassie Brilliant Blue, or transferred to nitrocellulose membrane and subjected to immunoblot analysis.

2.2.9 Binding experiments with recombinantly produced proteins

The following general protocol was used for *in vitro* binding experiments; modifications to this protocol are detailed in the figure legends: To set up binding reactions, an aliquot (generally 100μls) of 50% slurry of beads loaded with recombinantly produced fusion proteins (detailed in Section 2.2.6) was added to the protein of interest or competing protein (as detailed in the figure legends) in a 1.5 ml Eppendorf tube. Reaction volumes were normalised to a final volume of 1 ml with PBS, and binding reactions were allowed to take place for ~16 hrs at 4°C with gentle rotation. Following binding reactions, nonspecifically bound proteins were removed from the resin with 3 x 1 ml washes of the appropriate buffer (same as in the 50% slurry). PrA-tagged fusion

proteins and associated proteins were eluted from IgG-Sepharose beads with 0.5 M HAc pH 3.4 (generally in a ratio of 15 µls HAc : 25 µls of settled beads); an equivalent volume of 2xLSB, with saturated Tris-HCl added to a final concentration of 5%, was added to the HAc eluate). $His_{(6)}$-tagged or GST-tagged fusion proteins and associated proteins were eluted from Ni-NTA or GST-Sepharose beads with LSB (approximately 1 µl LSB/1 µl settled beads). In all cases, proteins were denatured for 5 min at 95°C and resolved by SDS-PAGE. Proteins were either visualised by staining with Coomassie Brilliant Blue, or transferred to nitrocellulose membrane and subjected to immunoblot analysis.

Amounts of protein (µgs) added, when stated, were roughly estimated by visual comparison of a known amount of sample to a known amount of protein standard. For this estimation, 5 µls of Broad Range Prestained Precision Protein Standards (Bio-Rad, catalogue no. 161-0372) were loaded onto the same gel as the samples; these protein standards are ~650 µg/500 µl (as detailed in the Product Manual), giving 6.5 µgs of protein/5 µls of protein standards. To estimate the amount of protein in each individual band of the standard, the total amount of protein (6.5 µgs) per volume loaded (5 µls) was divided by the number of bands visible on the gel. Of the ten bands in the standard, three of these are three times the intensity of the other bands (as detailed in the Product Information), giving a rough total of either $1 \times [(6.5)/(7 + (3 \times 3))] = 0.4$ µgs of protein in the bands of lower intensity, or $3 \times [(6.5)/(7 + (3 \times 3))] = 1.3$ µgs of protein in the bands of higher intensity.

2.2.10 Immunoprecipitation from yeast cell lysates

Yeast strains transformed with the appropriate plasmids were grown to mid-log phase (OD_{600} = 0.6-1.0) in 50 mls of medium. Cells were harvested and resuspended in 4 mls YPD-sorb (50% (v/v) YPD, 50% (v/v) 2.4 M sorbitol) to which 20 µls of a 15 mg/ml stock (in 50 mM Tris-HCl pH 7.7, 1 mM EDTA, 50% (v/v) glycerol) of yeast lytic enzyme (MP Biomedicals, Aurora, Ohio) and 250 µls of 1 M Tris-HCl (pH 7.4) were added. Cells were converted to spheroplasts during a one hour incubation, with shaking, at 30°C; spheroplasts were harvested at 500 *g* for 2 min and transferred to ice. Spheroplasts were disrupted by vortexing (1 min vortex, 1 min on ice, 30 sec vortex, 1 min on ice, 30 sec vortex) in 1.2 mls ice-cold lysis buffer (200 mM sorbitol, 100 mM KOAc, 1% (v/v) Triton X-100, 50 mM

KCl, 20 mM Tris-HCl pH 6.8). To reduce nonspecific binding, 50 µls of PrA-Agarose (Sigma) was added to the resultant lysates, and the mixture was allowed to incubate on ice for 15 min. Unlysed cells and PrA-agarose were removed by centrifugation for 1 min at 9,300 *g* at 4°C. After reserving an aliquot of cell lysate for SDS-PAGE analysis, 500 µls of lysate were transferred to a fresh tube. To each tube, an additional 500 µls of lysis buffer and appropriate primary antibody (10 µls α-HA; Roche, 100 µgs/ml) were added. Lysates and antibodies were mixed by rotation for 2 hrs at 4°C, prior to the addition of 50 µls PrA-Agarose and a subsequent additional hour of rotation at 4°C. PrA-Agarose and associated proteins were pelleted in a 1 min spin at 9,300 *g* at 4°C, and pellets were washed three times in 1 ml lysis buffer. Bound proteins were eluted in 25 µls LSB and denatured for 5 min at 100°C; PrA-Agarose was pelleted in a 5 min at top speed in a microcentrifuge. Immunoprecipitated proteins were resolved by SDS-PAGE, transferred to nitrocellulose membrane, and subjected to immunoblot analysis.

2.2.11 Subcellular fractionation

Differential centrifugation was used to generate membrane and cytosolic fractions as previously described (Horazdovsky and Emr, 1993), with modifications. Strains transformed with the appropriate plasmids were grown to mid-log phase in 20 mls of the appropriate drop-out medium. Cells were killed with the addition of NaN_3 to a final concentration of 10 mM, and 10 OD_{600} units of cells were immediately harvested. Cells were washed with sterile H_2O, resuspended in 1 ml of 50 mM Tris-HCl pH 9.5, 10 mM DTT, 10 mM NaN_3, and incubated at room temperature for 15 min. Cells were resuspended in 1 ml of 1.2 M sorbitol, 50 mM KP_i pH 7.4, 1 mM $MgCl_2$, 10 mM NaN_3, to which 20 µls of 15 mg/ml zymolase (in 50 mM Tris-HCl pH 7.7, 1 mM EDTA, 50% glycerol) were added. Cells were converted to spheroplasts during a 30 min incubation, with shaking, at 30°C; spheroplasts were washed twice in 1.2 M sorbitol. All steps onward were carried out at 4°C. Spheroplasts were lysed by trituration in 1.2 mls ice-cold 0.2 M sorbitol, 50 mM Tris-HCl pH 7.5, 1 mM EDTA, 10 mM NaN_3. Unlysed spheroplasts and cell debris were removed in a clearing spin in a microcentrifuge for 5 min at 500 *g*. 1 ml of the cleared lysate was removed. 50 µls of 50% TCA was added to 200 µls of the lysate; proteins were allowed to precipitate on ice for at least 30 min, generating the WCE (whole cell extract)

pellet. The remaining 800 µls of lysate were transferred to a fresh tube, and a 30 min spin at 100,000 *g* in a Beckman TLA100.3 rotor was performed to generate the P pellet. To the supernatant of this spin, 200 µls of 50% TCA were added and proteins were allowed to precipitate on ice for at least 45 min, generating the S pellet. TCA-precipitated proteins were harvested in a 10 min spin at 13,800 *g* at 4°C. The resulting pellets were washed once in ice-cold acetone and allowed to dry for at least one hour at 25 °C; proteins were then solubilised in 50 µls LSB (WCE) or 200 µls LSB (S). Proteins contained within the P pellet were resuspended in 200 µls LSB via trituration. Proteins contained within all samples were denatured for 5 min at 95°C, resolved by SDS-PAGE, transferred to nitrocellulose membrane, and subjected to immunoblot analysis.

Subcellular fractionation experiments with the temperature sensitive strain LCY006 (*sec18-1 vps45*Δ) were performed similarly, except that cells were grown to mid-log phase at 25°C before an additional 90 min incubation at either 25°C (permissive temperature) or 37°C (restrictive temperature) prior to fractionation.

2.2.12 Precipitation of proteins from extracellular media

To detect the presence of secreted CPY, it was necessary to concentrate the proteins present in the extracellular media into a smaller volume. This was achieved using trichloroacetic acid (TCA) to precipitate the proteins from the media according to the following protocol: Yeast strains transformed with the appropriate plasmids were grown to mid-log phase in 10 mls of the appropriate drop-out medium. Cells were harvested, and the resultant supernatants were added to ice-cold 50% (v/v) TCA for a final concentration of 10% (v/v). Proteins were allowed to precipitate for at least 1 hr on ice, after which time precipitated proteins were harvested in a 10 min spin at top speed at 4°C in a microcentrifuge. Pellets containing precipitated proteins were washed with 1 ml of ice-cold acetone and harvested at top speed at 4°C in a microcentrifuge. Excess acetone was allowed to evaporate, and precipitated proteins were solubilised in 15 µls LSB. Proteins were denatured for 5 min at 95°C, resolved by SDS-PAGE, and transferred to nitrocellulose membrane. The presence of CPY was assessed by immunoblot analysis with α-CPY antibodies.

Table 2.1 *E. coli* and *S. cerevisiae* strains used in this study

E. coli strains used in this study:			
Strain	Genotype		Source
BL-21(DE3)	F⁻ *ompT hsdS*$_B$($r_B^- m_B^-$) *gal dcm* (DE3)		Invitrogen
XL-1 Blue	*recA1 endA1 gyrA96 thi-1 hsdR17 supE44 relA1 lac* [F′ *proAB lacI*^{q}Z*ΔM15* Tn10 (Tet^r)]		Stratagene
S. cerevisiae strains used in this study:			
Strain	Genotype	Construction	Reference
LCY006	*MATα sec18-1 ura3-52 leu2-3, 112 vps45Δ::Kan*^{r}	*SmaI/SphI* digested pNOz13 (Bryant and James, 2001) used to disrupt *VPS45* in SEY5186 (Emr *et al.*, 1984)	This work
LCY008	*MATα ura3-52 leu2-3 112 his4-519 ade6 gal2 pep4-3 vps45Δ::Kan*^{r}	*SmaI/SphI* digested pNOz13 (Bryant and James, 2001) used to disrupt *VPS45* in SF838-9D	This work
NOzY2	*MATα ura3-52 leu2-3 112 his4-519 ade6 gal2 vps45Δ::Kan*^{r}		Bryant and James, 2001
NOzY3	*MATα ura3-52 leu2-3 112 his4-519 ade6 gal2 pep4-3 tlg2Δ::Kan*^{r}		Bryant and James, 2001
RPY10	*MATα ura3-52 leu2-3 112 his4-519 ade6 gal2*		Piper *et al.*, 1994
SF838-9D	*MATα ura3-52 leu2-3 112 his4-519 ade6 gal2 pep4-3*		Rothman and Stevens, 1986

Table 2.2 Oligonucleotides used in this study

Oligo	Description	Sequence (5' → 3')
2	*Xho*IstopTLG2	CTCGAGGTAGTGTGTTGCTTTATTCAAC
3	*Eco*RIinframeSNC2	GAATTCGATGTCGTCATCAGTGCCATAGC
4	*Hind*IIIstopstopSNC2	AAGCTTTTATTAATCTTTCCACCACATTTGCT
7	*Nco*IVTI1	CCATGGATGAGTTCCCTATTAATATCATAC
8	*Eco*RIstopstopVTI1	GAATTCTTATTAAGTCATTGTTTTTAGTGTCT TTAT
9	*Bam*HIinframeVPS45	GGATTCGATGAACCTTTTTGATGTGGCTG
10	*Pst*IadditionalstopVPS45	CTCGAGTTATTATTTTGCAGATCTAATAGAAT C
27	*Pac*IPROTEINA	TTAATTAATCACGAATTCGCGTCTACTTTCG G
44	*Nde*ITLG2	CATATGTTTAGAGATAGAACTAATTTA
45	*Nde*ITLG2	CATATGGGTACATACCCGATGATG
47	*Xho*IPROTEINA	CTCGAGCTGGTTCCGCGTGGATCCGTAGACA ACAAATTCAACAAAG
48	*Nde*ITLG2	CATATGACGTTGCAGAGACAGCAACAG
127	*Kpn*IstartSNC2	GGTACCATGTCGTCATCAGTGCCATACG
128	*Xho*ISNC2	CTCGAGATCTTTCCACCACATTTGCTTTC
129	*Kpn*IstartSNC2	GGTACCATGGCAAACCCAAATTCCCAAAAC
133	*Kpn*IstartVTI1	GGTACCATGAGTTCCCTATTAATATCATAC
134	*Xho*IVTI1	CTCGAGAGTCATTGTTTTTAGTGTCTTTAT
156	*upstreamofSNC2*	TTAATACGAACAAAATAAAAATATG
157	*downstreamfromSNC2*	AAGACGGCCACTAAAACTGATG
162	upstreamstart*Hpa*ISNC2	GAACGCGCAACGATGGTTAACTCGTCATCAG TGCCATAC
163	reverse complement of 162	GTATGGCACTGATGACGAGTTAACCATCGTT GCGCGTTC
190	*Eco*RI in frame w/$His_{(6)}$ tag HA tag *SNC2 ORF*	GAATTCGTACCCATACGATGTTCCGGATTAC GCT*ATGTCGTCATCAGTGCCATA*
191	upstreamstartHAtag*SNC2*	GAACGCGCAACGATGTACCCATACGATGTTC CGGATTACGCT TCGTCATCAGTGCCATAC
192	reverse complement of 191	GTATGGCACTGATGACGAAGCGTAATCCGGA ACATCGTATGGGTACATCGTTGCGCGTTC
200	**last 6 residues of HA tag** *TLG2 ORF* starting at residue 37	GATGTGCCTGACTACGCAATGGGTACATACC CGAT
201	reverse complement of 200	CATCGGGTATGTACCCATTGCGTAGTCAGGC ACATC
202	*VPS45*L117R*VPS45*	ATTGTCTCTAAATCTCAAAGAGAACGGCTAG' CTGAATC
203	reverse complement of 202	GATTCAGCTAGCCGTTCTCTTTGAGATTTAG AGACAAT
204	*VPS45*W244R*VPS45*	CACCTTTACTTCAACCTAGGACCTACCAATCA ATGATC
205	reverse complement of 204	GATCATTGATTGGTAGGTCCTAGGTTGAAGT AAAGGTG
214	*TLG2*K26R*TLG2*	ACTTTCTCATCTGGGAGAGCACCCTTGGGCG
215	reverse complement of 214	CGCCCAAGGGTGCTCTCCCAGATGAGAAAGT
322	*TLG2*F9A,L10A*TLG2*	TAAGAGATAGAACTAATTTAGCTGCATCATA

		CCGTAGGACTTTC
323	reverse complement of 322	GAAAGTCCTACGGTATGATGCAGCTAAATTA GTTCTATCTCTAA

Table 2.3 Plasmids constructed and/or used in this study

Plasmid	Description	Construction/Reference/Source
pACYC-Duet™-1	P15A *ori* Cm^r *lacI*; *E. coli* expression vector	Novagen
pCOG002	270 bp fragment encoding the cytosolic domain of Snc2p, flanked by *Eco*RI and *Hind*III sites, in pCR®2.1-TOPO®	Sequence encoding the cytosolic domain of Snc2p was PCR amplified from genomic DNA prepared from a 9Dα strain using oligos 3 and 4. The resulting PCR product was *Taq*-treated and subcloned into pCR®2.1-TOPO®.
pCOG003	560 bp fragment encoding the cytosolic domain of Vti1p, flanked by *Nco*I and *Eco*RI sites, in pCR®2.1-TOPO®	Sequence encoding cytosolic domain of Vti1p was PCR amplified from template pSN253 (kind gift from Tom Stevens, University of Oregon, USA) with oligos 7 and 8. Resulting PCR product was *Taq*-treated and subcloned into pCR®2.1-TOPO®.
pCOG006	*E. coli* expression vector encoding an N-terminally $His_{(6)}$-tagged version of the cytosolic domain of Snc2p	270 bp *Eco*RI/*Hind*III fragment subcloned from pCOG002 into pACYC™-Duet-1 cut with the same enzymes.
pCOG021	365 bp fragment encoding two synthetic repeats of the IgG binding domains of *S. aureus* protein A, flanked by *Pac*I and *Xho*I sites, in pCR®2.1-TOPO®	Sequence encoding two synthetic repeats of the IgG binding domains of *S. aureus* protein A was PCR amplified from template pZZ-HIS5 (Rayner and Munro, 1998) with oligos 27 and 47. Resulting PCR product was *Taq*-treated and subcloned into pCR®2.1-TOPO®.
pCOG022	*E. coli* expression vector encoding two repeats of the IgG binding domains of *S. aureus* protein A	365 bp *Pac*I/*Xho*I fragment from pCOG021 subcloned into pET-Duet™-1 cut with the same enzymes. Final subcloning step performed by Fiona Brandie (University of Glasgow).
pCOG025	*E. coli* expression vector encoding a C-terminally PrA -tagged version of the cytosolic domain of Tlg2p (residues 1-309)	pET-Duet™-1 containing 927 bp *Nde*I/*Xho*I fragment from pCOG028 and 365 bp *Pac*I/*Xho*I fragment from pCOG021.
pCOG026	*E. coli* expression vector encoding $Tlg2p_{cyto}\Delta 1$-36-PrA	819 bp *Nde*I/*Xho*I fragment subcloned from pCOG029 into pCOG022 cut with same enzymes.
pCOG027	*E. coli* expression vector encoding $Tlg2p_{cyto}\Delta 2$-230-PrA	237 bp *Nde*I/*Xho*I fragment subcloned from pCOG030 into pCOG022 cut with same enzymes.
pCOG028	927 bp fragment encoding the cytosolic domain of Tlg2p, flanked by *Nde*I and *Xho*I sites, in pCR®2.1-TOPO®	Sequence encoding cytosolic domain of Tlg2p was PCR amplified from template pYCG-YOL018c (Seron *et al.*, 1998) with oligos 44 and 2. Resulting PCR product was *Taq*-

		treated and subcloned into pCR®2.1-TOPO®.
pCOG029	*E. coli* expression vector encoding a C-terminally PrA -tagged truncation of the cytosolic domain of Tlg2p lacking residues 1-36	Created as pCOG025, but with oligos 45 and 2.
pCOG030	*E. coli* expression vector encoding a C-terminally PrA -tagged truncation of the cytosolic domain of Tlg2p lacking residues 2-230	Created as pCOG025, but with oligos 48 and 2.
pCOG032	*E. coli* expression vector designed for co-production of cytosolic domain of Vti1p (residues 1-187) and $Tlg2p_{cyto}$-PrA	560 bp *Nco*I/*Hind*III fragment subcloned from pCOG003 into pCOG025 cut with same enzymes.
pCOG033	As pCOG032, but encoding $Tlg2p_{cyto}\Delta 1$-36-PrA	560 bp *Nco*I/*Hind*III fragment subcloned from pCOG003 into pCOG026 cut with same enzymes.
pCOG034	As pCOG032, but encoding $Tlg2p_{cyto}\Delta 2$-230-PrA	560 bp *Nco*I/*Hind*III fragment subcloned from pCOG003 into pCOG026 cut with same enzymes.
pCOG043	270 bp fragment encoding the cytosolic domain of Snc2p, flanked by *Kpn*I and *Xho*I sites, in pCR®2.1-TOPO®	Sequence encoding cytosolic domain of Snc2p was PCR amplified from pCOG006 with oligos 127 and 128. Resulting PCR product was *Taq*-treated and subcloned into pCR®2.1-TOPO®.
pCOG044	210 bp fragment encoding a truncation of the cytosolic domain of Snc2p (lacking residues 2-19), flanked by *Kpn*I and *Xho*I sites, in pCR®2.1-TOPO®	Sequence encoding truncation of cytosolic domain of Snc2p was PCR amplified from pCOG006 with oligos 129 and 128. Resulting PCR product was *Taq*-treated and subcloned into pCR®2.1-TOPO®.
pCOG045	*E. coli* expression vector encoding a C-terminally PrA -tagged version of the cytosolic domain of Snc2p	270 bp *Kpn*I/*Xho*I fragment from pCOG043 was subcloned into pCOG022 cut with the same enzymes.
pCOG046	*E. coli* expression vector encoding a C-terminally PrA -tagged truncation of the cytosolic domain of Snc2p lacking residues 2-19.	210 bp *Kpn*I/*Xho*I fragment from pCOG044 was subcloned into pCOG022 cut with the same enzymes.
pCOG047	270 bp fragment encoding the cytosolic domain of Vti1p, flanked by *Kpn*I and *Xho*I sites, in pCR®2.1-TOPO®	Sequence encoding cytosolic domain of Vti1p was PCR amplified from pCOG032 with oligos 133 and 134. Resulting PCR product was *Taq*-treated and subcloned into pCR®2.1-TOPO®.
PCOG048	*E. coli* expression vector encoding a C-terminally PrA -tagged truncation of the	560 bp *Kpn*I/*Xho*I fragment was subcloned from pCOG047 into pCOG022 cut with the same

	cytosolic domain of Vti1p	enzymes.
pCOG049	Sequence beginning approximately 490 basepairs upstream from the start of *SNC2* ORF, extending to approximately 300 basepairs downstream from the stop codon, in pCR®2.1-TOPO®	PCR amplification was performed from genomic DNA (prepared from a 9Dα strain) with oligos 156 and 157. Resulting ~1.14 kb PCR product was *Taq*-treated and subcloned into pCR®2.1-TOPO®.
pCOG052	Same as pCOG049, but with a *Hpa*I site immediately preceding the start codon	SDM was performed on pCOG049 using oligos 162 and 163
pCOG053	Same as pCOG052, but in yeast expression plasmid	1.14 kb *Xho*I/*Kpn*I fragment from pCOG052 was subcloned into pRS426 cut with the same enzymes
pCOG054	Yeast expression plasmid (2μ, *URA3*) driving overproduction of HA-Snc2p.	SDM was performed on pCOG053 to remove the *Hpa*I site and introduce an N-terminal HA tag using oligos 191 and 192
pCOG055	270 bp fragment encoding the cytosolic domain of Snc2p, flanked by *Eco*RI and *Hind*III sites, in pCR®2.1-TOPO®	Sequence encoding truncation of cytosolic domain of Snc2p was PCR amplified from pCOG006 with oligos 190 and 4. Resulting PCR product was Taq-treated and subcloned into pCR®2.1-TOPO®.
pCOG056	*E. coli* expression vector encoding an N-terminally $His_{(6)}$-HA-tagged version of the cytosolic domain of Snc2p	Approximately 297 bp *Eco*RI/*Hind*III fragment liberated from pCOG055 and subcloned into pACYC-Duet™-1 cut with the same enzymes.
pCOG062	Yeast expression plasmid (2μ, *URA3*) driving production of HA-Tlg2p lacking residues 1-36	SDM performed to loop out the sequence encoding the first 36 residues of Tlg2p from pHA-TLG2 using oligos 200 and 201
pCOG063	Yeast expression plasmid (2μ, *URA3*) driving production of HA-Tlg2p(K26R)	SDM performed to introduce the K26R mutation into pHA-TLG2 using oligos 214 and 215
pCOG064	Yeast expression plasmid (2μ, *LEU2*) driving overproduction of Vps45p-HA	3.7 kb *Bam*HI/*Sph*I fragment from pCOG070 subcloned into YEplac181 cut with the same enzymes
pCOG065	Yeast expression plasmid (2μ, *LEU2*) driving overproduction of Vps45p(W244R)-HA	3.7 kb *Bam*HI/*Sph*I fragment from pCOG072 subcloned into YEplac181 cut with the same enzymes
pCOG067	*E. coli* expression vector encoding $His_{(6)}$-Vps45p(L117R)	SDM was performed on pNB710 using oligos 202 and 203
pCOG068	*E. coli* expression vector encoding $His_{(6)}$-Vps45p(W244R)	SDM was performed on pNB710 using oligos 204 and 205
pCOG070	Yeast expression plasmid (2μ, *URA3*) driving	Carpp *et al.*, 2006

	overproduction of Vps45p-HA	
pCOG071	Yeast expression plasmid (2μ, *URA3*) driving overproduction of Vps45p(L117R)-HA	Carpp *et al.*, 2006
pCOG072	Yeast expression plasmid (2μ, *URA3*) driving overproduction of Vps45p(W244R)-HA	Carpp *et al.*, 2006
pCOG073	Yeast expression plasmid (2μ, *URA3*) driving overproduction of Vps45p(L117R/W244R)-HA	Carpp *et al.*, 2006
pCOG076	*E. coli* expression vector encoding a C-terminally PrA -tagged version of the cytosolic domain of Tlg2p (residues 1-309) harbouring the F9A,L10A mutations	SDM was performed on pCOG025 using oligos 322 and 323
pCR®2.1-TOPO®	ColE *ori* Amp^r Kan^r *lacZα*; TA cloning vector	Invitrogen
pGST-Tlg1p	*E. coli* expression vector encoding a GST-tagged truncation of the cytosolic domain of Tlg1p	Kind gift from Wanjin Hong (Institute of Molecular and Cell Biology, Singapore) (Coe *et al.*, 1999)
pET-Duet™-1	ColE1 *ori* Amp^r *lacI*; *E. coli* expression vector	Novagen
pHA-TLG2	Yeast expression plasmid (2μ, *URA3*) driving production of HA-Tlg2p	Seron *et al.*, 1998
pNB706	Yeast expression plasmid (*CEN*, *LEU2*) driving production of Vps45p-HA	3.7 kb *Bam*HI/*Sph*I fragment from pCOG070 subcloned into YCplac111 cut with the same enzymes. Created by Nia Bryant.
pNB707	Yeast expression plasmid (*CEN*, *LEU2*) driving production of Vps45p(W244R)-HA	3.7 kb *Bam*HI/*Sph*I fragment from pCOG072 subcloned into YCplac111 cut with the same enzymes. Created by Nia Bryant.
pNB708	Yeast expression plasmid (*CEN*, *LEU2*) driving production of Vps45p(L117R)-HA	3.7 kb *Bam*HI/*Sph*I fragment from pCOG071 subcloned into YCplac111 cut with the same enzymes. Created by Nia Bryant.
pNB709	Yeast expression plasmid (*CEN*, *LEU2*) driving production of Vps45p(L117R/W244R)-HA	3.7 kb *Bam*HI/*Sph*I fragment from pCOG073 subcloned into YCplac111 cut with the same enzymes. Created by Nia Bryant.
pNB710	*E. coli* expression vector encoding $His_{(6)}$-Vps45p	Sequence encoding Vps45p was PCR amplified from genomic DNA (prepared from a 9Dα strain) with oligos 9 and 10. The resulting ~1.7 kb product was subcloned into pCR®2.1-TOPO® and the *Bam*HI/*Not*I

		fragment then subcloned into pET-Duet™-1 cut with the same enzymes. Created by Nia Bryant.
pRS426	2μ, *URA3*	Sikorski and Hieter, 1989
pVT-102U	2μ, *URA3*	Vernet *et al.*, 1987
YCplac111	CEN, *LEU2*	Gietz and Sugino, 1988
YEplac181	2μ, *LEU2*	Gietz and Sugino, 1988
YEplac195	2μ, *URA3*	Gietz and Sugino, 1988
pT-GroE	T7 promoter-driven vector for the co-expression of the *E.coli* chaperone proteins GroEL and GroES	Yasukawa *et al.*, 1995

Chapter Three: Investigation of Vps45p binding modes to cognate SNARE partners

3.1 Introduction

SM proteins are required for all SNARE-mediated membrane fusion events, but their mechanism of action is far from understood (Jahn, 2000; Toonen and Verhage, 2003). In support of the idea that SM proteins perform (a) common function(s), SM proteins are conserved across species: Munc18 and its isoforms share 44-63% sequence identity with *Drosophila* Rop and *C. elegans* Unc-18, and 20-29% sequence identity with yeast SM proteins (Halachmi and Lev, 1996; Piper *et al.*, 1994). Furthermore, this homology is distributed evenly across their entire sequences rather than concentrated to one particular domain (Halachmi and Lev, 1996), making it likely that SM proteins have similar overall structures. Consistent with this idea, crystallography studies have revealed that Munc18-1 and Sly1p, which share 22% sequence identity and 47% sequence similarity (Piper *et al.*, 1994), also share a common fold (Bracher and Weissenhorn, 2002). Both proteins are arch-shaped molecules, composed of three domains forming a central cavity of approximately 15 Å (Bracher and Weissenhorn, 2002; Misura *et al.*, 2000).

Considering this similarity, it was surprising that these SM proteins were found to bind their cognate syntaxins through strikingly distinct modes (Bracher and Weissenhorn, 2002; Misura *et al.*, 2000): Specifically, for Munc18-1 to bind syntaxin 1a with nanomolar affinity (Pevsner *et al.*, 1994b), almost the entire cytosolic domain of syntaxin 1a is required (Kee *et al.*, 1995), and syntaxin 1a must adopt its closed conformation (Dulubova *et al.*, 1999; Misura *et al.*, 2000). Consistent with these observations, the crystal structure of Munc18-1 in complex with syntaxin 1a (Munc18-1/Sx1a) reveals that the inner cavity formed by domains 1 and 3a of Munc18-1 contacts syntaxin 1a throughout its H_{abc} domain and SNARE motif (Misura *et al.*, 2000). In this mode of interaction, i.e. with syntaxin 1a in its closed conformation, the H_{abc} domain shields the SNARE motif and renders it inaccessible for participation in SNARE complexes. In accordance with this, Munc18-1 does not bind assembled complexes containing syntaxin 1a, where syntaxin 1a is in its open conformation (Yang *et al.*, 2000).

In stark contrast to the above, the yeast syntaxin Sed5p possesses a short N-terminal region of approximately 40 residues that is both necessary and sufficient to capture its cognate SM protein, Sly1p (Yamaguchi *et al.*, 2002). The crystal structure of Sly1p in complex with the N-terminal 45 residues of Sed5p [Sly1p/Sed5p(1-45)] reveals that the Sed5p peptide inserts into a hydrophobic pocket on the outer surface of domain I of Sly1p (Bracher and Weissenhorn, 2002). As the SNARE motif is not shielded in this mode of interaction, Sly1p binding does not prevent Sed5p from participating in SNARE complexes; on the contrary, Sly1p has been shown to bind to assembled complexes (Peng and Gallwitz, 2002).

Understanding SM protein/syntaxin interactions could be key to identifying the exact point(s) of the SNARE complex assembly/disassembly cycle at which SM proteins exert their effects. For example, the mode of interaction captured in the Munc18-1/Sx1a crystal structure (Misura *et al.*, 2000) implies that Munc18-1 acts upstream of complex assembly, because Munc18-1 must dissociate from syntaxin 1a before core complexes can be formed. In contrast, Sly1p could interact with Sed5p via the mode captured by the Sly1p/Sed5p(1-45) crystal structure prior to, during, or after complex assembly (Bracher and Weissenhorn, 2002). The striking differences between these modes of interaction have made a unifying model of SM protein function difficult to formulate, even though the even homology among SM proteins and their similar overall structures suggest that they share (a) common mode of action(s). With the goal of constructing a model which encompasses (a) universal action(s) performed by SM proteins, a hypothesis was proposed that the diverse binding modes captured by the Munc18-1/Sx1a and Sly1p/Sed5p(1-45) crystal structures correspond to intermediates in a series of distinct interactions undertaken by SM proteins and their cognate syntaxins throughout the SNARE complex assembly/disassembly cycle. To this end, it was aimed to characterise the interactions(s) undertaken by Vps45p and its cognate syntaxin Tlg2p.

Vps45p has previously been shown to interact with Tlg2p with high affinity (Bryant and James, 2001; Nichols *et al.*, 1998). Several pieces of evidence suggest that this high affinity interaction between Vps45p and Tlg2p occurs via a mode analogous to that captured in the Sly1p/Sed5p(1-45) crystal structure, i.e. with the N-terminus of Tlg2p inserting into a hydrophobic pocket in domain I of

Vps45p: Firstly, residue F10 of Sed5p (identified as the key residue in the Sly1p/Sed5p interaction) is conserved in Tlg2p (Bracher and Weissenhorn, 2002); secondly, all five residues of Sly1p which form the hydrophobic pocket are conserved in Vps45p (Bracher and Weissenhorn, 2002). Furthermore, a similar short N-terminal region of Tlg2p (33 residues) has been shown to be both necessary and sufficient to capture Vps45p (Dulubova *et al.*, 2002). To test the hypothesis that Vps45p and Tlg2p utilise a pocket mode of interaction analogous to that captured by the Sly1p/Sed5p(1-45) crystal structure, an approach consisting of mapping studies and site-directed mutagenesis was taken.

3.2 Results

3.2.1 The first N-terminal 36 residues of Tlg2p mediate binding to Vps45p

To map the region of Tlg2p required for Vps45p binding, a recombinant protein was designed, containing the entire cytosolic domain of Tlg2p (residues 1-309) fused in-frame to two repeats of a synthetic IgG binding domain based on staphylococcal protein A (PrA) (Nilsson *et al.*, 1987), with a thrombin cleavage site just prior to the PrA tag ($Tlg2p_{cyto}$-PrA, Figure 3.1). The PrA tag was placed at the C-terminus of the fusion protein, replacing both the transmembrane and luminal domains of Tlg2p; the luminal domain has previously been shown to be nonessential for Tlg2p function (Abeliovich *et al.*, 1998). The positioning of the PrA tag was in contrast to previous work, in which a GST tag was placed at the N-terminus of the fusion protein (Dulubova *et al.*, 2002). The rationale for placing the PrA tag at the C-terminus of the fusion protein was that the N-terminal region of Tlg2p is required for its interaction with Vps45p (Dulubova *et al.*, 2002); therefore, an N-terminal tag could potentially interfere with this interaction. Two truncations of $Tlg2p_{cyto}$-PrA were also created: $Tlg2p_{cyto}\Delta N36$-PrA (lacking residues 1-36; residue 37 is a methionine and serves as a start codon) and $Tlg2p_{cyto}\Delta N230$-PrA (lacking residues 2-230). $Tlg2p_{cyto}\Delta N36$-PrA lacks the short N-terminal region shown to be necessary and sufficient for Vps45p binding (Dulubova *et al.*, 2002), but contains both the H_{abc} domain and the SNARE motif; $Tlg2p_{cyto}\Delta N230$-PrA lacks both the N-terminal region and the H_{abc} domain and only contains the SNARE motif.

When these proteins were produced recombinantly in *E. coli* and immobilised on IgG-Sepharose beads, only the full-length cytosolic domain of Tlg2p bound an HA-tagged version of Vps45p (Vps45p-HA) provided by a yeast lysate (Figure 3.1b, upper panel, lane 1). Note that $Tlg2p_{cyto}$-PrA is particularly subject to proteolysis; multiple bands corresponding to its degradation products are observed in Figure 3.1b, lane 1 (lower panel). These degradation products likely result from proteolytic cleavage at the N-terminus, since immunoblot analysis reveals that they still harbour the C-terminal PrA tag (for example, see Figure 3.7). The increased susceptibility of the N-terminal region of $Tlg2p_{cyto}$-PrA to proteolytic degradation can likely be attributed to its unstructured nature (Dulubova *et al.*, 2002).

3.2.2 Tlg2p and Vps45p interact in a "pocket mode" analogous to that undertaken by Sed5p and Sly1p

In the Sly1p/Sed5p(1-45) crystal structure, an α-helical peptide from the N-terminus of Sed5p inserts into a hydrophobic pocket on the outer surface of domain I of Sly1p (Bracher and Weissenhorn, 2002). The data presented in Figure 3.1, in which the truncation of a similar (36 residue) N-terminal region of Tlg2p abolished its ability to capture Vps45p, suggested that Vps45p and Tlg2p undergo a similar mode of interaction; this mode of interaction will henceforth be referred to as the "pocket mode". The hypothesis that this Vps45p/Tlg2p interaction is analogous to the Sly1p/Sed5p(1-45) interaction was supported by a sequence alignment of Sly1p and Vps45p; Figure 3.2a illustrates the precise conservation of four of the five residues of Sly1p (L137, L140, A141, and V156) which constitute the hydrophobic pocket. The only residue not exactly conserved is I153 in Sly1p, with a valine (V129) being present at this position in Vps45p; valines are also present at this position in Sly1p from other species including *C. elegans*, *D. melanogaster*, *A. thalianis*, and *H. sapiens* (Bracher and Weissenhorn, 2002). In an extensive mutagenesis study of several residues of Sly1p, aimed at disrupting the interaction between Sly1p and Sed5p, an L137R point mutation in Sly1p abolished its binding to Sed5p (Peng and Gallwitz, 2004). The interaction was likely abolished because the basic, hydrophilic, and bulky arginine residue (R137) chosen to replace the neutral, hydrophobic, and small leucine residue (L137) filled the space in the hydrophobic pocket, thereby preventing the N-terminal peptide of Sed5p from inserting into the pocket.

Considering that Sly1p and Vps45p share similar levels of sequence identity and similarity with Munc18-1 (22%/47% and 22%/46%, respectively (Piper *et al.*, 1994)), and the conservation of the five residues comprising the hydrophobic pocket of Sly1p in Vps45p (Bracher and Weissenhorn, 2002), it was hypothesised that a mutation analogous to L137R in Sly1p made in Vps45p would have a similar effect, i.e. abrogate Vps45p binding to Tlg2p. As shown in Figure 3.2a, residue L137 in Sly1p is analogous to L117 of Vps45p; therefore, Vps45p(L117R) should be analogous to Sly1p(L137R). Consistent with this hypothesis, the data presented in Figure 3.2b show that while Vps45p-HA provided by a yeast lysate bound $Tlg2p_{cyto}$-PrA (lane 1), the L117R mutation in Vps45p-HA severely abrogated this interaction (lane 2).

The pocket mode of interaction can also be disrupted via mutations in the syntaxin; residue F10 of Sed5p inserts into the hydrophobic pocket of Sly1p and has been identified as key for the Sly1p/Sed5p interaction (Bracher and Weissenhorn, 2002). As predicted, a version of Sed5p harbouring an F10A mutation was unable to bind to Sly1p (Yamaguchi *et al.*, 2002). Residue F10 of Sed5p is conserved in Tlg2p (F9; marked with an asterisk in Figure 3.2a), suggesting that a mutation analogous to F10A in Sed5p would also abolish Vps45p binding to Tlg2p. The combination of F9A/L10A mutations in Tlg2p abolished Vps45p binding in previous work (Dulubova *et al.*, 2002); to corroborate this result, F9A and L10A mutations were introduced into $Tlg2p_{cyto}$-PrA, a version of Tlg2p previously demonstrated to bind Vps45p-HA (Figures 3.1 and 3.2b). The ability of purified $His_{(6)}$-Vps45p to bind $Tlg2p_{cyto}$-PrA and $Tlg2p(F9A/L10A)_{cyto}$-PrA was then assessed. As displayed in Figure 3.2c, $His_{(6)}$-Vps45p bound $Tlg2p_{cyto}$-PrA (lane 2), but its binding to $Tlg2p(F9A/L10A)_{cyto}$-PrA was markedly decreased (lane 3), suggesting that the F9A/L10A mutations in Tlg2p impair the pocket mode interaction between Vps45p and Tlg2p.

The data presented in Figures 3.1 and 3.2c suggest that truncating the N-terminal 36 residues of Tlg2p is a more effective way of abolishing its interaction with Vps45p than the introduction of the F9A/L10A mutations; the N-terminus of Tlg2p(F9A/L10A) may retain some ability to insert into the putative hydrophobic pocket of domain I of Vps45p. Although other studies showed that F9A/L10A mutations in Tlg2p abolished its ability to interact with Vps45p (Dulubova *et al.*, 2002), it is worth noting that these mutations were made in the context of an N-

terminally tagged GST-fusion protein, rather than the C-terminally tagged PrA-fusion protein used here. The data presented in Figure 3.2 also indicate that the L117R mutation in Vps45p is a more effective means of abolishing the Vps45p/Tlg2p interaction than are the F9A/L10A mutations in Tlg2p. As a caveat to this conclusion, Vps45p-HA and Vps45p(L117R)-HA were provided by yeast lysates in the experiment shown in Figure 3.2b, while recombinantly produced $His_{(6)}$-Vps45p was used in the experiment shown in Figure 3.2c; endogenous Tlg2p from the lysates may have competed for interaction sites in the first case and masked a weak interaction between Vps45p(L117R)-HA and $Tlg2p_{cyto}$-PrA. Alternatively, the L117R mutation in Vps45p may simply be a more effective way of disrupting the pocket mode interaction than are the F9A/L10A mutations in Tlg2p.

To complement these *in vitro* binding studies, and to assess whether the L117R mutation in Vps45p also abolished its ability to associate with Tlg2p *in vivo*, an immunoprecipitation (IP) approach was undertaken. Vps45p-HA and Vps45p(L117R)-HA were immunoprecipitated from yeast cell lysates with α-HA antibodies, and immunoblot analysis was used to detect the presence of co-precipitated Tlg2p. Figure 3.3 shows that whereas Vps45p-HA efficiently co-precipitated endogenous Tlg2p, the introduction of the L117R mutation abolished this interaction (compare lanes 3 and 4 of the bottom panel). Comparison of the amount of immunoprecipitated material with the sample of lysate run on the same immunoblot indicates that in cells producing Vps45p-HA, ~4% of the total population of Tlg2p was co-precipitated by ~8% of the total population of Vps45p-HA (lane 3). It may be possible to extrapolate from this ratio that the entire population of Vps45p-HA would co-precipitate 50% of the total population of Tlg2p. This high level of association is consistent with the observation that Vps45p associates both with monomeric Tlg2p and with *cis*-complexes (Bryant and James, 2003). In a similar experiment, a myc-tagged version of Sec1p (precipitated with 50% efficiency by α-myc antibodies) co-precipitated 0.2% of its cognate syntaxin Sso1p (Carr *et al.*, 1999). The lower percentage of total Sso1p co-precipitated by MYC-Sec1p is consistent with the observations that Sec1p does not associate with monomeric Sso1p *in vivo* (Carr *et al.*, 1999), and that only ~1% of the total populations of the SNAREs involved in exocytosis (Sso1p, Sec9p, Sncp) exist in complexes (Grote *et al.*, 2000).

Two conclusions can be drawn from the data presented in Figures 3.2 and 3.3: One, Vps45p and Tlg2p likely undergo a pocket mode interaction analogous to that revealed by the Sly1p/Sed5p(1-45) crystal structure. Two, this pocket mode interaction can be disrupted by mutations in either Vps45p or Tlg2p; the L117R mutation in Vps45p severely abrogates its interaction with Tlg2p both *in vitro* (Figure 3.2b) and *in vivo* (Figure 3.3), and F9A/L10A mutations in Tlg2p strongly impair its interaction with Vps45p *in vitro* (Figure 3.2c).

3.2.3 Vps45p interacts with its cognate v-SNARE, Snc2p, via its SNARE motif

SM proteins have traditionally been thought to regulate membrane fusion via interaction with their cognate syntaxin. However, it was recently found that Sly1p interacts with the v-SNAREs Bet1p and Sft1p, and the nonsyntaxin t-SNAREs Bos1p and Gos1p (Peng and Gallwitz, 2004), in addition to its cognate syntaxin Sed5p (Grabowski and Gallwitz, 1997) (N.B. Sed5p participates in two SNARE complexes: Sed5p/Bos1p/Sec22p/Bet1p, which controls ER-to-Golgi traffic (Parlati *et al.*, 2000), and Sed5p/Gos1p/Ykt6p/Sft1p, which controls intra-Golgi traffic (Parlati *et al.*, 2002)). This finding supports a model in which SM proteins act as physical bridges between t-SNAREs and v-SNAREs to facilitate complex assembly. To investigate whether the ability to interact with nonsyntaxin SNARE proteins is a common feature of SM proteins, the ability of Vps45p to bind each of its cognate SNARE proteins was investigated. Tlg2p forms a functional SNARE complex with Tlg1p, Vti1p, and Snc2p, as demonstrated by the co-precipitation of these SNARE proteins from yeast cell lysates (Bryant and James, 2001; Coe *et al.*, 1999), and the ability of this complex to drive fusion of artificial liposomes (Paumet *et al.*, 2001).

To examine Vps45p binding to the individual SNARE proteins in this complex, the ability of purified $His_{(6)}$-Vps45p to bind fusion proteins containing the cytosolic domains of Tlg2p, Snc2p, Vti1p, and Tlg1p was assessed. Purified proteins were used to eliminate the possibility of indirect interactions being bridged by additional factors in yeast lysates. The cytosolic domains of Tlg2p, Snc2p, and Vti1p were produced as C-terminally tagged PrA fusion proteins and immobilised on IgG-Sepharose; the cytosolic domain of Tlg1p was produced as a GST fusion protein and recovered on GST-Sepharose. Beads loaded with cytosolic SNARE

proteins were then incubated with purified $His_{(6)}$-Vps45p. Of the proteins tested, only $Tlg2p_{cyto}$-PrA and $Snc2p_{cyto}$-PrA bound $His_{(6)}$-Vps45p at levels above background and visible by staining with Coomassie Brilliant Blue (lanes 1 and 2 compared to lane 4, upper panel, Figure 3.4). The identity of this band as $His_{(6)}$-Vps45p was confirmed by immunoblot analysis with α-Vps45p antibodies (bottom panel, Figure 3.4). No interaction was observed between $His_{(6)}$-Vps45p and the cytosolic domains of Vti1p or Tlg1p (lanes 3 and 5, Figure 3.4). The data presented in Figure 3.4 indicate that in addition to Tlg2p, Vps45p interacts specifically and directly with the v-SNARE Snc2p.

The region of Snc2p mediating its interaction with Vps45p was next investigated. Unlike syntaxins, which contain large, independently structured N-terminal domains preceding their SNARE motifs, Snc2p possesses only a short N-terminal region of 19 amino acids prior to its SNARE motif (Paumet *et al.*, 2001). To determine whether this region was required for its interaction with Vps45p, a construct was created to produce a C-terminally PrA-tagged version of the cytosolic domain of Snc2p lacking the 18 amino acids which precede the SNARE motif (Δ2-19; Figure 3.5a). Figure 3.5b shows that the SNARE motif of Snc2p is sufficient to bind Vps45p. $Tlg2p_{cyto}$-PrA, $Snc2p_{cyto}$-PrA, and $Snc2p_{cyto}$Δ2-19-PrA were immobilised on IgG-Sepharose beads and incubated with purified $His_{(6)}$-Vps45p. $Snc2p_{cyto}$Δ2-19-PrA bound $His_{(6)}$-Vps45p as efficiently as $Snc2p_{cyto}$-PrA, at levels visible by staining with Coomassie Brilliant Blue (lane 3 compared with lane 2, lower panel, Figure 3.5b). The identity of this band as $His_{(6)}$-Vps45p was confirmed by immunoblot analysis with α-Vps45p antibodies (upper panel, Figure 3.5b). These data demonstrate that the SNARE motif of Snc2p mediates its interaction with Vps45p. Importantly, this differs from the interaction between Tlg2p and Vps45p; a similar truncation of Tlg2p comprised of only its SNARE motif was unable to bind Vps45p (Figure 3.1b). Furthermore, this observation is consistent with the finding that the interactions of the v-SNAREs Bet1p and Sft1p with Sly1p are mediated by their SNARE motifs (Peng and Gallwitz, 2004).

3.2.4 Vps45p interacts with Tlg2p and Snc2p via distinct mechanisms

Since an N-terminal portion of the syntaxin inserts into the hydrophobic pocket of the SM protein in the pocket mode, the observation that the N-terminal 19

residues of Snc2p were not required for Vps45p binding (Figure 3.5b) suggested that Snc2p interacts with Vps45p via an alternative mode. Therefore, the effect of the pocket filling L117R mutation on the ability of Vps45p to bind Snc2p was examined. The results from this experiment are presented in Figure 3.6. Consistent with the data presented in Figures 3.2 and 3.3, the L117R mutation severely abrogated the ability of Vps45p-HA (provided by a yeast lysate) to bind to $Tlg2p_{cyto}$-PrA (compare lanes 1 and 2). In contrast to this finding, the L117R mutation did not affect the ability of $His_{(6)}$-Vps45p to bind to $Snc2p_{cyto}$-PrA (compare lanes 3 and 4). Collectively, the findings that the N-terminal 19 residues of Snc2p were not required for Vps45p binding (Figure 3.5b), and that the L117R pocket-filling mutation did not impair the Vps45p/Snc2p interaction (Figure 3.6), suggest that Snc2p does not bind Vps45p via the pocket mode.

3.2.5 Vps45p does not appear to bind Tlg2p and Snc2p simultaneously

The finding that Tlg2p and Snc2p bound distinct regions of Vps45p (Figure 3.6) suggested that Vps45p may act as a physical bridge between Tlg2p and Snc2p, perhaps helping to regulate the fidelity of t-SNARE/v-SNARE pairing *in vivo*, or to influence the kinetics of SNARE complex assembly. This model predicts that the SM protein would be able to bind the two SNARE proteins simultaneously, via distinct modes. Such a model has previously been postulated, although distinct binding modes for the syntaxin and the v-SNARE to the SM protein were not demonstrated (Peng and Gallwitz, 2002). To assess whether Vps45p could bind Tlg2p and Snc2p simultaneously, the ability of $His_{(6)}$-Vps45p to physically bridge $Tlg2p_{cyto}$ and $His_{(6)}$-HA-$Snc2p_{cyto}$ was assessed. In this experiment, bacterial lysates containing recombinantly produced proteins were mixed in the following combinations: 1) $His_{(6)}$-HA-$Snc2p_{cyto}$ and $Tlg2p_{cyto}$-PrA, 2) $His_{(6)}$-HA-$Snc2p_{cyto}$, $Tlg2p_{cyto}$-PrA, and GroEL/GroES, and 3) $His_{(6)}$-HA-$Snc2p_{cyto}$, $Tlg2p_{cyto}$-PrA, $His_{(6)}$-Vps45p, and GroEL/GroES. The second condition, in which only the chaperone proteins GroEL/GroES were added to $His_{(6)}$-HA-$Snc2p_{cyto}$ and $Tlg2p_{cyto}$-PrA, was included because significant amounts of GroEL and GroES often remained complexed with purified $His_{(6)}$-Vps45p (for examples, see $His_{(6)}$-Vps45p input in Figures 3.4 and 3.5). After mixing of the bacterial lysates, $Tlg2p_{cyto}$-PrA and any associated proteins were recovered via affinity purification onto IgG-Sepharose; a thrombin cleavage step was next performed to liberate $Tlg2p_{cyto}$ (and any

bound proteins) from the PrA tag, which remained bound to the IgG-Sepharose beads. The presence of $His_{(6)}$-HA-Snc2p in the thrombin cleaved supernatant was then assessed through immunoblot analysis with α-HA antibodies (many of the degradation products of $Tlg2p_{cyto}$-PrA migrated at similar molecular weights as $His_{(6)}$-HA-$Snc2p_{cyto}$, making it difficult to assess the presence of $His_{(6)}$-HA-Snc2p in the thrombin cleaved supernatant by Coomassie staining alone). The data presented in Figure 3.7 show that $Tlg2p_{cyto}$-PrA/$His_{(6)}$-Vps45p dimers were successfully recovered, and that $His_{(6)}$-Vps45p could be detected following their cleavage from the PrA tag (lane 3, middle and lower panels), but no $His_{(6)}$-HA-$Snc2p_{cyto}$ was detected to be associated with the $Tlg2p_{cyto}$/$His_{(6)}$-Vps45p dimers (lane 3, bottom panel). From these data, it does not appear that Vps45p acts as a physical bridge between $His_{(6)}$-HA-$Snc2p_{cyto}$ and $Tlg2p_{cyto}$-PrA.

It is worth bearing in mind that that the version of Snc2p shown to interact with Vps45p (Figure 3.4) harboured a C-terminal PrA tag ($Snc2p_{cyto}$-PrA). Therefore, the formal possibility remained that either the N-terminal $His_{(6)}$- tag, or the HA tag, on $His_{(6)}$-HA-$Snc2p_{cyto}$ interfered with its interaction with $His_{(6)}$-Vps45p. This control could not be performed, due to the presence of the $His_{(6)}$- tag on both $His_{(6)}$-HA-$Snc2p_{cyto}$ and $His_{(6)}$-Vps45p. As a complementary approach, using an untagged version of the cytosolic domain of Snc2p, a second experiment to examine the ability of Vps45p to bind Tlg2p and Snc2p simultaneously was performed in collaboration with Nia Bryant and Scott Shanks (University of Glasgow). In contrast to the experiment shown in Figure 3.7, in which bacterial lysates containing recombinant proteins were mixed, this experiment utilised purified proteins. The inputs of each protein are shown in lanes 1-3 of Figure 3.8: lane 1, $His_{(6)}$-Vps45p; lane 2, $Tlg2p_{cyto}$-PrA; lane 3, $Snc2p_{cyto}$ (generated from thrombin cleavage of the PrA tag from $Snc2p_{cyto}$-PrA). IgG-Sepharose beads loaded with $Tlg2p_{cyto}$-PrA (~1 nmol) were incubated with either $Snc2p_{cyto}$ alone (lane 4) or both $His_{(6)}$-Vps45p and $Snc2p_{cyto}$ (lane 5). Both $Snc2p_{cyto}$ and $His_{(6)}$-Vps45p were added in excess (~5- and ~2-fold, respectively) relative to $Tlg2p_{cyto}$-PrA. Although $His_{(6)}$-Vps45p bound the immobilised $Tlg2p_{cyto}$-PrA, no $Snc2p_{cyto}$ was present in the protein complexes (lane 5). As an additional control, the ability of $His_{(6)}$-Vps45p immobilised on Ni-NTA beads to bind $Snc2p_{cyto}$ was assessed (lane 6), demonstrating that the lack of observed $His_{(6)}$-Vps45p bridging between $Tlg2p_{cyto}$-PrA and $Snc2p_{cyto}$ is not due to the inability of $His_{(6)}$-Vps45p to bind $Snc2p_{cyto}$. Together, the data presented in Figures 3.7 and 3.8 suggest that

Vps45p does not appear to bind Tlg2p and Snc2p simultaneously. These experiments were unable to yield evidence in support of the bridging hypothesis; however, it is worth noting that if such a bridging intermediate exists, it is likely to be tightly regulated, and may require a transient conformation of the SM protein that is not accessed in this experimental system.

3.2.6 Tlg2p displaces Snc2p from Vps45p

The finding that the L117R mutation in Vps45p severely abrogated its ability to bind to Tlg2p, but did not affect its ability to bind to Snc2p (Figure 3.6), suggested that the two SNARE proteins bind distinct regions of Vps45p rather than competing for the same region. However, the observation that Vps45p could not be observed to bind Tlg2p and Snc2p simultaneously (Figures 3.7 and 3.8) raised the possibility that the Tlg2p and Snc2p binding sites overlap. It was aimed to determine whether one SNARE could displace the other from the SM protein; to this end, competition binding experiments were performed. In these experiments, the first SNARE protein was allowed to bind to Vps45p, and the ability of the second SNARE protein to displace the first SNARE protein was investigated.

First, the ability of $Tlg2p_{cyto}$-PrA to displace $Snc2p_{cyto}$-PrA from $His_{(6)}$-Vps45p was assessed. $Snc2p_{cyto}$-PrA/$His_{(6)}$-Vps45p complexes were recovered on Ni-NTA agarose, and increasing amounts of $Tlg2p_{cyto}$-PrA were added to attempt to displace $Snc2p_{cyto}$-PrA. The results of a typical experiment are shown in Figure 3.9a. In lane 1, the amount of $Snc2p_{cyto}$-PrA (lower band, upper panel) bound to immobilised $His_{(6)}$-Vps45p (upper band, upper panel) is shown. In lanes 3-5, the amounts of $Snc2p_{cyto}$-PrA bound to immobilised $His_{(6)}$-Vps45p after incubation with increasing amounts of $Tlg2p_{cyto}$-PrA are shown. A Coomassie stained gel displaying 2.5% of the inputs of $Tlg2p_{cyto}$-PrA added to each reaction is also shown in Figure 3.9a (lower panel). The amount of bound $Snc2p_{cyto}$-PrA decreased as the amount of added $Tlg2p_{cyto}$-PrA increased, with 60 μgs of $Tlg2p_{cyto}$-PrA being sufficient to displace all bound $Snc2p_{cyto}$-PrA from $His_{(6)}$-Vps45p (lane 5, lower band, upper panel).

To ensure that this result reflected a specifically executed displacement by Tlg2p, rather than a general effect mediated by any SNARE protein, a SNARE

protein from a different transport step (syntaxin 4, which plays a role in the fusion of GLUT4-containing vesicles with the plasma membrane in insulin responsive tissues (Jagadish *et al.*, 1996)) was also added to $Snc2p_{cyto}$-PrA/$His_{(6)}$-Vps45p complexes. Although a slight reduction in the amount of bound $Snc2p_{cyto}$-PrA could be observed with the addition of GST-$Sx4_{cyto}$ (bottom band, lane 2 vs. lane 1, upper panel), GST-$Sx4_{cyto}$ did not completely displace $Snc2p_{cyto}$-PrA (as did $Tlg2p_{cyto}$-PrA) when equivalent amounts of the two proteins were added (bottom band, lane 5, upper panel).

Second, the ability of $Snc2p_{cyto}$-PrA to displace bound $Tlg2p_{cyto}$-PrA from $His_{(6)}$-Vps45p was assessed. Binary $Tlg2p_{cyto}$-PrA/$His_{(6)}$-Vps45p complexes were immobilised on Ni-NTA agarose, and increasing amounts of $Snc2p_{cyto}$-PrA (or $Vti1p_{cyto}$-PrA as a negative control) were added to attempt to displace $Tlg2p_{cyto}$-PrA. The results from a typical competition experiment are shown in Figure 3.9b. In lane 1, the amount of $Tlg2p_{cyto}$-PrA bound to $His_{(6)}$-Vps45p is shown (bottom band, upper panel). In lanes 2-4, the amounts of $Tlg2p_{cyto}$-PrA bound to immobilised $His_{(6)}$-Vps45p after incubation with increasing amounts of $Snc2p_{cyto}$-PrA are shown. A Coomassie stained gel displaying 3% of the inputs of $Snc2p_{cyto}$-PrA added to each reaction is also shown in Figure 3.9b (lower panel). The amount of bound $Tlg2p_{cyto}$-PrA did not decrease in any of the reactions, even when the amount of $Snc2p_{cyto}$-PrA added to attempt to displace $Tlg2p_{cyto}$-PrA from $His_{(6)}$-Vps45p (125 μg, lane 4) was more than twice the amount of $Tlg2p_{cyto}$-PrA which was sufficient to displace bound $Snc2p_{cyto}$-PrA from $His_{(6)}$-Vps45p (60 μg, lane 5 in Figure 3.9a). Collectively, the data presented in Figure 3.9 suggest that Tlg2p can displace Snc2p from Vps45p, while Snc2p is unable to displace Tlg2p from Vps45p.

3.2.7 The displacement of Snc2p from Vps45p does not require the pocket mode interaction between Vps45p and Tlg2p

To determine whether the displacement of Snc2p from Vps45p required Vps45p and Tlg2p to interact via the pocket mode, the pocket-filling L117R mutation in Vps45p and the F9A/L10A mutations in Tlg2p were exploited to disrupt this interaction (Figure 3.2). Once again, the displacement of $Snc2p_{cyto}$-PrA from $His_{(6)}$-Vps45p was examined by competition binding assays. This time, $His_{(6)}$-

Vps45p(L117R) and Tlg2p(F9A/L10A)$_{cyto}$-PrA were also used in the binding reactions to assess their abilities to execute the displacement of Snc2p$_{cyto}$-PrA.

First, the ability of Tlg2p$_{cyto}$-PrA to displace Snc2p$_{cyto}$-PrA from His$_{(6)}$-Vps45p(L117R) was assessed; the L117R mutation in Vps45p was previously demonstrated to severely abrogate the pocket mode interaction between Vps45p and Tlg2p (Figure 3.2). The data presented in Figure 3.10a show that Tlg2p$_{cyto}$-PrA completely displaced Snc2p$_{cyto}$-PrA from both wild-type His$_{(6)}$-Vps45p (lane 3) and His$_{(6)}$-Vps45p(L117R) (lane 6). As a negative control, GST-Sx4$_{cyto}$ did not completely displace Snc2p$_{cyto}$-PrA from either wild-type His$_{(6)}$-Vps45p (lane 2), or from His$_{(6)}$-Vps45p(L117R) (lane 5). These data suggest that the mechanism by which Snc2p is displaced from Vps45p does not involve the pocket mode interaction between Vps45p and Tlg2p. As a second approach to test this hypothesis, the ability of Tlg2p(F9A/L10A)$_{cyto}$-PrA to displace Snc2p$_{cyto}$-PrA from His$_{(6)}$-Vps45p(L117R) was assessed; the F9A/L10A mutations in Tlg2p were previously demonstrated to strongly impair the pocket mode interaction between Vps45p and Tlg2p (Figure 3.2). The data presented in Figure 3.10b show that both Tlg2p$_{cyto}$-PrA and Tlg2p(F9A/L10A)$_{cyto}$-PrA were able to displace Snc2p$_{cyto}$-PrA from His$_{(6)}$-Vps45p (lanes 3 and 4, respectively). The negative control, GST-Sx4$_{cyto}$, was unable to completely displace Snc2p$_{cyto}$-PrA (lane 2). This result is consistent with the finding that Tlg2p$_{cyto}$-PrA can displace Snc2p$_{cyto}$-PrA from His$_{(6)}$-Vps45p(L117R) (Figure 3.10a); collectively, these data strongly suggest that the mechanism of this displacement does not occur via the pocket mode interaction between Vps45p and Tlg2p.

This is a surprising finding, as no evidence was found to suggest that Vps45p and Tlg2p undergo any mode of interaction alternative to the pocket mode (Figures 3.1b and 3.2b) through which Tlg2p could execute this displacement. Two possible explanations are: One, the L117R and F9A/L10A mutations do not completely abolish the pocket mode interaction. To fully address this possibility, the affinities of Vps45p(L117R) for Tlg2p, and of Tlg2p(F9A/L10A) for Vps45p, would need to be determined. If the L117R and F9A/L10A mutations do not completely abolish the pocket mode interaction, the insertion of the N-terminal portion of Tlg2p into the putative hydrophobic pocket of domain I of Vps45p could trigger a conformational change of Vps45p, causing the displacement of Snc2p. Such a conformational change has been observed in

domain I of rSly1, triggered by the binding of an N-terminal peptide from its cognate syntaxin (Arac *et al.*, 2005). This suggests a model in which Vps45p associates with vesicles via its interaction with the SNARE motif of Snc2p (Figure 3.5), perhaps preventing Snc2p from forming complexes until the vesicle is transported to a potential site of fusion. Upon reaching the target membrane, interaction with Tlg2p via the pocket mode causes a conformational change in Vps45p, which releases Snc2p and frees its SNARE motif for participation in complexes. In this model, Vps45p ensures that Snc2p does not enter complexes until the appropriate time (i.e. until the vesicle reaches its cognate syntaxin at the target membrane).

A second explanation is that Tlg2p and Snc2p bind the same (or overlapping) site(s) of Vps45p, and that Tlg2p has a higher affinity for this region than does Snc2p. Since the hydrophobic pocket of Vps45p does not mediate its interaction with Snc2p (Figure 3.6), this would imply that Tlg2p and Vps45p also undertake a similar interaction (i.e. distinct from the pocket mode). To test this hypothesis, it will be important to characterise the Vps45p/Snc2p interaction; this could be addressed through yeast two-hybrid work directed towards this aim. If Tlg2p and Snc2p do bind the same region of Vps45p, this would be consistent with the finding that Vps45p did not appear to simultaneously bind Tlg2p and Snc2p (Figures 3.7 and 3.8). This hypothesis is also consistent with a model in which Vps45p associates with Snc2p-containing vesicles and releases Snc2p when brought into proximity with Tlg2p (i.e. upon reaching the target membrane).

3.3 Discussion

The data presented in this chapter indicate that a short N-terminal region of Tlg2p inserts into a putative hydrophobic pocket on the outer surface of domain I of Vps45p, in a mode similar to that captured by the crystal structure of Sly1p/Sed5p(1-45) (Bracher and Weissenhorn, 2002). The finding that the removal of this short N-terminal region from Tlg2p abolishes its ability to bind to Vps45p-HA (Figure 3.1) corroborates previous reports (Dulubova *et al.*, 2002). To further characterise this interaction, key contact residues were identified (L117 of Vps45p and F9/L10 of Tlg2p); point mutations of these residues either severely abrogated or impaired the pocket mode interaction between Vps45p and Tlg2p (Figure 3.2). Several syntaxins have now been demonstrated to

interact with their cognate SM proteins via this mode, including Sed5p and its mammalian homologue syntaxin 5 (Yamaguchi *et al.*, 2002), Ufe1p and its mammalian homologue syntaxin 18 (Yamaguchi *et al.*, 2002), and Tlg2p and its mammalian homologue syntaxin 16 (Dulubova *et al.*, 2002). From the work presented in this chapter, no evidence was found to suggest that Vps45p and Tlg2p undertake an interaction analogous to that observed in the Munc18-1/syntaxin 1a crystal structure (Misura *et al.*, 2000), i.e. with the syntaxin cradled in its closed conformation in the inner cavity of the SM protein.

Although most models of SM protein function have focused on the ways in which they regulate syntaxin (Toonen and Verhage, 2003), the SM protein Sly1p has recently been demonstrated to interact with non-syntaxin members of its cognate SNARE complex (Peng and Gallwitz, 2004). The data presented in this chapter have extended this observation by identifying Vps45p as an additional SM protein capable of interacting with multiple SNARE partners. Specifically, Vps45p was shown to interact specifically and directly with both its cognate syntaxin, Tlg2p, and its cognate v-SNARE, Snc2p (Figure 3.4); this latter interaction has not been previously demonstrated. Vps45p interacts with the SNARE motif of Snc2p (Figure 3.5), and this interaction does not occur via the same mechanism as its interaction with Tlg2p (i.e. the pocket mode, Figure 3.6). While this finding suggests that distinct regions of Vps45p are involved in its interactions with Tlg2p and Snc2p, no evidence was found to indicate that Vps45p acts as a physical bridge between Snc2p and Tlg2p (Figures 3.7 and 3.8). Instead, the finding that Tlg2p can displace Snc2p from Vps45p (Figure3.9) suggests that Tlg2p binding disrupts the Vps45p/Snc2p interaction.

From the data presented in this chapter, a preliminary model to describe the role of Vps45p in SNARE complex assembly can be formulated. In this initial working model, Vps45p associates with vesicles destined for the endosomal system via interaction with Snc2p; these vesicles are transported to target membranes characterised by the presence of Tlg2p. In this model, the specific recognition of two cognate SNARE partners (Tlg2p and Snc2p) by one SM protein (Vps45p) helps direct the Snc2p-containing vesicle to its proper destination, i.e. endosomes rather than the plasma membrane. Upon reaching the target membrane, Vps45p interacts with Tlg2p (via a mode distinct from the pocket mode), thereby releasing Snc2p. The interaction between Vps45p and Tlg2p

primes Tlg2p into a complex-receptive conformation (perhaps analogous to the open conformation of syntaxin 1a) and would account for the *in vivo* requirement of Vps45p in complex assembly (Bryant and James, 2001). This model does not assign any function to the pocket mode interaction between Vps45p and Tlg2p; the work presented in the following chapter is aimed at investigating this point.

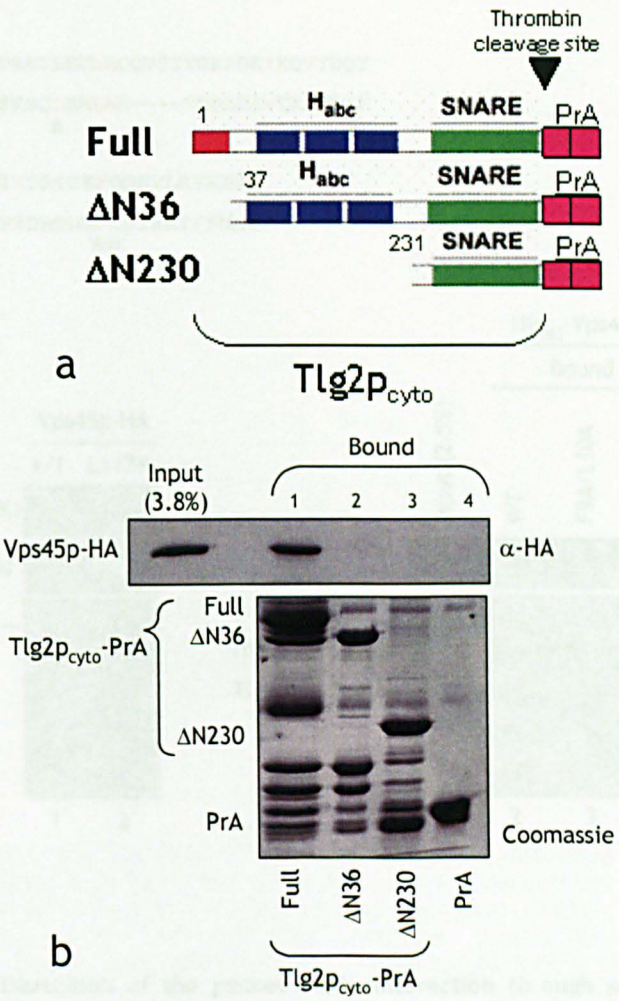

Figure 3.1 The first N-terminal 36 residues of Tlg2p mediate Vps45p binding. a) Schematic diagram of full length $Tlg2p_{cyto}$-PrA and two truncations thereof, ΔN36 and ΔN230. b) Plasmids pCOG025, pCOG029, pCOG030, and pCOG022 were used to recombinantly produce $Tlg2p_{cyto}$-PrA, $Tlg2p_{cyto}$ ΔN36-PrA, $Tlg2p_{cyto}$ ΔN230-PrA, and PrA. Purified proteins were eluted from IgG-Sepharose beads, resolved by SDS-PAGE, and visualised by staining with Coomassie Brilliant Blue (bottom panel). IgG-Sepharose beads loaded with $Tlg2p_{cyto}$-PrA (lane 1), $Tlg2p_{cyto}$ ΔN36-PrA (lane 2), $Tlg2p_{cyto}$ ΔN230-PrA (lane 3), or PrA (lane 4) were incubated with a yeast lysate from *vps45Δ* (LCY008) cells transformed with pCOG070 (driving the production of Vps45p-HA). After extensive washing to remove nonspecifically bound proteins, bound proteins were eluted, resolved by SDS-PAGE, and transferred to nitrocellulose membrane. The amount of bound Vps45p-HA was then assessed using immunoblot analysis with α-HA antibodies (upper panel).

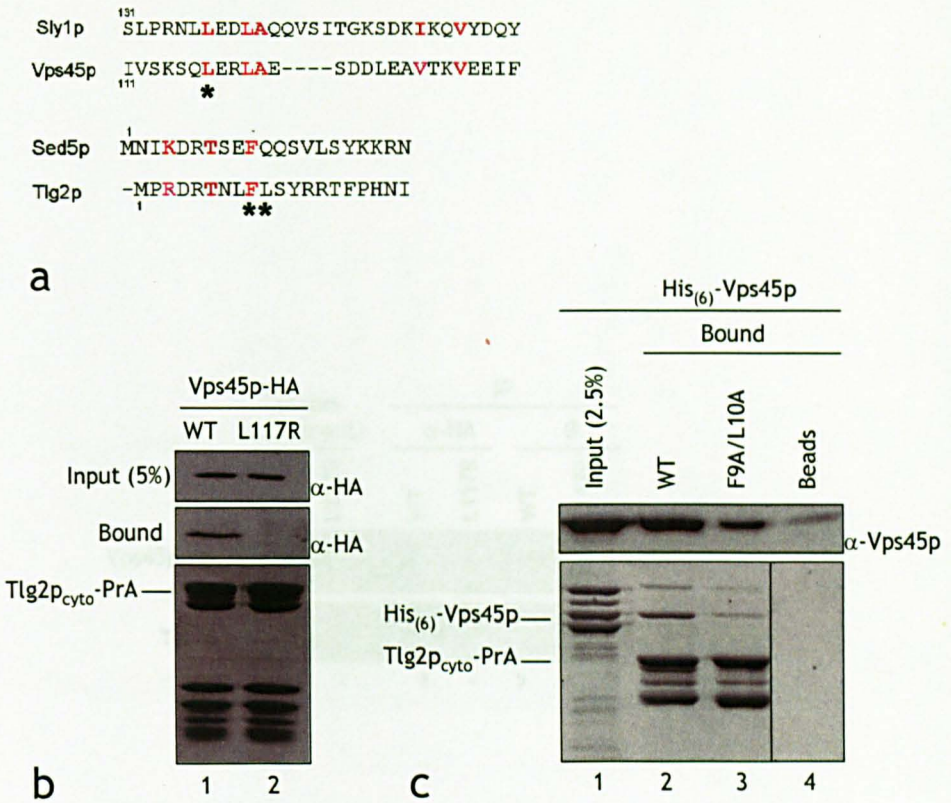

Figure 3.2 Disruption of the pocket mode interaction through point mutations in Vps45p and Tlg2p. a) Alignments of Sly1p/Vps45p and Sed5p/Tlg2p, modified from Bracher and Weissenhorn (2002). Vps45p(L117) and Tlg2p(F9/L10) are designated with asterisks. b) The L117R mutation in Vps45p-HA severely abrogates its binding to Tlg2p$_{cyto}$-PrA: pCOG025 was used to recombinantly produce Tlg2p$_{cyto}$-PrA; IgG-Sepharose beads loaded with Tlg2p$_{cyto}$-PrA were incubated with lysates from *vps45*Δ cells (LCY008) transformed with either pCOG070 (driving the production of Vps45p-HA, lane 1) or pCOG071 (driving the production of Vps45p(L117R)-HA, lane 2). Following extensive washing to remove nonspecifically bound proteins, bound proteins were eluted, resolved by SDS-PAGE, and either visualised by staining with Coomassie Brilliant Blue (bottom panel) or transferred to nitrocellulose membrane and subjected to immunoblot analysis with α-HA antibodies (middle panel). Samples of lysate inputs were similarly analysed (upper panel). c) The F9A/L10A mutations in Tlg2p$_{cyto}$-PrA strongly interfere with its interaction with His$_{(6)}$-Vps45p: Plasmids pCOG025/pT-GroE, pCOG076/pT-GroE, or pNB710/pT-GroE were used to recombinantly produce Tlg2p$_{cyto}$-PrA, Tlg2p$_{cyto}$(F9A/L10A)-PrA, or His$_{(6)}$-Vps45p. IgG-Sepharose beads loaded with either Tlg2p$_{cyto}$-PrA (lane 2), Tlg2p$_{cyto}$(F9A/L10A)-PrA (lane 3), or no protein (lane 4) were incubated with purified His$_{(6)}$-Vps45p (2.5% of the input is shown in lane 1). Following extensive washing to remove nonspecifically bound proteins, bound proteins were eluted, resolved by SDS-PAGE, and either visualised by staining with Coomassie Brilliant Blue (bottom panel) or transferred to nitrocellulose membrane and subjected to immunoblot analysis with α-Vps45p antibodies (upper panel).

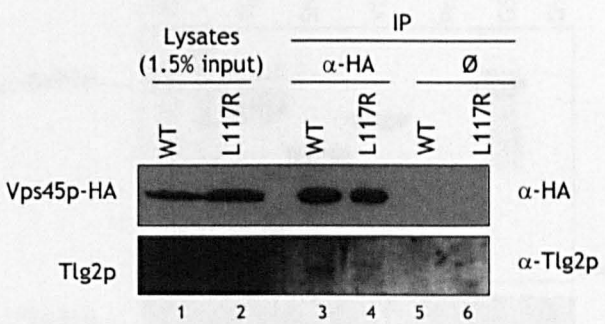

Figure 3.3 Vps45p(L117R) does not associate with Tlg2p *in vivo*. α-HA antibodies were used to immunoprecipitate Vps45p-HA or Vps45p(L117R)-HA, and associated proteins, from lysates obtained from wild-type yeast (9Dα) transformed with either pCOG070 (driving the production of Vps45p-HA) or pCOG071 (driving the production of Vps45p(L117R)-HA). Proteins from samples representing either 1.5% of the total lysate input for each immunoprecipitation (left panels), or 40% of the total immunoprecipitated material (right panels), were resolved by SDS-PAGE and transferred to nitrocellulose membrane. The presence of co-immunoprecipitated Tlg2p was then assessed through immunoblot analysis with α-Tlg2p antibodies.

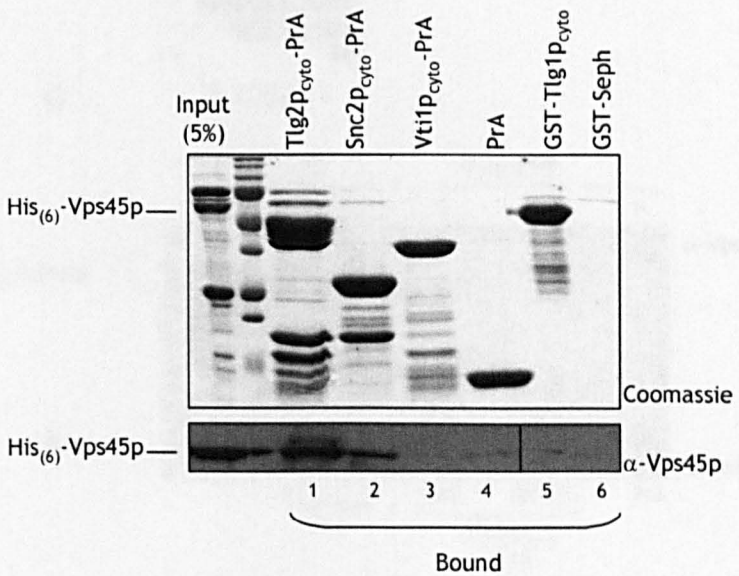

Figure 3.4 Vps45p interacts specifically and directly with both Tlg2p and Snc2p. Plasmids pCOG025, pCOG045, pCOG048, pCOG022, and pGST-Tlg1p were used to recombinantly produce Tlg2p$_{cyto}$-PrA, Snc2p$_{cyto}$-PrA, Vti1p$_{cyto}$-PrA, PrA, and GST-Tlg1p$_{cyto}$. Fusion proteins were immobilised on either IgG-Sepharose or GST-Sepharose, incubated with purified His$_{(6)}$-Vps45p (produced recombinantly from pNB710/pT-GroE), and washed extensively. Bound proteins were eluted, resolved by SDS-PAGE, and either visualised by staining with Coomassie Brilliant Blue (upper panel) or transferred to nitrocellulose membrane and subjected to immunoblot analysis with α-Vps45p antibodies (lower panel).

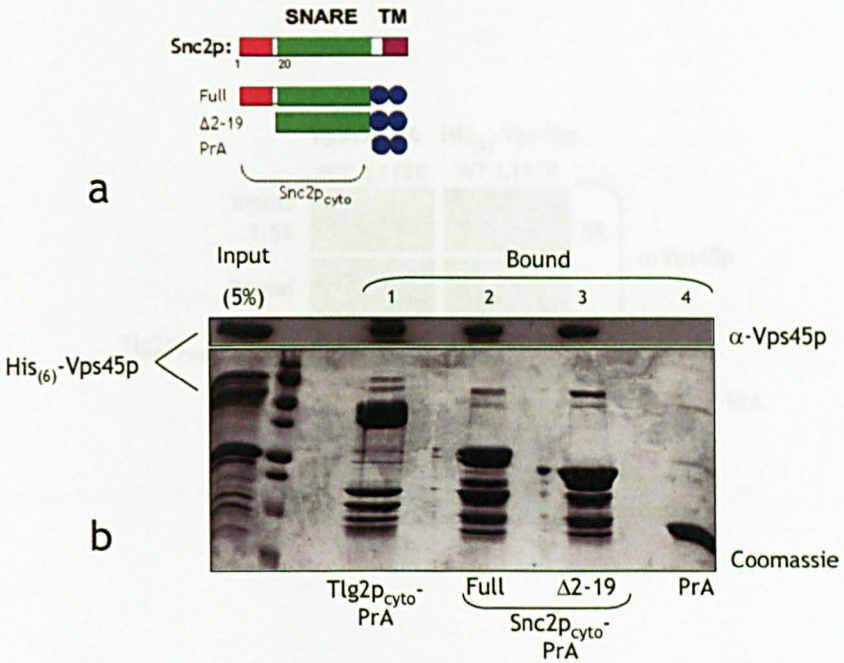

Figure 3.5 Vps45p binds the SNARE motif of Snc2p. a) Schematic diagram of versions of the cytosolic domain of Snc2p-PrA used to map Vps45p binding. b) Plasmids pCOG025, pCOG045, pCOG046, or pCOG022 were used to recombinantly produce Tlg2p$_{cyto}$-PrA, Snc2p$_{cyto}$-PrA, Snc2p$_{cyto}$Δ2-19-PrA or PrA, respectively. Fusion proteins immobilised on IgG-Sepharose beads were incubated with purified His$_{(6)}$-Vps45 (produced recombinantly from pNB710/pT-GroE). Following extensive washing, bound proteins were eluted, resolved by SDS-PAGE, and either visualised by staining with Coomassie Brilliant Blue (bottom panel) or transferred to nitrocellulose membrane and subjected to immunoblot analysis with α-Vps45p antibodies (upper panel).

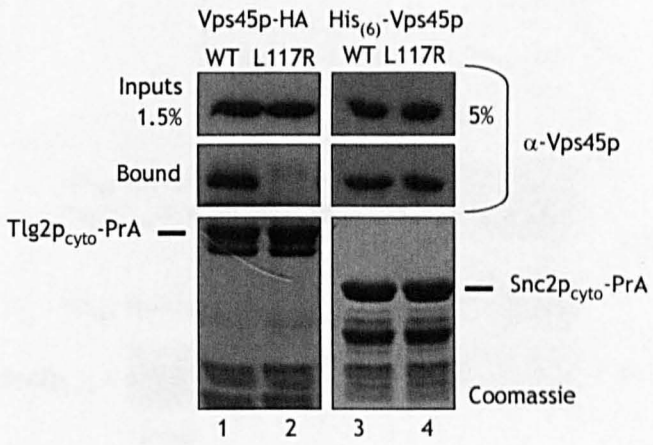

Figure 3.6 Vps45p binds Snc2p and Tlg2p through distinct modes. $Tlg2p_{cyto}$-PrA and $Snc2p_{cyto}$-PrA were produced recombinantly from plasmids pCOG025 and pCOG045; fusion proteins were immobilised on IgG-Sepharose resin. Beads loaded with $Tlg2p_{cyto}$-PrA (left panels) were incubated with either Vps45p-HA or Vps45p(L117R)-HA, provided by lysates from *vps45*Δ cells (LCY008) transformed with either pCOG070 (driving the production of Vps45p-HA) or pCOG071 (driving the production of Vps45p(L117R)-HA). Beads loaded with $Snc2p_{cyto}$-PrA (right panels) were incubated with either purified $His_{(6)}$-Vps45p or $His_{(6)}$-Vps45p(L117R), produced recombinantly from plasmids pNB710/pT-GroE or pCOG067/pT-GroE, respectively. After extensive washing to remove nonspecifically bound proteins, bound proteins were eluted, resolved by SDS-PAGE, and either visualised by staining with Coomassie Brilliant Blue (bottom panels) or transferred to nitrocellulose membrane and subjected to immunoblot analysis with α-Vps45p antibodies (middle panels). Samples of inputs were also analysed by immunoblotting with α-Vps45p antibodies (upper panels).

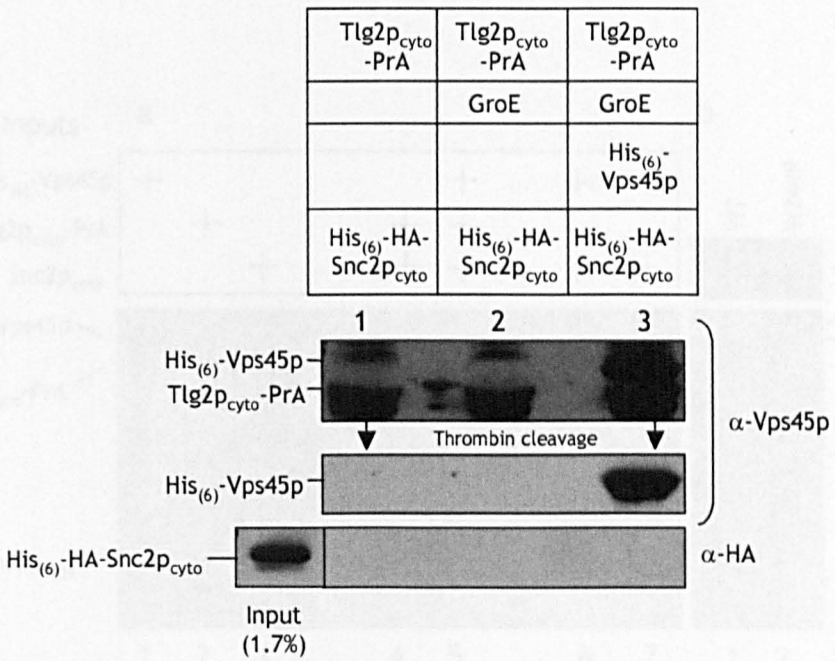

Figure 3.7 Vps45p does not appear to bind Tlg2p and Snc2p simultaneously. a) Lysates containing recombinantly produced proteins were mixed overnight at 4°C in the following combinations: Tlg2p$_{cyto}$-PrA and His$_{(6)}$-HA-Snc2p$_{cyto}$ (lane 1; produced from plasmids pCOG025 and pCOG056), Tlg2p$_{cyto}$-PrA, GroEL/GroES, and His$_{(6)}$-HA-Snc2p$_{cyto}$ (lane 2; produced from plasmids pCOG025, pT-GroE, and pCOG056), or Tlg2p$_{cyto}$-PrA, GroEL/GroES, His$_{(6)}$-Vps45p and His$_{(6)}$-HA-Snc2p$_{cyto}$ (lane 3; produced from plasmids pCOG025, pT-GroE, pNB710, and pCOG056). IgG-Sepharose beads were then added to each mixture and proteins were allowed to bind for 1 hr at 4°C. Following extensive washing to remove nonspecifically bound proteins, bound proteins were eluted from an aliquot of IgG-Sepharose beads with HAc (pH 3.4). Eluted proteins were resolved by SDS-PAGE, transferred to nitrocellulose membrane, and subjected to immunoblot analysis with α-Vps45p antibodies to confirm that His$_{(6)}$-Vps45p was bound to Tlg2p$_{cyto}$-PrA when appropriate (lane 3). The remaining portion of IgG-Sepharose beads was subjected to a thrombin cleavage step to remove Tlg2p$_{cyto}$ (and any associated proteins). Proteins present in the thrombin cleaved supernatant were resolved by SDS-PAGE, transferred to nitrocellulose membrane, and subjected to immunoblot analysis using α-Vps45p and α-HA antibodies (middle and lower panels). To confirm the presence of His$_{(6)}$-HA-Snc2p$_{cyto}$ in the starting lysate mixtures, an aliquot of the original lysate was included alongside the thrombin cleaved supernatants (lower left panel).

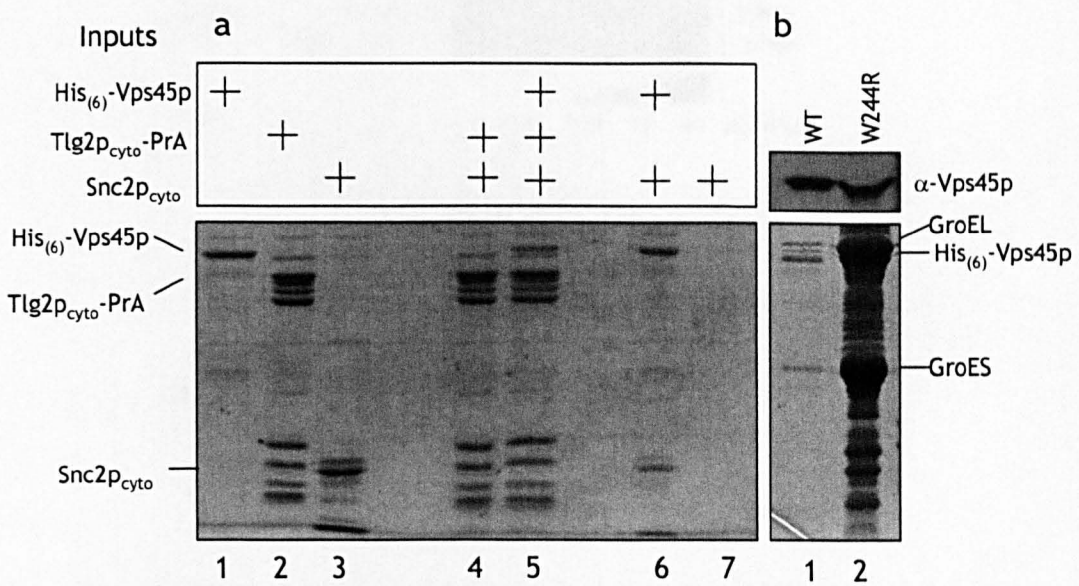

Figure 3.8 Simultaneous binding between Vps45p/Tlg2p/Snc2p is also not observed using purified proteins. a) Plasmids pNB710/pT-GroE, pCOG025/pT-GroE, and pCOG045 were used to recombinantly produce $His_{(6)}$-Vps45p, $Tlg2p_{cyto}$-PrA, and $Snc2p_{cyto}$-PrA, respectively. Fusion proteins were immobilised on the appropriate resins. $His_{(6)}$-Vps45p was eluted with imidazole and dialysed against PBS; $Snc2p_{cyto}$ was liberated from IgG-Sepharose via thrombin cleavage. IgG-Sepharose beads loaded with $Tlg2p_{cyto}$-PrA (~1 nmol) were then incubated simultaneously with either $Snc2p_{cyto}$ alone (lane 4), or both $His_{(6)}$-Vps45p and $Snc2p_{cyto}$ (lane 5). After extensive washing, bound proteins were eluted with HAc, resolved by SDS-PAGE, and visualised by staining with Coomassie Brilliant Blue. As an additional control, $Snc2p_{cyto}$ was incubated either with (lane 6) or without (lane 7) $His_{(6)}$-Vps45p. Excess amounts of Ni-NTA agarose resin were added for the last hour of the binding reactions, after which time bound proteins were eluted with LSB, resolved by SDS-PAGE, and visualised by staining with Coomassie Brilliant Blue. b) Plasmids pNB710/pT-GroE and pCOG068/pT-GroE were used to recombinantly produce $His_{(6)}$-Vps45p and $His_{(6)}$-Vps45p(W244R), respectively. Fusion proteins were recovered on Ni-NTA agarose resin, eluted with LSB, resolved by SDS-PAGE, and either visualised by staining with Coomassie Brilliant Blue (lower panel) or transferred to nitrocellulose membrane and subjected to immunoblot analysis with α-Vps45p antibodies (upper panel).

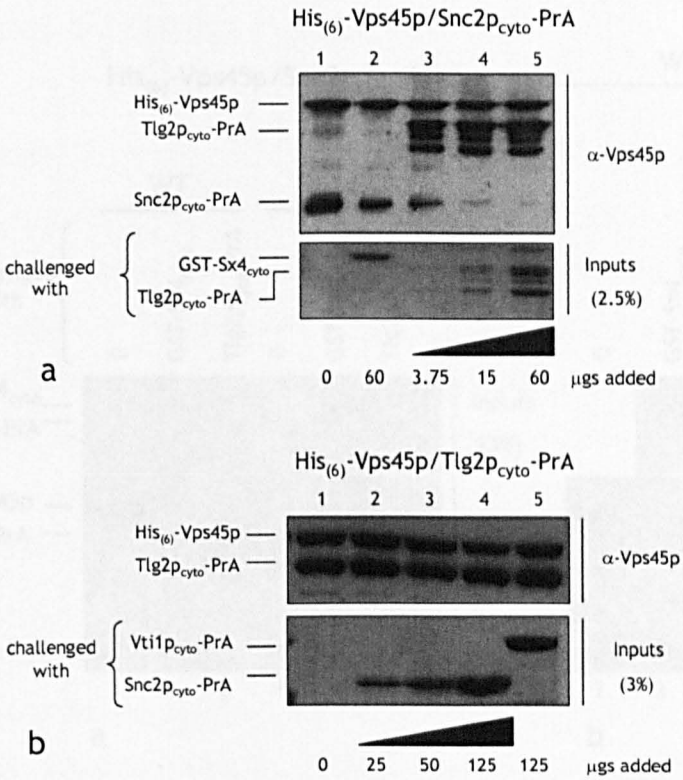

Figure 3.9 Tlg2p displaces Snc2p from Vps45p. Plasmids pNB710/pT-GroE, pCOG025/pT-GroE, pCOG045, and pCOG048 were used to recombinantly produce $His_{(6)}$-Vps45p, $Tlg2p_{cyto}$-PrA, $Snc2p_{cyto}$-PrA, and $Vti1p_{cyto}$-PrA, respectively. Fusion proteins were recovered on the appropriate resins; PrA-tagged SNARE proteins were eluted in 0.5 M HAc (pH 3.4) and dialysed against PBS. When appropriate, $His_{(6)}$-Vps45p was eluted in 250 mM imidazole in PBS and dialysed against PBS. Purified GST-$Sx4_{cyto}$ was kindly provided by Fiona Brandie (University of Glasgow). a) Challenging Vps45p/Snc2p complexes with Tlg2p: $His_{(6)}$-Vps45p and $Snc2p_{cyto}$-PrA were allowed to bind for 16 hrs at 4°C. Binary complexes were recovered in a one hour incubation with Ni-NTA beads, followed by extensive washing with 20 mM imidazole in PBS to remove nonspecifically bound proteins. To attempt to displace bound $Snc2p_{cyto}$-PrA, increasing amounts of either $Tlg2p_{cyto}$-PrA or GST-$Sx4_{cyto}$ (as a negative control) were added to the binding reactions. $His_{(6)}$-Vps45p/$Snc2p_{cyto}$-PrA dimers were challenged with the following: Lane 1, nothing; Lane 2, 60 μgs GST-$Sx4_{cyto}$; Lane 3, 3.75 μgs $Tlg2p_{cyto}$-PrA; Lane 4, 15 μgs $Tlg2p_{cyto}$-PrA; Lane 5, 60 μgs $Tlg2p_{cyto}$-PrA. PBS (to a final volume of 1 ml) was also added to each reaction. After two hours of rotation at 4°C, beads were washed extensively with 20 mM imidazole in PBS. Bound proteins were eluted with LSB, resolved by SDS-PAGE, and transferred to nitrocellulose membrane for immunoblot analysis with α-Vps45p antibodies (upper panel). Samples representing 2.5% of the input of competing proteins were also resolved by SDS-PAGE and visualised by staining with Coomassie Brilliant Blue (lower panel). b) Challenging Vps45p/Tlg2p complexes with Snc2p: Ni-NTA beads loaded with $His_{(6)}$-Vps45p were incubated for ~16 hrs at 4°C with $Tlg2p_{cyto}$-PrA to form binary complexes. Beads were then washed extensively with 20 mM imidazole in PBS to remove nonspecifically bound proteins, before adding increasing amounts of $Snc2p_{cyto}$-PrA or $Vti1p_{cyto}$-PrA (as a negative control). $His_{(6)}$-Vps45p/$Tlg2p_{cyto}$-PrA dimers were challenged with the following: Lane 1, nothing; Lane 2, 25 μgs $Snc2p_{cyto}$-PrA; Lane 3, 50 μgs $Snc2p_{cyto}$-PrA; Lane 4, 125 μgs $Snc2p_{cyto}$-PrA; Lane 5, 125 μgs $Vti1p_{cyto}$-PrA. PBS (to a final volume of 1 ml) was also added to each reaction. After ~16 hours of rotation at 4°C, beads were washed extensively with 20 mM imidazole in PBS. Bound proteins were eluted with LSB, resolved by SDS-PAGE, and transferred to nitrocellulose membrane for immunoblot analysis with α-Vps45p antibodies (upper panel). Samples representing 3% of the input of competing proteins were also resolved by SDS-PAGE and visualised by staining with Coomassie Brilliant Blue (lower panel).

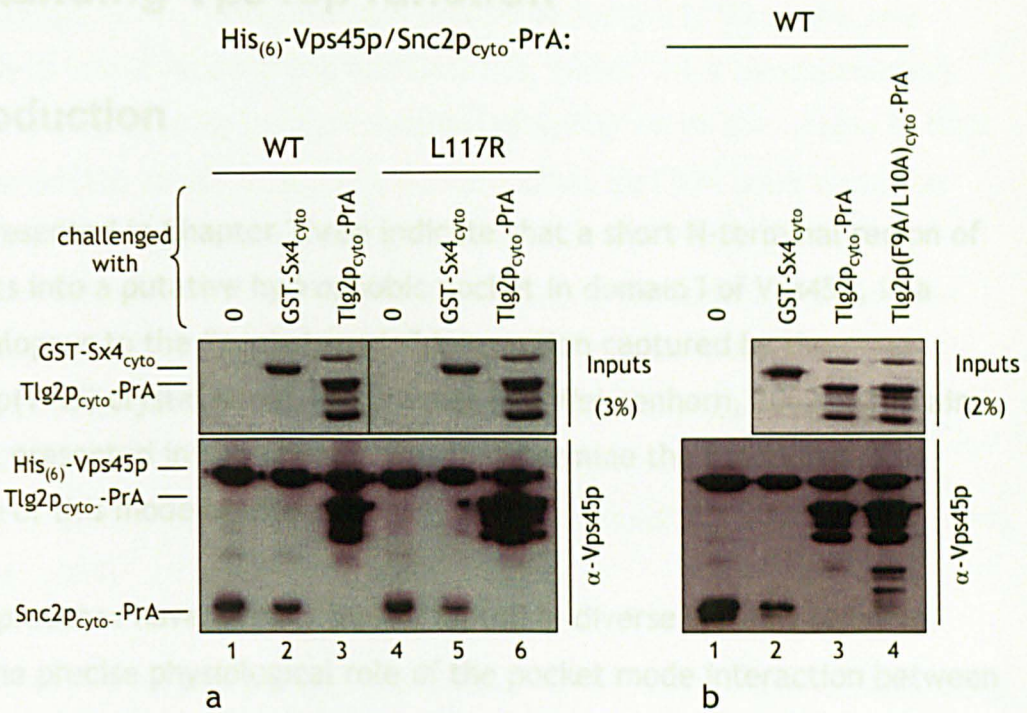

Figure 3.10 The displacement of Snc2p from Vps45p is not facilitated via the pocket mode interaction between Vps45p and Tlg2p. Plasmids pNB710/pT-GroE, pCOG067/pT-GroE, pCOG025/pT-GroE, and pCOG076/pT-GroE were used to recombinantly produce $His_{(6)}$-Vps45p, $His_{(6)}$-Vps45p(L117R), $Tlg2p_{cyto}$-PrA, and $Tlg2p(F9A/L10A)_{cyto}$-PrA, respectively. Fusion proteins were immobilised on the appropriate resins; PrA-tagged SNARE proteins were eluted with 0.5 M HAc (pH 3.4) and dialysed against PBS, while $His_{(6)}$-Vps45p and $His_{(6)}$-Vps45p(L117R) were eluted in 250 mM imidazole in PBS and dialysed against PBS. Purified $GST\text{-}Sx4_{cyto}$ was kindly provided by Fiona Brandie (University of Glasgow). $His_{(6)}$-Vps45p (WT or L117R) and $Snc2p_{cyto}$-PrA were allowed to bind for 16 hrs at 4°C. Binary complexes were recovered through a one hour incubation with Ni-NTA beads, followed by extensive washing with 20 mM imidazole in PBS to remove unbound proteins.

a) To attempt to displace $Snc2p_{cyto}$-PrA from $His_{(6)}$-Vps45p and $His_{(6)}$-Vps45p(L117R), ~50 μgs of either $GST\text{-}Sx4_{cyto}$ (as a negative control) or $Tlg2p_{cyto}$-PrA were added to Ni-NTA beads loaded with the appropriate complexes. PBS was also added to each reaction for a final volume of 1 ml. After two hours of rotation at 4°C to allow displacement to occur, beads were washed extensively with 20 mM imidazole in PBS. Bound proteins were then eluted in LSB, resolved by SDS-PAGE, and transferred to nitrocellulose membrane prior to immunoblot analysis with α-Vps45p antibodies (lower panel). Lane 1: $His_{(6)}$-Vps45p/$Snc2p_{cyto}$-PrA with no competing protein, Lane 2: $His_{(6)}$-Vps45p/$Snc2p_{cyto}$-PrA plus $GST\text{-}Sx4_{cyto}$, Lane 3: $His_{(6)}$-Vps45p/$Snc2p_{cyto}$-PrA plus $Tlg2p_{cyto}$-PrA, Lane 4: $His_{(6)}$-Vps45p(L117R)/$Snc2p_{cyto}$-PrA with no competing protein, Lane 5: $His_{(6)}$-Vps45p(L117R)/$Snc2p_{cyto}$-PrA plus $GST\text{-}Sx4_{cyto}$, Lane 6: $His_{(6)}$-Vps45p(L117R)/$Snc2p_{cyto}$-PrA plus $Tlg2p_{cyto}$-PrA. Samples representing 3% of the input of competing protein were resolved by SDS-PAGE and visualised by staining with Coomassie Brilliant Blue (upper panel).

b) The same as (a), except ~40 μgs of either $GST\text{-}Sx4_{cyto}$, $Tlg2p_{cyto}$-PrA, or $Tlg2p(F9A/L10A)_{cyto}$-PrA were added to Ni-NTA beads loaded with $His_{(6)}$Vps45p/$Snc2p_{cyto}$-PrA complexes; displacement reactions were allowed to occur for ~16 hours at 4°C. Lane 1: $His_{(6)}$-Vps45p/$Snc2p_{cyto}$-PrA with no competing protein, Lane 2: $His_{(6)}$-Vps45p/$Snc2p_{cyto}$-PrA plus $GST\text{-}Sx4_{cyto}$, Lane 3: $His_{(6)}$-Vps45p/$Snc2p_{cyto}$-PrA plus $Tlg2p_{cyto}$-PrA, Lane 4: $His_{(6)}$-Vps45p/$Snc2p_{cyto}$-PrA plus $Tlg2p(F9A/L10A)_{cyto}$-PrA. Samples representing 2% of the input of competing protein were resolved by SDS-PAGE and visualised by staining with Coomassie Brilliant Blue (upper panel).

Chapter Four: A genetic approach to understanding Vps45p function

4.1 Introduction

The data presented in Chapter Three indicate that a short N-terminal region of Tlg2p inserts into a putative hydrophobic pocket in domain I of Vps45p, in a manner analogous to the "pocket mode" interaction captured by the Sly1p/Sed5p(1-45) crystal structure (Bracher and Weissenhorn, 2002). The aim of the work presented in this chapter was to determine the functional significance of this mode of interaction.

Multiple approaches have already been adopted in diverse systems to try to elucidate the precise physiological role of the pocket mode interaction between SM proteins and their cognate syntaxins. These studies have yielded conflicting conclusions. In African green monkey kidney (Vero) cells, the production of an N-terminal fragment of syntaxin 5 (the mammalian homologue of Sed5p) resulted in disruption of the structure of the Golgi complex (Yamaguchi *et al.*, 2002). This was interpreted as resulting from nonproductive saturation of the syntaxin 5 binding sites in the hydrophobic pocket of Sly1 by the N-terminal fragment of syntaxin 5 (Yamaguchi *et al.*, 2002). This study suggested that Sly1 executes at least one of its functions via the pocket mode of interaction with syntaxin 5. In another study, fusion measured by an *in vitro* assay designed to reconstitute ER-to-Golgi transport was strongly inhibited when Fab fragments derived from either α-rsly1 antibodies, or a monoclonal antibody raised against the SNARE motif of syntaxin 5, were added (Williams *et al.*, 2004). In addition, transport was also inhibited when a recombinantly produced N-terminal fragment of syntaxin 5 (residues 1-43) was added to the *in vitro* assay (Williams *et al.*, 2004). Together, these data suggested that blocking the pocket mode of rsly1/syntaxin 5 interaction inhibited membrane fusion, again implying a physiological role for this mode.

In contrast to the above, work in yeast has suggested that SM proteins need not interact with their cognate syntaxins via the pocket mode in order to function. One study utilised mutant versions of the SM protein Sly1p which are unable to

bind its cognate syntaxin Sed5p via the pocket mode, including one harbouring an L137R point mutation, Sly1p(L137R). Although Sly1p is essential for cell viability (Dascher *et al.*, 1991), a strain producing Sly1p(L137R) as the sole source of Sly1p is still viable (Peng and Gallwitz, 2004). As a complementary approach in the same study, mutant versions of Sed5p which are unable to bind Sly1p via the pocket mode, including one harbouring an F10A point mutation [Sed5p(F10A)], were generated. Sed5p is also required for cell growth (Hardwick and Pelham, 1992), and a strain producing Sed5p(F10A) as the sole source of Sed5p exhibited no obvious defects with respect to cell growth, viability, or the trafficking of carboxypeptidase Y and invertase (Peng and Gallwitz, 2004). This study concluded that the pocket mode of interaction between Sly1p and Sed5p is dispensable for the functions of these proteins (Peng and Gallwitz, 2004).

In Chapter Three, a version of Vps45p analogous to Sly1p(L137R), Vps45p(L117R) (harbouring a pocket filling mutation and unable to interact with its cognate syntaxin Tlg2p), was characterised (Figures 3.2 and 3.3). The aim of the work presented in this chapter was to functionally analyse Vps45p(L117R), with the ultimate goal of understanding the precise physiological role of the pocket mode of interaction between Vps45p and Tlg2p.

4.2 Results

4.2.1 Vps45p(L117R) can perform the function of wild-type Vps45p-HA with respect to CPY sorting

As mentioned above, previous work performed in yeast utilised point mutations to disrupt the interaction between an SM protein and its cognate syntaxin (Peng and Gallwitz, 2004). The L137R mutation in Sly1p abolished the Sly1p/Sed5p interaction as determined by *in vitro* pull down assays; somewhat surprisingly, cells producing Sly1p(L137R) as the sole source of the essential protein Sly1p were still viable (Peng and Gallwitz, 2004). This study concluded that Sly1p(L137R) was fully functional; however, these data should be interpreted with the caveat that if Sly1p performs multiple functions, Sly1p(L137R) may be able to perform the essential function of Sly1p, yet be defective in non-essential

functions which manifest themselves in a subtle phenotype not examined in this study.

A similar point mutation (L117R) in Vps45p severely abrogated its interaction with Tlg2p (Figures 3.2 and 3.3). To investigate whether interaction with Tlg2p via the pocket mode was required for Vps45p to perform its function in the *VPS* pathway, the ability of Vps45p(L117R)-HA to sort the vacuolar hydrolase carboxypeptidase Y (CPY) to the vacuole was examined. The trafficking of CPY has been extremely well characterised, making it an ideal marker protein to monitor the integrity of trafficking through the *VPS* pathway. CPY undergoes oligosaccharide modifications in the ER and Golgi, generating its precursor form p2CPY, before being redirected out of the secretory pathway and into the *VPS* pathway at the *trans*-Golgi network (TGN) (Bryant and Stevens, 1998). p2CPY is delivered to the vacuole via the endosomal system and undergoes proteolytic cleavage to generate its mature, active form, mCPY (Bryant and Stevens, 1998). Vps45p regulates transport through the endosomal system (Rothman and Stevens, 1986), and like other class D *vps* mutants (Raymond *et al.*, 1992), *vps45*Δ cells are defective in their sorting of CPY to the vacuole. Approximately 75-85% of the total CPY in *vps45*Δ cells fails to be diverted from the secretory pathway, and is secreted into the extracellular media as its Golgi-modified precursor, p2CPY (Cowles *et al.*, 1994; Piper *et al.*, 1994).

To assess the abilities of Vps45p-HA and Vps45p(L117R)-HA to complement the CPY sorting defect of *vps45*Δ cells, the amount of CPY present in the extracellular media of the appropriate strains was assessed using immunoblot analysis. As shown in Figure 4.1, wild-type cells secreted little, if any, CPY (lane 5). In contrast to wild-type cells, *vps45*Δ cells secreted a detectable amount of CPY (lane 6). The C-terminal HA tag did not interfere with Vps45p-HA function, since Vps45p-HA complemented the CPY sorting defect of *vps45*Δ cells when produced at either 2μ or *CEN* levels, (demonstrated by a lack of secreted CPY in lane 1: upper panel, 2μ; lower panel, *CEN*). Importantly, Vps45p(L117R)-HA also complemented the CPY sorting defect of *vps45*Δ cells when produced at both 2μ and *CEN* levels (demonstrated by the lack of detectable CPY in lane 3: upper panel, 2μ; lower panel, *CEN*). In addition, *vps45*Δ cells producing Vps45p(L117R)-HA processed CPY normally, as assessed by pulse-chase immunoprecipitation experiments (Carpp *et al.*, 2006). Together, these results

suggest that although Vps45p(L117R)-HA is severely impaired in its ability to interact with Tlg2p (Figures 3.2 and 3.3), it is still able to perform the function of the wild-type protein with respect to the trafficking of CPY to the vacuole.

Although this finding is consistent with previous work in yeast (Peng and Gallwitz, 2004), it conflicts with work in mammalian systems which suggested that disruption of the pocket mode of interaction between SM proteins and their cognate syntaxins affects membrane trafficking (Williams *et al.*, 2004; Yamaguchi *et al.*, 2002). It is worth noting that these latter studies perturbed the pocket mode interaction either through the production of an N-terminal portion of the syntaxin *in vivo* (Yamaguchi *et al.*, 2002) or the addition of a similar fragment (produced recombinantly) to an *in vitro* assay system (Williams *et al.*, 2004); this was in contrast to the work in yeast, which was performed in strains whose sole versions of the SM protein (or syntaxin) were unable to undertake the pocket mode interaction. It may be insightful to investigate the yeast system via the same approach as that used to investigate the mammalian system; that is, overproduce fragments consisting of the first N-terminal 36 residues of Tlg2p and/or domain I of Vps45p *in vivo*, and assess the effects (if any) on CPY processing. As an alternative explanation for the discrepancy between the yeast and mammalian data, additional compensatory mechanisms may exist in yeast by which SM proteins can perform their function(s), which have been lost throughout evolution.

4.2.2 Overproduction of Vps45p(W244R) confers a dominant negative effect on CPY sorting

Considering that the pocket mode interaction between Vps45p and Tlg2p is of high affinity (Bryant and James, 2001; Nichols *et al.*, 1998), it was surprising that the pocket filled version of Vps45p exhibited no observable functional defects. With the goal of generating additional tools for understanding the role(s) performed by Vps45p, a screen designed to isolate dominant negative versions of Vps45p was performed by Alan Boyd and Leonora Ciufo (University of Liverpool). One such version created in this screen harbours a single point mutation, W244R. Overproduction of Vps45p(W244R) in the presence of endogenous Vps45p was found to confer a dominant negative effect with respect to the sorting of CPY to the vacuole, as assessed by a filter overlay assay.

To confirm this result, the presence of CPY in the extracellular media of strains producing either Vps45p-HA, or a version harbouring the W244R mutation, was investigated using immunoblot analysis. The results from this experiment are shown in Figure 4.2a. Once again, wild-type cells secreted little, if any, CPY (lane 3) while *vps45*Δ cells secreted a detectable amount of CPY (lane 4). The overproduction of Vps45p-HA itself in wild-type cells was not detrimental (demonstrated by the lack of CPY in lane 1). The overproduction of Vps45p(W244R)-HA in wild-type cells, however, had a dominant negative effect on CPY sorting (demonstrated by the presence of CPY in lane 2). Consistent with Vps45p(W244R)-HA being a dysfunctional version of the protein, it was unable to complement the CPY sorting defect of *vps45*Δ cells (see lane 2, Figure 4.1; upper panel 2μ, lower panel *CEN*).

As a second approach to investigate the effects of overproduction of Vps45p(W244R)-HA on CPY sorting, a pulse-chase experiment following the fate of newly synthesized CPY containing radiolabelled methionine-S^{35} was performed in collaboration with Nia Bryant. This approach provided more information than the TCA precipitation approach, because the pulse-chase experiment assessed the presence of CPY in both internal and external fractions, and followed the maturation of CPY into its processed forms. The results of this experiment are also shown in Figure 4.2. Following 5 minutes of pulse labelling and a chase period of 30 minutes, the majority (>95%) of the CPY in wild-type cells was found in its properly processed form in the intracellular fraction (4.2b), whereas the majority (~80%) of the CPY in *vps45*Δ cells was found in its unprocessed form in the extracellular fraction (4.2e). This observation is consistent with previous reports that *vps45*Δ cells missort 75-85% of their newly synthesised CPY (Cowles *et al.*, 1994; Piper *et al.*, 1994). Consistent with the data presented in Figure 4.2a, overproduction of Vps45p(W244R)-HA from a multicopy (2μ) plasmid resulted in the secretion of CPY, with ~60% of the total CPY found in its unprocessed form in the extracellular fraction (4.2c).

Production of Vps45p(W244R)-HA at *CEN* levels did not confer missorting of CPY (Carpp *et al.*, 2006), suggesting that the mutant protein needs to be present in excess relative to the wild-type protein in order to interfere with its function. To test this hypothesis, a second multicopy (2μ) plasmid driving the overproduction of wild-type Vps45p-HA was introduced into cells already

overproducing Vps45(W244R)-HA, and the ability of this strain to process CPY was examined in the same pulse-chase experiment. The data in Figure 4.2 show that the CPY missorting defect exhibited by a strain overproducing Vps45p(W244R)-HA is rescued by the simultaneous overproduction of wild-type Vps45p-HA, with ~95% of the total CPY properly processed and in the intracellular fraction under this condition (4.2d). The titration of the detrimental effect on CPY sorting conferred by overproduction of Vps45p(W244R)-HA by an increased dosage of the wild-type protein identifies the mutant protein as an antimorph; a competitive inhibitor to the wild-type protein. A possible mechanism of action of an antimorph is to sequester (a) downstream effector(s) in non-productive complexes, resulting in the accumulation of an intermediate. This mechanism is in contrast to the mechanisms of other classes of mutant proteins, such as neomorphs, which have acquired (a) novel or altered function(s). Based on this finding, it was hypothesised that this dominant negative version of Vps45p, Vps45p(W244R)-HA, interferes with the function of wild-type Vps45p by binding to its effectors and forming a non-productive complex which is likely a *bona fide* physiological intermediate.

4.2.3 The W244R mutation does not affect Vps45p binding to Tlg2p

As a first step towards characterising Vps45p(W244R)-HA, the ability of the mutant protein to bind Tlg2p was assessed. Since W244 is not one of the residues that constitute the hydrophobic pocket of Vps45p (Bracher and Weissenhorn, 2002), the W244R mutation was predicted not to affect the pocket mode interaction between Vps45p and Tlg2p. The data presented in Figure 4.3 show that Vps45p-HA and Vps45p(W244R)-HA, provided by yeast lysates, exhibit no observable differences with respect to their binding to the cytosolic domain of Tlg2p ($Tlg2p_{cyto}$-PrA; see Figure 3.1) immobilised on IgG-Sepharose (lanes 1 and 3). These data indicate that the W244R mutation does not affect the interaction between Vps45p and Tlg2p facilitated through the pocket mode, which was described in Chapter Three.

The data presented in Figure 4.3 raised the possibility that the W244R mutation locks Vps45p in a conformation favouring an alternative mode of binding to

Tlg2p, i.e. distinct from the pocket mode. Some evidence exists to suggest that SM proteins are capable of conformational changes; structural studies of the N-terminal domain of the mammalian SM protein, rSly1, have revealed that it undergoes a conformational change upon binding of syntaxin 5, which potentially alters the overall conformation of rSly1 (Arac *et al.*, 2005). In addition, the determination of several crystal forms of unliganded sSec-1 revealed that the region between domains 1 and 2 potentially act as a hinge, around which domain 1 rotates (Bracher and Weissenhorn, 2001). Therefore, the W244R mutation may interfere with the ability of Vps45p to undergo a conformational change, so that the mutant protein is locked in a conformation favouring an alternative mode of interaction with Tlg2p. To test this hypothesis, the ability of Vps45p(W244R)-HA to bind to $Tlg2p_{cyto}\Delta N36$-PrA was examined, since Vps45p-HA cannot bind this version of Tlg2p via the pocket mode (Figure 3.1). The results from this experiment are presented in Figure 4.3. Like the wild-type version of Vps45p-HA, Vps45p(W244R)-HA did not bind $Tlg2p_{cyto}\Delta N36$-PrA (lanes 1 and 3). These data suggest that if Vps45p interacts with monomeric Tlg2p in a second mode, i.e. distinct from the pocket mode, the W244R mutation does not lock Vps45p in an alternative conformation that favours this mode of interaction.

4.2.4 The L117R mutation severely abrogates the binding of Vps45p(W244R) to Tlg2p

With the aim of gaining insight into its mechanism of action, the L117R mutation was introduced into Vps45p(W244R)-HA by Leonora Ciufo (University of Liverpool). Based on the data presented in Figures 3.2 and 3.3, the introduction of the L117R mutation was predicted to remove the ability of Vps45p(W244R)-HA to bind Tlg2p via the pocket mode. The rationale behind this experiment was that the dominant negative version of Vps45p might accumulate an intermediate at some stage of the SNARE cycle which would reveal a role for the pocket mode of interaction between Vps45p and Tlg2p. To test this prediction, recombinantly produced $Tlg2p_{cyto}$-PrA, which was previously demonstrated to capture wild-type Vps45p-HA from a yeast lysate (Figure 3.1), was used to investigate the binding properties of Vps45p(L117R/W244R)-HA. The data presented in Figure 4.3 show that despite the slightly elevated (~two fold) levels of Vps45p(L117R/W244R)-HA compared to wild-type Vps45p-HA in the respective input lysates, no Vps45p(L117R/W244R)-HA bound $Tlg2p_{cyto}$-PrA, in contrast to the wild-type

version of Vps45p-HA, which bound $Tlg2p_{cyto}$-PrA robustly (lane 4 vs. lane 1). This finding affirms the prediction that the L117R mutation would abolish the ability of the dominant negative version of Vps45p to bind Tlg2p.

4.2.5 The L117R mutation removes the ability of Vps45p(W244R) to exert its dominant negative effect on CPY sorting

Having established that Vps45p(L117R/W244R)-HA does not bind $Tlg2p_{cyto}$-PrA (Figure 4.3), its ability to exert a dominant negative effect on CPY sorting was examined. Once again, the amounts of CPY present in the extracellular media of strains overproducing Vps45p-HA, and mutants thereof, were assessed using immunoblot analysis. The results of a typical experiment are shown in Figure 4.4. In contrast to cells overproducing Vps45p(W244R)-HA, which secreted CPY (lane 2), cells overproducing Vps45p(L117R/W244R)-HA secreted little, if any, CPY (lane 4). The inability of Vps45p(L117R/W244R)-HA to interfere with CPY sorting when overproduced in wild-type cells, coupled with its inability to bind $Tlg2p_{cyto}$-PrA (Figure 4.2), suggest that Vps45p(W244R)-HA exerts its dominant negative effect after binding to Tlg2p via the hydrophobic pocket mode. This interpretation confirms the data presented in Figure 3.3, which suggest that Vps45p associates *in vivo* with Tlg2p via the hydrophobic pocket mode of interaction. More importantly, however, it demonstrates that this interaction has a functional role, in agreement with studies in mammalian systems (Williams *et al.*, 2004; Yamaguchi *et al.*, 2002).

4.2.6 The W244R mutation does not affect Vps45p binding to Snc2p

In Chapter Three, Vps45p was demonstrated to interact directly and specifically with both its cognate syntaxin, Tlg2p, and its cognate v-SNARE, Snc2p (Figure 3.4). Since Vps45p(W244R)-HA did not exhibit any observable differences from the wild-type protein with respect to its ability to bind to Tlg2p, and with the aim of further characterising the mutant protein, the ability of Vps45p(W244R)-HA to bind to Snc2p was investigated. The data presented in Figure 4.5 indicate that both Vps45p-HA and Vps45p(W244R)-HA, provided by yeast lysates, bind the cytosolic domain of Snc2p ($Snc2p_{cyto}$-PrA; see Figure 3.5) similarly (lanes 1 and 2). Neither Vps45p-HA nor Vps45p(W244R)-HA bound to the PrA moiety alone.

4.2.7 The dominant negative effect on CPY sorting conferred by Vps45p(W244R) is rescued by overproduction of Snc2p

To further test the hypothesis that Vps45p(W244R)-HA acts through the accumulation of a normal physiological intermediate, the ability of overproduction of Snc2p to suppress the dominant negative effect conferred by Vps45p(W244R)-HA was examined. The rationale behind this experiment was that Vps45p(W244R)-HA may interact normally with Snc2p, but fail to perform some subsequent function, resulting in the accumulation of non-functional intermediates which sequester Snc2p away from endogenous Vps45p. Overproduction of Snc2p would therefore be predicted to alleviate the dominant negative effect of Vps45p(W244R)-HA by making Snc2p available to endogenous Vps45p. To test this hypothesis, the amounts of CPY present in the extracellular media of the appropriate strains were once again examined (Figure 4.6a). As expected, wild-type cells secreted little, if any, CPY (lane 1) while *vps45*Δ cells secreted a detectable amount of CPY (lane 2). The dominant negative effect caused by overproduction of Vps45p(W244R)-HA was again demonstrated by the presence of CPY in lane 3. Importantly, cells overproducing both Vps45p(W244R)-HA and an HA-tagged version of Snc2p secreted little, if any, CPY (lane 4). This result suggests that Vps45p(W244R)-HA acts through the accumulation of a *bona fide* physiological intermediate, as its effects can be suppressed by the overexpression of a relevant SNARE protein.

To investigate whether this suppression specifically resulted from overproduction of Snc2p, or whether it was a general effect conferred by increased levels of any SNARE protein, the effect of overproduction of Tlg2p in a strain overproducing Vps45p(W244R)-HA was examined. Figure 4.6 shows an experiment performed in collaboration with Nia Bryant, in which the fate of newly synthesised CPY containing radiolabelled methionine-S^{35} was examined in various strains. Following 5 minutes of pulse labelling and a chase period of 30 minutes, the majority (>95%) of the CPY in wild-type cells was found in its properly processed form in the intracellular fraction (4.6b), whereas the majority (~80%) of the CPY in *vps45*Δ cells was found in its unprocessed form in the extracellular fraction (4.6f). Consistent with the data presented in Figure 4.2, overproduction of Vps45p(W244R)-HA resulted in the secretion of CPY, with ~60% of the total CPY found in its unprocessed form in the extracellular fraction

(4.6c). Simultaneous overproduction of HA-Snc2p rescued the CPY missorting defect associated with overproduction of Vps45p(W244R)-HA, with ~90% of the total CPY now properly processed and in the intracellular fraction (4.6d), consistent with the data shown in Figure 4.6a. Importantly, the CPY missorting defect associated with overproduction of Vps45p(W244R)-HA could not be alleviated by simultaneous overproduction of HA-Tlg2p; under these conditions, ~40% of the total CPY remained in its unprocessed form and was found in the extracellular fraction (4.6e). These results suggest that Vps45p(W244R)-HA specifically sequesters the v-SNARE Snc2p in a non-productive manner.

One possible explanation for the manner by which Vps45p(W244R)-HA sequesters Snc2p is that the mutant protein has a higher affinity for Snc2p, outcompeting endogenous Vps45p for Snc2p. Although no observable differences between the binding of Vps45p-HA and Vps45p(W244R)-HA (provided by yeast lysates) to recombinantly produced $Snc2p_{cyto}$-PrA were observed (Figure 4.5), it is worth noting that endogenous Snc2p would also have been present in the yeast lysates. Therefore, some Vps45p-HA (or the W244R version) may have been complexed with Snc2p in the lysate, making this population of Vps45p-HA (or the W244R version) unable to bind the immobilised $Snc2p_{cyto}$-PrA. To address this possibility, it was aimed to examine the binding of recombinantly produced $His_{(6)}$-Vps45p and $His_{(6)}$-Vps45p(W244R) to $Snc2p_{cyto}$-PrA; however, $His_{(6)}$-Vps45p(W244R) was difficult to purify. Figure 3.8b shows equal amounts of purified $His_{(6)}$-Vps45p (lane 1) and $His_{(6)}$-Vps45p(W244R) (lane 2) as assessed by immunoblot analysis with α-Vps45p antibodies (upper panel). Significantly more of the chaperone proteins GroEL and GroES were found complexed with $His_{(6)}$-Vps45p(W244R) than with wild-type $His_{(6)}$-Vps45p, probably due to misfolding of the mutant protein. In addition, several bands corresponding to degradation products of $His_{(6)}$-Vps45p(W244R) were visible after staining with Coomassie Brilliant Blue; this is probably also due to misfolding of the mutant protein, which makes it a better substrate for proteolytic degradation. Protease inhibitors were included in the buffers used in the purification of $His_{(6)}$-Vps45p(W244R), but were unable to remedy this problem. One goal of future work is to optimise the purification of $His_{(6)}$-Vps45p(W244R), in order to compare its affinity for $Snc2p_{cyto}$-PrA with that of wild-type $His_{(6)}$-Vps45p for $Snc2p_{cyto}$-PrA.

The hypothesis that Vps45p(W244R)-HA sequesters Snc2p away from wild-type Vps45p could also be tested with respect to other transport pathways, in addition to the work performed on the *VPS* pathway (Figure 4.6). Snc2p is also required (along with its functionally redundant partner, Snc1p) for the fusion of secretory vesicles with the plasma membrane (Protopopov *et al.*, 1993); therefore, *snc1*Δ *snc2*Δ cells either exhibit severe defects in both growth and secretion (Protopopov *et al.*, 1993), or are inviable (Gurunathan *et al.*, 2000). If Vps45p(W244R)-HA does sequester Snc2p away from endogenous Vps45p, the reduced availability of Snc2p to the secretory pathway may confer growth and/or secretory defects; the growth and/or invertase secretion of a strain producing Vps45p(W244R)-HA could be examined to test this hypothesis. Preliminary observations of cells producing Vps45p(W244R)-HA indicate that their growth is slightly impaired on solid and in liquid medium; to quantify this observation, growth curves examining the effect of Vps45p(W244R)-HA production on growth rate could be generated.

4.2.8 Tlg2p displaces Snc2p from Vps45p(W244R)

In the light of the finding that Snc2p acts as a suppressor of the dominant negative effect conferred by Vps45p(W244R)-HA (Figure 4.6), it was hypothesised that this version of Vps45p sequesters Snc2p in a non-productive complex. Since Snc2p can be displaced from Vps45p by Tlg2p (Figure 3.9), Vps45p(W244R)-HA may be defective in this mechanism and physically bridge both SNAREs as a non-functional intermediate. To test this hypothesis, the ability of $Tlg2p_{cyto}$-PrA to displace bound $Snc2p_{cyto}$-PrA from $His_{(6)}$-Vps45p(W244R) was investigated. Figure 4.7 shows that $Tlg2p_{cyto}$-PrA displaced all $Snc2p_{cyto}$-PrA from $His_{(6)}$-Vps45p (while GST-$Sx4_{cyto}$, a negative control, did not); this finding was consistent with the data presented in Figure 3.9. Similar results were obtained when $Tlg2p_{cyto}$-PrA was added to $Snc2p_{cyto}$-PrA/$His_{(6)}$-Vps45p(W244R) complexes. In this case, $Tlg2p_{cyto}$-PrA displaced nearly all $Snc2p_{cyto}$-PrA from $His_{(6)}$-Vps45p(W244R) (GST-$Sx4_{cyto}$, again used as a negative control, only displaced a small amount of $Snc2p_{cyto}$-PrA). This suggests that the W244R mutation does not interfere with the mechanism of displacement of Snc2p from Vps45p by Tlg2p. Note that $His_{(6)}$-Vps45p(W244R) migrates at a slightly different molecular weight than does $His_{(6)}$-Vps45p; this may be due to the increased levels of GroEL in the $His_{(6)}$-Vps45p(W244R) preparation (see Figure 3.8b).

To further examine the possibility that Vps45p(W244R) bridges Snc2p and Tlg2p non-productively, the ability of Vps45p(W244R) to bind both SNAREs simultaneously was investigated. Although no Tlg2p/Vps45p/Snc2p complexes were observed in previous experiments (Figures 3.7 and 3.8), such a bridging intermediate might only occur transiently and/or be of low affinity, making such a complex difficult to detect. If Vps45p(W244R) accumulates bridging intermediates, it may make the detection of Vps45p/Tlg2p/Snc2p complexes easier. However, the instability of recombinantly produced $His_{(6)}$-Vps45p(W244R), as previously discussed, complicated this experiment. Furthermore, several degradation products of $His_{(6)}$-Vps45p(W244R) migrated at similar molecular weights to $Snc2p_{cyto}$ (Figure 3.8), making $His_{(6)}$-Vps45p(W244R) difficult to utilise in a bridging experiment similar to the one presented in Figure 3.8a.

4.2.9 Vps45p interacts with SNARE complexes via two modes

Since no evidence was found to suggest that Vps45p(W244R)-HA binds the two individual SNARE proteins with which Vps45p interacts (Tlg2p and Snc2p) any differently than wild-type Vps45p (Figure 4.3 and 4.5), the binding of Vps45p(W244R)-HA to another candidate, the SNARE complex, was investigated. Vps45p has previously been shown to interact with *cis*-complexes (Bryant and James, 2003); however, this interaction had not yet been characterised.

4.2.9.1 Recombinant production of SNARE complexes

To characterise the binding of Vps45p to assembled complexes, a protocol to produce these complexes *in vitro* was developed. Constructs were created to produce, as recombinant proteins, three versions of the cytosolic domain of Tlg2p (full, ΔN36, and ΔN230; see section 3.2.1), along with the cytosolic domains of its cognate SNARE partners Tlg1p, Vti1p, and Snc2p (with the latter harbouring an N-terminal $His_{(6)}$- tag). As illustrated in Figure 4.8a, assembled complexes were produced and purified in a four step process: 1) co-production of all four fusion proteins in *E. coli*, 2) purification via the PrA tag by incubating bacterial lysate with IgG-Sepharose resin, 3) thrombin cleavage to remove the PrA tag from $Tlg2p_{cyto}$, 4) purification via the $His_{(6)}$ tag by incubating the thrombin cleaved supernatant with Ni-NTA resin. This strategy was designed for

the specific purification of quaternary complexes, free from monomers and partially assembled complexes, which would also have been recovered in a single-tag purification strategy. Figure 4.8b compares the products recovered after step 3 (thrombin cleavage; T) and step 4 (incubation with Ni-NTA resin; Ni-NTA) in the purification of complexes containing all three versions of $Tlg2p_{cyto}$ (Full, lanes 1 and 2; ΔN36, lanes 3 and 4; ΔN230, lanes 5 and 6). All three truncations of $Tlg2p_{cyto}$ formed complexes; the identities of $Tlg1p_{cyto}$ and $Vti1p_{cyto}$ were confirmed by immunoblot analysis. Note that the apparently less than stoichiometric amounts of $His_{(6)}$-$Snc2p_{cyto}$ in each complex are due to the inefficient Coomassie staining of Snc2p, as previously noted by Rothman and colleagues (McNew *et al.*, 2000).

4.2.9.2 Tlg2p and Snc2p do not form a dimer

The double-tag purification strategy left open the possibility of the recovery of $Tlg2p_{cyto}$/$His_{(6)}$-$Snc2p_{cyto}$ dimers; this was addressed by two approaches. In the first experiment, Ni-NTA agarose was used to recover $His_{(6)}$-HA-$Snc2p_{cyto}$, and any associated proteins, from a bacterial lysate containing both $Tlg2p_{cyto}$-PrA and $His_{(6)}$-HA-$Snc2p_{cyto}$. Proteins bound to Ni-NTA agarose were eluted with imidazole, and the eluates were incubated with IgG-Sepharose in an attempt to recover any $Tlg2p_{cyto}$-PrA which may have been associated with $His_{(6)}$-HA-$Snc2p_{cyto}$. Figure 4.9 shows that although $His_{(6)}$-HA-$Snc2p_{cyto}$ is successfully recovered from the Ni-NTA beads (lane 1), no $His_{(6)}$-HA-$Snc2p_{cyto}$ from the eluate binds to IgG-Sepharose beads, as assessed by immunoblot analysis with α-HA antibodies (lane 2). This observation suggests that $Tlg2p_{cyto}$/$His_{(6)}$-HA-$Snc2p_{cyto}$ dimers are not recovered in the purification of assembled complexes. However, because $Tlg2p_{cyto}$-PrA and $His_{(6)}$-HA-$Snc2p_{cyto}$ were co-produced in the same cells, the ratio of the two proteins in the resulting lysate could not be manipulated. If the lysate contained a great excess of $His_{(6)}$-HA-$Snc2p_{cyto}$, only a small population of this would be able to bind to $Tlg2p_{cyto}$-PrA. Then, if the population of $His_{(6)}$-HA-$Snc2p_{cyto}$ was incompletely recovered onto Ni-NTA agarose, $Tlg2p_{cyto}$/$His_{(6)}$-HA-$Snc2p_{cyto}$ dimers might have been present in the lysate which were not detected. The experiment shown in Figure 4.9 did not determine the proportion of $His_{(6)}$-HA-$Snc2p_{cyto}$ that was recovered on the Ni-NTA agarose out of the total amount of $His_{(6)}$-HA-$Snc2p_{cyto}$ input, so this possibility remained.

To control the ratio of the two input proteins, a second approach was taken utilising purified proteins. Figure 3.8 shows an experiment performed in collaboration with Nia Bryant and Scott Shanks (University of Glasgow), in which ~1 nmol of $Tlg2p_{cyto}$-PrA immobilised on IgG-Sepharose beads (lane 2) was incubated with an ~5-fold molar excess of $Snc2p_{cyto}$ (lane 3). After extensive washing and elution of bound proteins, no $Snc2p_{cyto}$ was found in the eluate (as assessed by staining with Coomassie Brilliant Blue, lane 4), providing further evidence that Tlg2p and Snc2p do not form a dimer.

4.2.9.3 Characterisation of binding of Vps45p (and mutant versions thereof) to recombinantly produced SNARE complexes

To investigate the binding of Vps45p to complexes containing full, ΔN36, and ΔN230 versions of the cytosolic domain of Tlg2p (described in Figure 3.1), complexes were generated according to the protocol outlined in Figure 4.8a, henceforth referred to as full-length complexes, ΔN36 complexes, and ΔN230 complexes, respectively. Ni-NTA agarose beads loaded with complexes were used to assess the binding of Vps45p-HA, obtained from a yeast lysate. The results of a typical binding experiment are shown in Figure 4.10. Consistent with the observation that Vps45p associates with *cis*-complexes *in vivo* (Bryant and James, 2003), Vps45p-HA bound recombinantly produced full-length complexes (row 1). However, Vps45p-HA did not bind ΔN36 or ΔN230 complexes (row 1). Since the N-terminal 36 residues of Tlg2p mediate its interaction with Vps45p via the pocket mode (Figure 3.1), this result suggests that Vps45p also interacts with SNARE complexes via this mode. Based on the data presented in Figure 3.2b, it was predicted that the pocket filling L117R mutation in Vps45p would therefore also abolish its interaction with SNARE complexes. Consistent with this prediction, Vps45p(L117R)-HA did not bind any version of complexes, including full-length (row 3).

Surprisingly, Vps45p(L117R/W244R)-HA, a version of Vps45p-HA which harbours the pocket filling L117R mutation, bound both full-length and ΔN36 complexes (row 4). Since the N-terminal 36 residues of Tlg2p are not required for this mode of interaction, and the pocket filling L117R mutation in Vps45p does not abolish it, this finding suggests that Vps45p can also interact with complexes via a second mode (i.e. distinct from the pocket mode). Consistent with the idea

that this interaction occurs via an alternative mode, Vps45p(L117R/W244R)-HA binds less well to complexes than does Vps45p-HA (compare rows 1 and 4). The failure to observe an interaction between Vps45p-HA (wild-type) and ΔN36 complexes (row 1) suggests that the W244R mutation is required to lock Vps45p in a conformation favouring this second mode of interaction in order to observe it in this experimental system.

If the W244R mutation locks Vps45p in a conformation which favours its interaction with complexes via this second mode, Vps45p(W244R)-HA would be predicted to bind ΔN36 complexes. In this experiment, however, no interaction was observed between Vps45p(W244R)-HA and ΔN36 or ΔN230 complexes (row 2). However, in a similar experiment performed by Scott Shanks (University of Glasgow), Vps45p(W244R)-HA was observed to bind both full-length and ΔN36 complexes. The results of this experiment are shown in Figure 4.11. In this experiment, both Vps45p-HA and Vps45p(W244R)-HA bound full-length complexes (lanes 1 and 2), consistent with an interaction facilitated via the hydrophobic pocket. Furthermore, Vps45p(L117R/W244R) bound full-length complexes weakly (lane 4), and both Vps45p(W244R)-HA and Vps45p(L117R/W244R) bound ΔN36 complexes weakly (lanes 6 and 8). Again, the weaker nature of these latter interactions is consistent with the hypothesis that they are facilitated by a mechanism distinct from the hydrophobic pocket. The stronger binding of Vps45p(W244R)-HA to full-length complexes (lane 2) compared to ΔN36 complexes (lane 6) can probably be explained by the ability of Vps45p(W244R)-HA to bind to full-length complexes via both modes. The conflicting results between the data presented in Figures 4.10 and 4.11 regarding the interaction between Vps45p(W244R)-HA and ΔN36 complexes may reflect the difficulty in capturing this weaker mode of interaction in *in vitro* pull-down assays.

4.2.10 Vps45p(L117R/W244R) is partly membrane associated

As a complementary approach to the *in vitro* experiments which investigated the interactions between Vps45p and recombinantly produced complexes, the membrane association of Vps45p (and mutants thereof) was investigated. Vps45p is normally present in both cytosolic and membrane bound pools, with approximately 75-90% of the total pool associated with membranes (Cowles *et*

al., 1994; Piper *et al.*, 1994). In *tlg2Δ* cells, however, the majority of Vps45p localises to the cytosol, suggesting that Tlg2p mediates the association of Vps45p with membranes (Bryant and James, 2001; Nichols *et al.*, 1998). Furthermore, Vps45p has been shown to associate with membranes at two distinct stages of the SNARE cycle; Vps45p associates with monomeric Tlg2p (prior to complex assembly), dissociates from membranes upon formation of *trans*-complexes, and reassociates with formation of *cis*-complexes (Bryant and James, 2003). Since Vps45p(L117R/W244R)-HA did not bind monomeric Tlg2p (Figure 4.3), but did bind SNARE complexes (Figures 4.10 and 4.11), subcellular fractionation experiments were performed to investigate its membrane association.

Differential centrifugation was used to generate membrane (P; pellet) and cytosolic (S; soluble) fractions from *vps45Δ* cells producing various versions of Vps45p-HA. The distribution of the cytosolic enzyme phosphoglycerate kinase (PGK) and the vacuolar membrane protein alkaline phosphatase (ALP) were also examined as markers of the cytosolic and membrane fractions, respectively (Scopes, 1975; Klionsky and Emr, 1989). Figure 4.12 shows the fractionation of endogenous Vps45p (upper panel), PGK (middle panel), and ALP (lower panel) in wild-type cells. Approximately 40% of the total pool of Vps45p was membrane associated, consistent with previous reports that Vps45p is present in both cytosolic and membrane-bound pools (Cowles *et al.*, 1994; Piper *et al.*, 1994). The exclusive presence of PGK in the cytosolic fraction, and of ALP in the membrane fraction, suggest that neither fraction is contaminated with the other.

The distribution of Vps45p-HA was next examined, to confirm that the C-terminal HA tag did not alter its membrane association. Figure 4.12 shows that Vps45p-HA was distributed between membrane-bound and cytosolic pools, in similar proportion to endogenous Vps45p. As predicted by the inability of Vps45p(L117R)-HA to associate with Tlg2p *in vivo* (Figure 3.3), Vps45p(L117R)-HA was found exclusively in the cytosol (lanes 7-9). This contrasts with Peng and Gallwitz's observation that GFP-Sly1p(L140K) (another version unable to interact with Sed5p) was still partly membrane associated (Peng and Gallwitz, 2004). However, it is worth noting that a different approach (immunofluorescence) was used in this study. Vps45p(W244R)-HA showed a similar fractionation pattern as wild-type Vps45p-HA, and was distributed evenly between membrane-bound and

cytosolic pools (lanes 10-12). Surprisingly, approximately one-third of the total pool of Vps45p(L117R/W244R)-HA was membrane-bound, with the remaining two-thirds present in the soluble fraction (lanes 13-15).

4.2.11 The accumulation of cis*-complexes in* sec18-1 *cells does not increase the extent of membrane association of Vps45p(L117R/W244R)*

The unexpected findings that Vps45p(L117R/W244R)-HA bound recombinantly produced SNARE complexes (Figures 4.10 and 4.11) and was partially membrane associated (Figure 4.12) prompted an investigation of the membrane association of Vps45p(L117R/W244R)-HA under conditions favouring the accumulation of SNARE complexes. Post-fusion *cis*-complexes are normally disassembled by the ATPase Sec18p, in concert with its attachment protein, Sec17p (Mayer *et al.*, 1996). The temperature sensitive *sec18-1* allele encodes a mutant version of Sec18p (G89D), which is strongly impaired in its binding to Sec17p (Horsnell *et al.*, 2002). Consequently, *sec18-1* cells incubated at the restrictive temperature are unable to disassemble *cis*-complexes, and these cells accumulate *cis*-complexes at levels approximately 3-4 times of that observed in wild-type cells (Grote *et al.*, 2000). To examine the membrane association of mutant versions of Vps45p-HA after the accumulation of *cis*-complexes, subcellular fractionation was performed on cell lysates obtained from *sec18-1* cells after incubation at both permissive (25°C) and restrictive (37°C) temperatures. The results of these fractionations are shown in Figure 4.13.

Approximately two-fold more Vps45p-HA was membrane associated in *sec18-1* cells after a 90 minute incubation at the restrictive temperature, compared to those incubated only at the permissive temperature (lane 5 compared to lane 2, upper panels). In contrast, Vps45p(L117R)-HA was not present on membranes, even after incubation at the restrictive temperature (lanes 2 and 5, second panels). Vps45p(W244R)-HA showed approximately three-fold greater membrane association after incubation at the restrictive temperature (lanes 2 and 5, third panels), consistent with its robust binding to recombinantly produced SNARE complexes (Figures 4.10 and 4.11). Based on the weak interaction between Vps45p(L117R/W244R)-HA and recombinantly produced complexes (Figures 4.10 and 4.11), it was hypothesised that the pool of membrane associated

Vps45p(L117R/W244R)-HA (approximately 10-20% of the total pool) might exhibit a similar two- to three-fold increase upon *cis*-complex accumulation. However, the data presented in Figure 4.13 show that the amount of membrane associated Vps45p(L117R/W244R)-HA does not increase, even after incubation at the restrictive temperature (lanes 2 and 5, bottom panels).

Several points are worth bearing in mind when interpreting these data: Firstly, Vps45p(L117R/W244R)-HA interacted weakly with recombinantly produced SNARE complexes (Figures 4.10 and 4.11); therefore the kinetics of this interaction may not allow Vps45p(L117R/W244R)-HA to accumulate on membranes, even with elevated levels of *cis*-complexes, because Vps45p(L117R/W244R)-HA may dissociate so rapidly. As a second possibility, Vps45p(L117R/W244R)-HA may interact with *trans*- rather than *cis*-complexes. Although Vps45p was not found associated with *trans*-complexes in a previous study (Bryant and James, 2003), it is possible that this interaction may have been disrupted during some stage of these experiments. Thirdly, the membrane association of Vps45p(L117R/W244R)-HA may not be mediated through its interaction with SNARE complexes, but rather via interaction with another protein. As a final point, these experiments were performed in *vps45*Δ cells to ensure that endogenous Vps45p was not competing for binding sites on Tlg2p and assembled complexes. As will be discussed in Chapter Five, *vps45*Δ cells producing Vps45p(L117R/W244R)-HA as their sole source of Vps45p have reduced levels of Tlg2p (approximately 20-25% that of wild-type cells; see Figure 5.1). Therefore, the amount of *cis*-complexes that accumulate in *sec18-1 vps45*Δ cells producing Vps45p(L117R/W244R)-HA could be limited by the reduced amount of Tlg2p in these cells.

4.3 Discussion

Several syntaxins, including the yeast syntaxins Sed5p, Ufe1p, and Tlg2p (Dulubova *et al.*, 2002; Yamaguchi *et al.*, 2002), and their mammalian counterparts syntaxin 5, syntaxin 18, and syntaxin 16 (Dulubova *et al.*, 2002; Yamaguchi *et al.*, 2002), have been demonstrated to interact with their cognate SM proteins via the pocket mode characterised in Chapter Three. However, the functional significance of this mode of interaction has remained unclear. Work in yeast has suggested that the pocket mode interaction between SM proteins

and their cognate syntaxins is not required for SM proteins to execute their function (Peng and Gallwitz, 2004), while studies in mammalian systems implied that SM proteins do execute at least some function(s) via this mode (Williams *et al.*, 2004; Yamaguchi *et al.*, 2002).

The work presented here aimed to investigate the precise physiological role of the pocket mode interaction between Vps45p and Tlg2p. It was demonstrated in the functional studies presented at the beginning of the chapter that Vps45p(L117R)-HA, a version of Vps45p unable to bind to Tlg2p via the pocket mode (Figures 3.2 and 3.3), complemented the CPY sorting defect of *vps45Δ* cells (Figure 4.1). This finding is consistent with previous work in yeast concluding that the pocket mode interaction between SM proteins and their cognate syntaxins is not required for membrane traffic through the early stages of the secretory pathway (Peng and Gallwitz, 2004), and extends this finding to include membrane traffic through the *VPS* pathway.

This chapter also introduced a dominant negative version of Vps45p, which harbours a W244R point mutation. This version of Vps45p helped uncover how Vps45p might perform its function(s) via interactions other than the pocket mode of interaction with Tlg2p. Evidence for a second mode of interaction, i.e. distinct from the pocket mode, between Vps45p and its cognate SNARE complex was provided by *in vitro* binding experiments with versions of Vps45p containing the W244R mutation and recombinantly produced complexes (Figures 4.10 and 4.11). Because only versions of Vps45p containing the W244R mutation were observed to bind to SNARE complexes via this alternative mode, it was hypothesised that Vps45p(W244R) is locked in a conformation which favours this alternative mode of interaction. In order to better understand this mode of interaction, it would be informative to determine the contact sites between Vps45p(W244R) and SNARE complexes.

This chapter also demonstrated that the CPY missorting defect conferred by Vps45p(W244R)-HA could be suppressed by simultaneous overproduction of the wild-type protein (Figure 4.6), suggesting that the mutant protein interferes with a physiologically relevant intermediate of the SNARE cycle. Furthermore, overproduction of the v-SNARE Snc2p was also shown to suppress the CPY missorting defect conferred by Vps45p(W244R)-HA (Figure 4.2). This finding was

important, as it suggested that the interaction between Vps45p and Snc2p uncovered by *in vitro* binding experiments (Figure 3.4) is also relevant *in vivo*.

In an attempt to gain insight into the stage of the SNARE cycle at which Vps45p(W244R)-HA accumulates such an intermediate, the pocket-filling mutation L117R was introduced into the dominant negative protein, creating a version which was unable to bind to Tlg2p (Figure 4.3). Intriguingly, Vps45p(L117R/W244R)-HA no longer had a dominant negative effect on CPY sorting (Figure 4.4). This finding suggests that Vps45p(W244R)-HA exerts its dominant negative effect after binding to Tlg2p via the pocket mode; more importantly, however, it demonstrates that the pocket mode of interaction has a functional role, in agreement with studies in mammalian systems.

In summary, the data presented in this chapter suggest that Vps45p is capable of interacting with assembled complexes via a mode distinct from the pocket mode (Figures 4.10 and 4.11). The data presented in this chapter also suggest that Vps45p executes at least one role via the pocket mode, although this role is not an essential one (Figures 4.4 and 4.1). Consequently, the working hypothesis presented in Chapter Six attempts to account for these data by postulating that Vps45p performs two roles; one to facilitate the entry of Tlg2p into complexes and a second regulatory (non-essential) one (executed via the pocket mode).

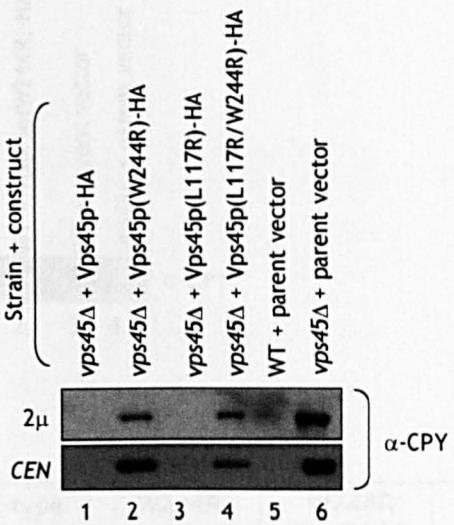

Figure 4.1 Vps45p(L117R) can perform the function of the wild-type protein with respect to CPY sorting. Proteins secreted by cells producing Vps45p-HA (and mutant versions thereof) were concentrated from the extracellular media with trichloroacetic acid (TCA), resolved by SDS-PAGE, and transferred to nitrocellulose membrane. Immunoblot analysis with α-CPY antibodies was used to assess the presence of CPY in the precipitations. Upper panel: Lanes 1-4: *vps45Δ* (LCY008) cells were transformed with either pCOG070 (2μ; driving the production of Vps45p-HA), pCOG072 (2μ; driving the production of Vps45p(W244R)-HA), pCOG071 (2μ; driving the production of Vps45p(L117R)-HA), or pCOG073 (2μ; driving the production of Vps45p(L117R/W244R)-HA). Lanes 5 and 6: Wild-type (9Dα) or *vps45Δ* (LCY008) cells were transformed with YEplac195 (parent vector). Lower panel: Lanes 1-4: *vps45Δ* (LCY008) cells were transformed with either pNB706 (*CEN*; driving the production of Vps45p-HA), pNB707 (*CEN*; driving the production of Vps45p(W244R)-HA), pNB708 (*CEN*; driving the production of Vps45p(L117R)-HA), or pNB709 (*CEN*; driving the production of Vps45p(L117R/W244R)-HA). Lanes 5 and 6: Wild-type (9Dα) or *vps45Δ* (LCY008) cells were transformed with YCplac111 (parent vector).

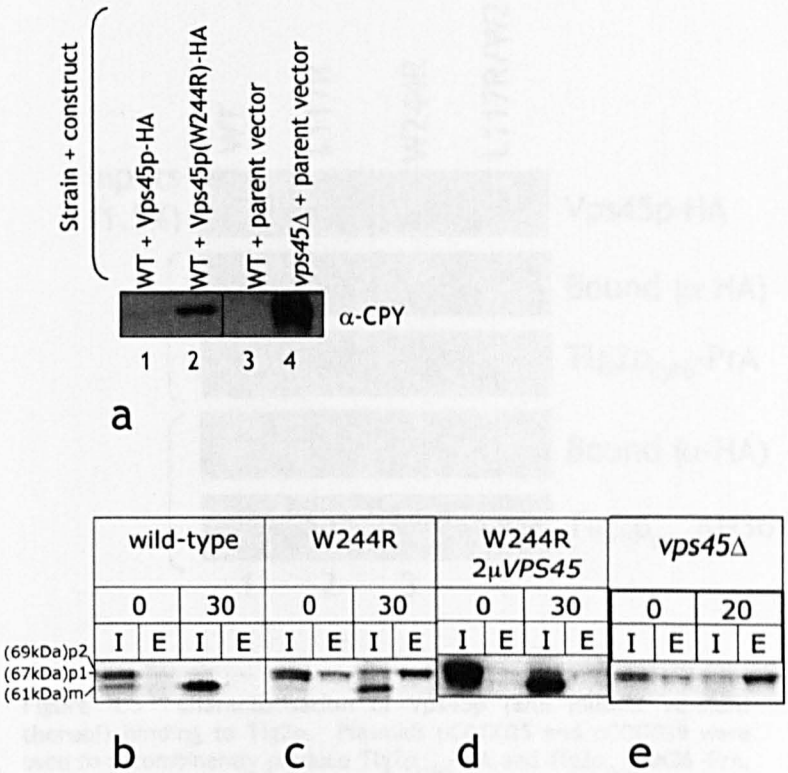

Figure 4.2 Vps45p(W244R) confers a dominant negative effect on CPY sorting. a) Proteins secreted by cells producing the indicated versions of Vps45p-HA were concentrated from the extracellular media with trichloroacetic acid (TCA), resolved by SDS-PAGE, and transferred to nitrocellulose membrane. Immunoblot analysis with α-CPY antibodies was used to assess the presence of CPY in the precipitations. Lane 1: Wild-type (9Dα) cells harbouring pCOG070 (2μ; driving the production of Vps45p-HA), Lane 2: Wild-type (9Dα) cells harbouring pCOG072 (2μ; driving the production of Vps45p(W244R)-HA), Lane 3: Wild-type (9Dα) cells harbouring YEplac195 (parent vector), Lane 4: *vps45*Δ (LCY008) cells harbouring YEplac195 (parent vector). b-e) Cells were allowed to incorporate methionine-S^{35} into newly synthesised proteins for a 5 min pulse period. After a 30 min chase period, radiolabelled CPY was immunoprecipitated from intracellular and extracellular fractions of cells (Piper *et al.*, 1994). The fate of newly synthesised CPY was followed in (b-d) wild-type cells (RPY10) harbouring the following plasmid(s): (b) YEplac195 (parent vector), (c) pCOG065 (2μ; driving the production of Vps45p(W244R)-HA; (d) pCOG070 (2μ; driving the production of Vps45p-HA) and pCOG065 (2μ; driving the production of Vps45p(W244R)-HA, or (e) *vps45*Δ cells (NOzY2) harbouring YEplac195 (parent vector).

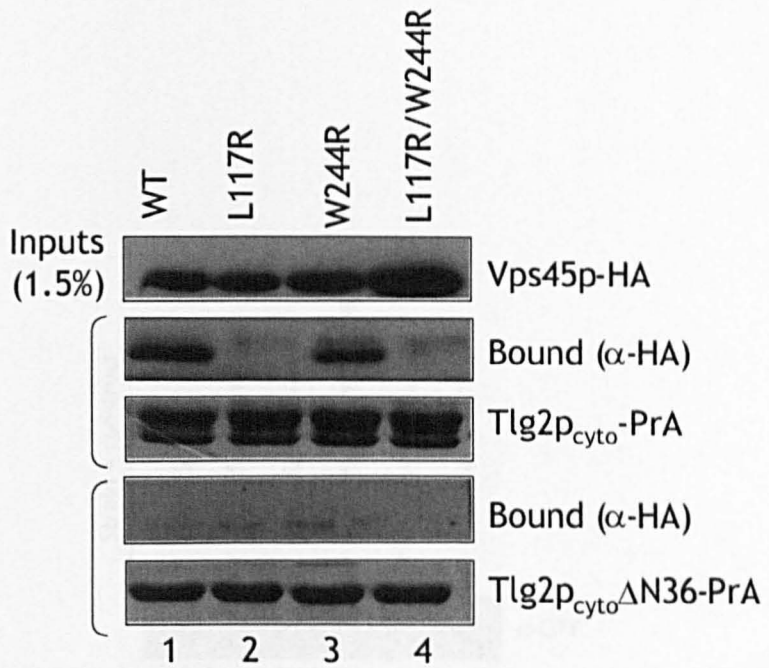

Figure 4.3 Characterisation of Vps45p (and mutant versions thereof) binding to Tlg2p. Plasmids pCOG025 and pCOG029 were used to recombinantly produce Tlg2p$_{cyto}$-PrA and Tlg2p$_{cyto}$ΔN36-PrA. Fusion proteins immobilised on IgG-Sepharose beads were incubated with lysates obtained from either 50 or 150 mls of mid-log phase *vps45*Δ (LCY008) cells transformed with either pCOG070 (driving the production of Vps45p-HA), pCOG071 (driving the production of Vps45p(L117R)-HA), pCOG072 (driving the production of Vps45p(W244R)-HA), or pCOG073 (driving the production of Vps45p(L117R/W244R)-HA. Strains producing Vps45p(W244R)-HA or Vps45p(L117R/W244R)-HA were grown in three times the volume of medium as those producing Vps45p-HA or Vps45p(L117R)-HA, due to the reduced levels of versions of Vps45p harbouring the W244R mutation (see Figure 5.1). Following extensive washing to remove nonspecifically bound proteins, bound proteins were eluted, resolved by SDS-PAGE, transferred to nitrocellulose membrane, and subjected to immunoblot analysis with α-HA antibodies to assess the amounts of bound Vps45p-HA (upper panels). Vps45p-HA inputs from the initial lysates were also analysed similarly (top panel). To ensure equal loading of beads with purified proteins, samples were also visualised by staining with Coomassie Brilliant Blue (bottom panels).

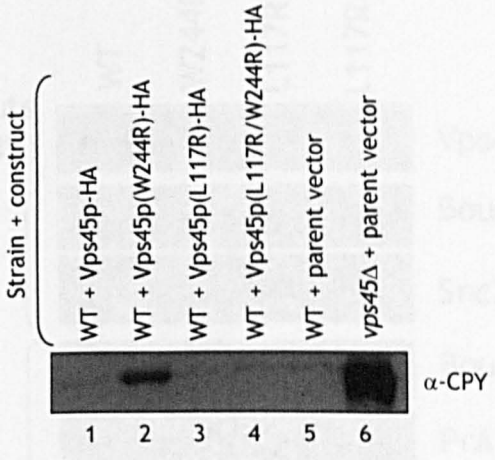

Figure 4.4 The L117R mutation removes the ability of Vps45p(W244R)-HA to exert its dominant negative effect on CPY sorting. Proteins secreted by cells producing the indicated versions of Vps45p-HA were concentrated from the extracellular media with trichloroacetic acid (TCA), resolved by SDS-PAGE, and transferred to nitrocellulose membrane. Immunoblot analysis with α-CPY antibodies was used to assess the presence of CPY in the precipitations. Lanes 1-4: Wild-type (9Dα) cells were transformed with either pCOG070 (2μ; driving the production of Vps45p-HA), pCOG072 (2μ; driving the production of Vps45p(W244R)-HA), pCOG071 (2μ; driving the production of Vps45p(L117R)-HA), or pCOG073 (2μ; driving the production of Vps45p(L117R/W244R)-HA). Lanes 5 and 6: Wild-type (9Dα) or *vps45*Δ (LCY008) cells were transformed with YEplac195 (parent vector).

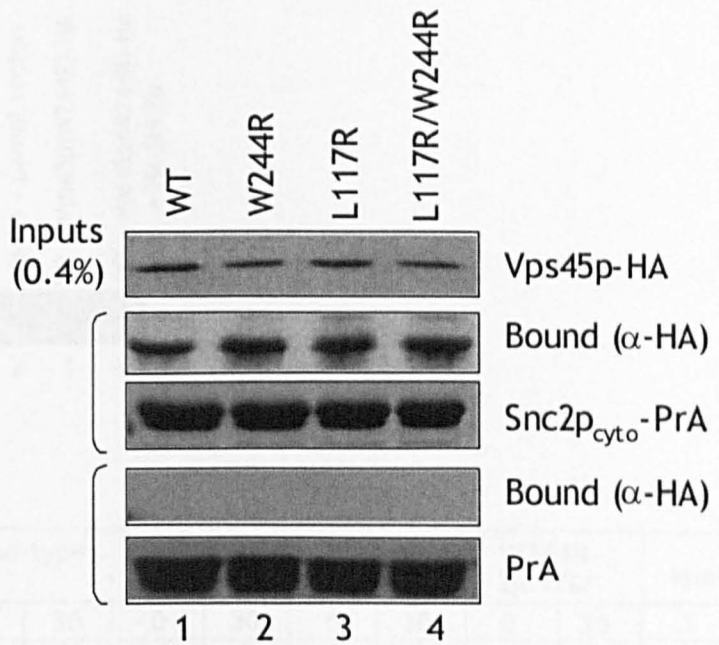

Figure 4.5 Characterisation of Vps45p (and mutant versions thereof) binding to Snc2p. Plasmids pCOG045 and pCOG022 were used to recombinantly produce Snc2p$_{cyto}$-PrA and PrA. Fusion proteins immobilised on IgG-Sepharose beads were incubated with lysates obtained from either 150 or 450 mls of mid-log phase *tlg2*Δ (NOzY3) cells transformed with either pCOG070 (driving the production of Vps45p-HA), pCOG072 (driving the production of Vps45p(W244R)-HA), pCOG071 (driving the production of Vps45p(L117R)-HA), or pCOG073 (driving the production of Vps45p(L117R/W244R)-HA). Strains producing Vps45p(W244R)-HA or Vps45p(L117R/W244R)-HA were grown in three times the volume of medium as those producing Vps45p-HA or Vps45p(L117R)-HA, due to the reduced levels of versions of Vps45p harbouring the W244R mutation (see Figure 5.1). Following extensive washing to remove nonspecifically bound proteins, bound proteins were eluted, resolved by SDS-PAGE, transferred to nitrocellulose membrane, and subjected to immunoblot analysis with α-HA antibodies to assess the amounts of bound Vps45p-HA (upper panels). Vps45p-HA inputs from the initial lysates were also analysed similarly (top panel). To ensure equal loading of beads with purified proteins, samples were also visualised by staining with Coomassie Brilliant Blue (bottom panels).

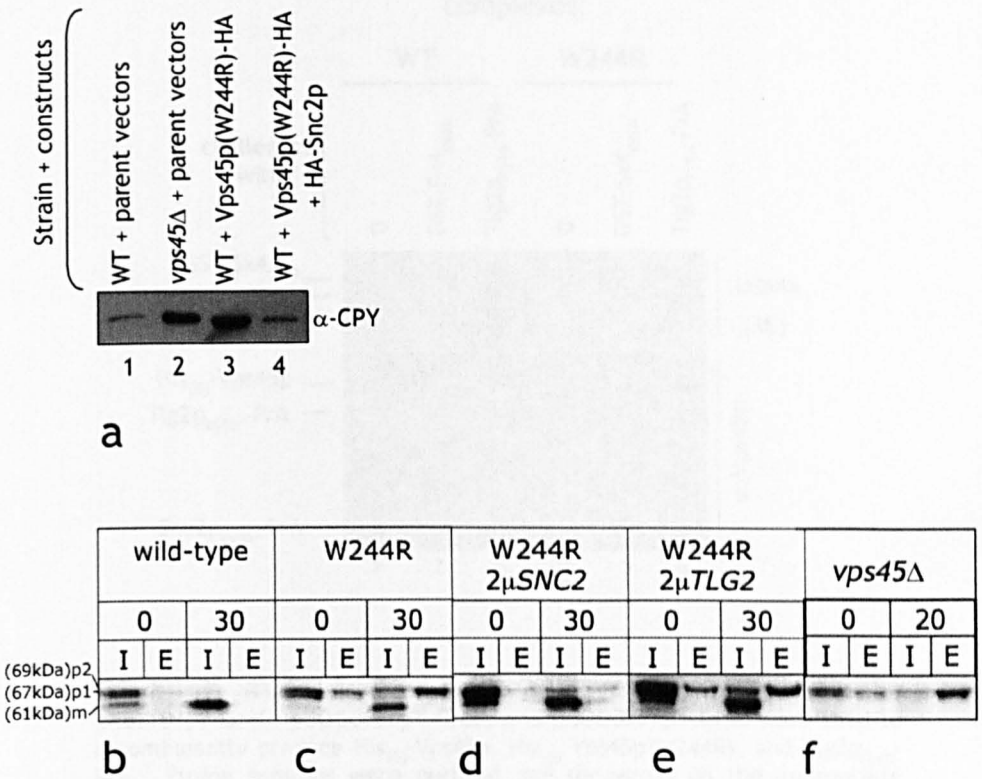

Figure 4.6 Overproduction of HA-Snc2p relieves the dominant negative effect on CPY sorting conferred by Vps45p(W244R)-HA. a) Proteins secreted by cells producing the indicated versions of Vps45p-HA were concentrated from the extracellular media with trichloroacetic acid (TCA), resolved by SDS-PAGE, and transferred to nitrocellulose membrane. Immunoblot analysis with α-CPY antibodies was used to assess the presence of CPY in the precipitations. Lane 1: Wild-type (9Dα) cells were co-transformed with pRS426 (parent vector) and YEplac181 (parent vector). Lane 2: *vps45*Δ (LCY008) cells were co-transformed with pRS426 (parent vector) and YEplac181 (parent vector). Lane 3: Wild-type (9Dα) cells were co-transformed with pRS426 (parent vector) and pCOG065 (2μ; driving the production of Vps45p(W244R)-HA). Lane 4: Wild-type (9Dα) cells were co-transformed with pCOG054 (2μ; driving the production of HA-Snc2p) and pCOG065 (2μ; driving the production of Vps45p(W244R)-HA). b-f) Cells were allowed to incorporate methionine-S^{35} into newly synthesised proteins for a 5 min pulse period. After a 30 min chase period, radiolabelled CPY was immunoprecipitated from intracellular and extracellular fractions of cells (Piper *et al.*, 1994). The fate of newly synthesised CPY was followed in (b-e) wild-type cells (RPY10) harbouring the following plasmid(s): (b) YEplac195 (parent vector), (c) pCOG065 (2μ; driving the production of Vps45p(W244R)-HA), (d) pCOG065 (2μ; driving the production of Vps45p(W244R)-HA) and pCOG054 (2μ; driving the production of HA-Snc2p), (e) pCOG065 (2μ; driving the production of Vps45p(W244R)-HA) and pHA-TLG2 (2μ; driving the production of HA-Tlg2p), and (f) *vps45*Δ cells (NOzY2) harbouring YEplac195 (parent vector).

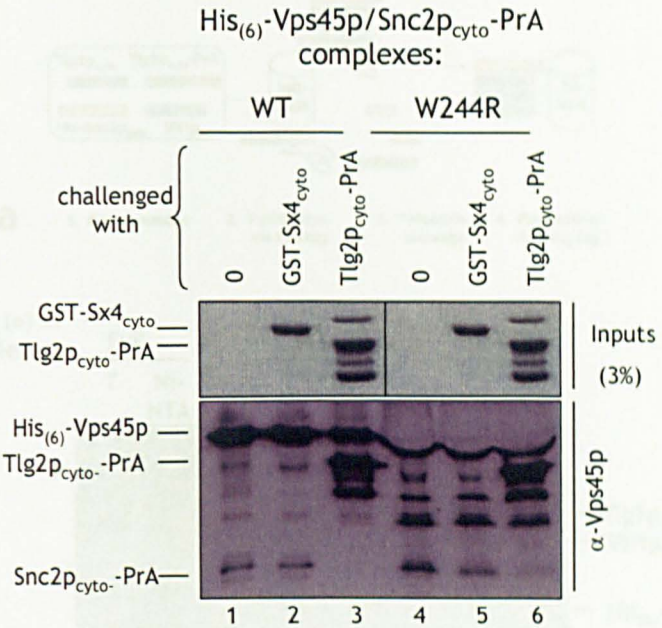

Figure 4.7 Tlg2p displaces Snc2p from Vps45p(W244R). Plasmids pNB710/pT-GroE, pCOG068/pT-GroE, and pCOG025/pT-GroE were used to recombinantly produce $His_{(6)}$-Vps45p, $His_{(6)}$-Vps45p(W244R), and $Tlg2p_{cyto}$-PrA. Fusion proteins were purified and recovered on the appropriate resins. PrA-tagged SNARE proteins were eluted in 0.5 M HAc (pH 3.4) and dialysed against PBS. $His_{(6)}$-Vps45p and $His_{(6)}$-Vps45p(W244R) were eluted in 250 mM imidazole in PBS and dialysed against PBS. Purified recombinant $GST\text{-}Sx4_{cyto}$ was kindly provided by Fiona Brandie (University of Glasgow). $His_{(6)}$-Vps45p (WT or W244R) and $Snc2p_{cyto}$-PrA were allowed to bind for 16 hrs at 4°C. Binary complexes were recovered through a one hour incubation with Ni-NTA beads, followed by extensive washing with 20 mM imidazole in PBS to remove unbound proteins. To attempt to displace $Snc2p_{cyto}$-PrA, ~50 μgs of either $Tlg2p_{cyto}$-PrA or $GST\text{-}Sx4_{cyto}$ (as a negative control) were added to the binding reactions. PBS was also added to each reaction for a final volume of 1 ml. After two hours of rotation at 4°C, beads were washed extensively with 20 mM imidazole in PBS. Bound proteins were eluted in LSB, resolved by SDS-PAGE, and transferred to nitrocellulose membrane for immunoblot analysis with α-Vps45p antibodies (lower panel). Lane 1: $His_{(6)}$-Vps45p/$Snc2p_{cyto}$-PrA dimers with no competing protein, Lane 2: $His_{(6)}$-Vps45p/$Snc2p_{cyto}$-PrA dimers plus $GST\text{-}Sx4_{cyto}$, Lane 3: $His_{(6)}$-Vps45p/$Snc2p_{cyto}$-PrA plus $Tlg2p_{cyto}$-PrA, Lane 4: $His_{(6)}$-Vps45p(W244R)/$Snc2p_{cyto}$-PrA with no competing protein, Lane 5: $His_{(6)}$-Vps45p(W244R)/$Snc2p_{cyto}$-PrA plus $GST\text{-}Sx4_{cyto}$, Lane 6: $His_{(6)}$-Vps45p(W244R)/$Snc2p_{cyto}$-PrA plus $Tlg2p_{cyto}$-PrA. Samples representing 3% of the input of competing protein were also resolved by SDS-PAGE and visualised by staining with Coomassie Brilliant Blue (upper panel).

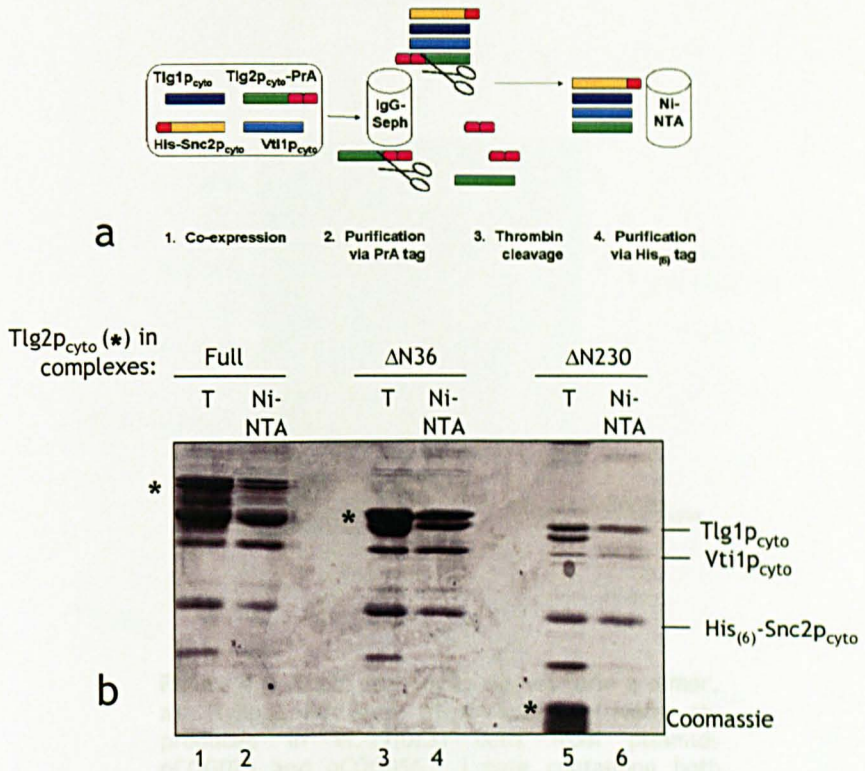

Figure 4.8 Recombinant production and purification of SNARE complexes. a) The four step strategy used: 1) Co-production of Tlg2p$_{cyto}$-PrA/Tlg1p$_{cyto}$/Vti1p$_{cyto}$/His$_{(6)}$-Snc2p$_{cyto}$ in *E. coli*. 2) Affinity purification of Tlg2p$_{cyto}$-PrA and Tlg2p$_{cyto}$-PrA/Tlg1p$_{cyto}$/Vti1p$_{cyto}$/His$_{(6)}$-Snc2p$_{cyto}$ complexes onto IgG-Sepharose. 3) Liberation of complexes from resin via thrombin cleavage (thrombin cleavage site just prior to PrA tag in Tlg2p$_{cyto}$-PrA). 4) Affinity purification of complexes onto Ni-NTA agarose via His$_{(6)}$ tag. b) To produce complexes containing the three truncations of Tlg2p$_{cyto}$, BL-21(DE3) cells were co-transformed with either pCOG032 and pCOG038 (full, lanes 1 and 2); pCOG033 and pCOG038 (ΔN36, lanes 3 and 4), or pCOG034 and pCOG038 (ΔN230, lanes 5 and 6). Following recombinant protein production and cell lysis, protein complexes contained within bacterial lysates were affinity purified onto IgG-Sepharose, liberated by thrombin cleavage (T; lanes 1, 3, and 5), and affinity purified again onto Ni-NTA agarose (Ni-NTA; lanes 2, 4, and 6). Proteins contained in samples from each stage were resolved by SDS-PAGE and visualised by staining with Coomassie Brilliant Blue. The three versions of Tlg2p$_{cyto}$ are marked with asterisks. Note: the bands migrating between Tlg2p$_{cyto}$-PrA and Tlg1p$_{cyto}$ in lane 1 correspond to degradation products of Tlg2p.

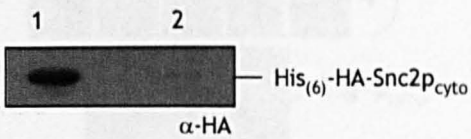

Figure 4.9 Tlg2p and Snc2p do not form a dimer. a) $Tlg2p_{cyto}$-PrA and His-HA-$Snc2p_{cyto}$ were co-produced in BL-21(DE3) cells from plasmids pCOG025 and pCOG056. Lysate containing both proteins was then incubated with Ni-NTA agarose (lane 1). Bound proteins were eluted and affinity purified in a second step onto IgG-Sepharose (lane 2). Samples at each stage were eluted, resolved by SDS-PAGE, transferred to nitrocellulose membrane, and subjected to immunoblot analysis with α-HA antibodies.

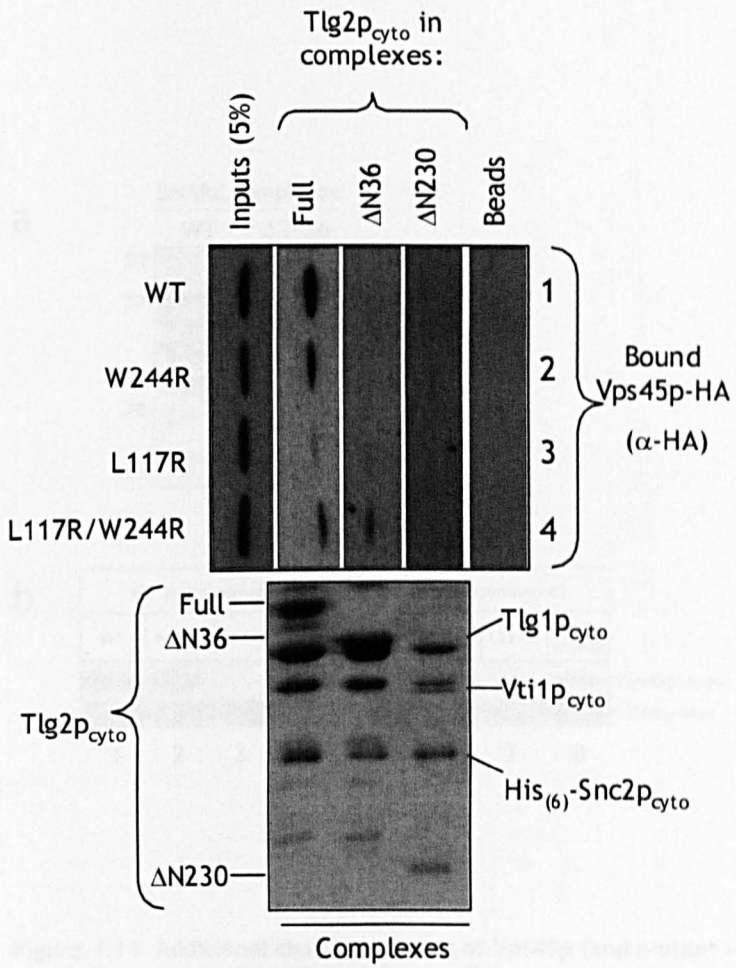

Figure 4.10 Characterisation of Vps45p (and mutant versions thereof) binding to SNARE complexes. Bottom panel: SNARE complexes containing full length, ΔN36, or Δ230 versions of the cytosolic domain of Tlg2p were produced from plasmids pCOG032 and pCOG038 (full), pCOG033 and pCOG038 (ΔN36), or pCOG034 and pCOG038 (ΔN230). Complexes were affinity purified onto IgG-Sepharose resin, liberated by thrombin cleavage, and affinity purified again onto Ni-NTA agarose resin as detailed in Figure 4.8. Bound proteins were eluted, resolved by SDS-PAGE, and visualised by staining with Coomassie Brilliant Blue. Upper columns: Ni-NTA beads loaded with complexes were incubated with lysates from *vps45Δ* (LCY008) cells transformed with either pCOG070 (driving the production of Vps45p-HA), pCOG072 (driving the production of Vps45p(W244R)-HA), pCOG071 (driving the production of Vps45p(L117R)-HA), or pCOG073 (driving the production of Vps45p(L117R/W244R)-HA). After extensive washing to remove nonspecifically bound proteins, bound proteins were eluted in LSB, resolved by SDS-PAGE, and subjected to immunoblot analysis with α-HA antibodies to assess the amounts of bound Vps45p-HA. Vps45p-HA inputs from the initial lysates were also analysed similarly (upper leftmost column).

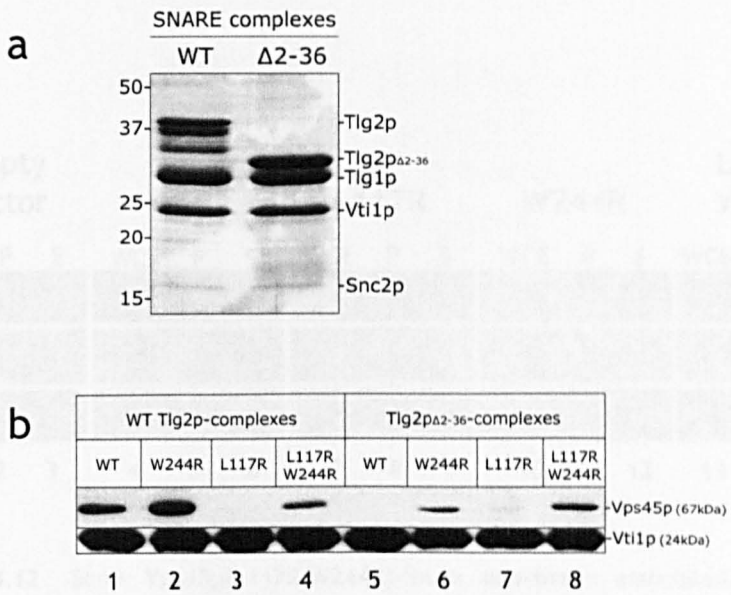

Figure 4.11 Additional characterisation of Vps45p (and mutant versions thereof) binding to SNARE complexes. This experiment was performed by Scott Shanks (University of Glasgow). a) SNARE complexes containing either full length (full), or a version lacking residues 2-36 (ΔN36), of the cytosolic domain of Tlg2p were produced from plasmids pCOG032 and pCOG038 (full) or pCOG033 and pCOG038 (ΔN36). Complexes were affinity purified onto IgG-Sepharose resin, liberated by thrombin cleavage, and affinity purified again onto Ni-NTA agarose resin as detailed in Figure 4.8. a) Bound proteins were eluted, resolved by SDS-PAGE, and visualised by staining with Coomassie Brilliant Blue. b) Lanes 1-4: Ni-NTA beads loaded with complexes (full) were incubated with lysates from *vps45*Δ (LCY008) cells transformed with either pCOG070 (driving the production of Vps45p-HA), pCOG072 (driving the production of Vps45p(W244R)-HA), pCOG071 (driving the production of Vps45p(L117R)-HA), or pCOG073 (driving the production of Vps45p(L117R/W244R)-HA). Lanes 5-8: Same as lanes 1-4, except that Ni-NTA beads were loaded with ΔN36 complexes. After extensive washing to remove nonspecifically bound proteins, bound proteins were eluted in LSB, resolved by SDS-PAGE, and subjected to immunoblot analysis with α-HA antibodies to assess the amounts of bound Vps45p-HA (upper panel). Immunoblot analysis with α-Vti1p antibodies was also performed to ensure equal loading of beads with recombinantly produced complexes (lower panel).

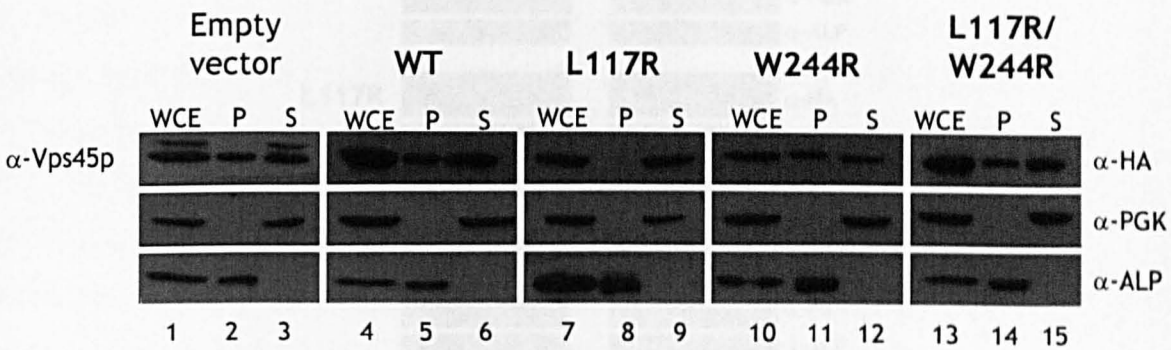

Figure 4.12 Some Vps45p(L117R/W244R)-HA is membrane associated. Differential centrifugation was performed to generate membrane (P; pellet) and cytosolic (S; soluble) fractions from lysates (WCE; whole cell extract) from wild-type (9Dα) cells transformed with YCplac111 (parent vector; lanes 1-3) or *vps45*Δ (LCY008) cells transformed with pNB706 (*CEN*, driving the production of Vps45p-HA; lanes 4-6), pNB708 (*CEN*, driving the production of Vps45p(L117R)-HA; lanes 7-9), pNB707 (*CEN*, driving the production of Vps45p(W244R)-HA; lanes 10-12), or pNB709 (*CEN*, driving the production of Vps45p(L117R/W244R)-HA; lanes 13-15). Proteins contained within each fraction were resolved by SDS-PAGE and transferred to nitrocellulose membrane. Immunoblot analysis was performed with α-Vps45p antibodies, α-HA antibodies, α-PGK antibodies, and α-ALP antibodies to assess the distributions of endogenous Vps45p, Vps45p-HA, and the cytosolic and membrane marker proteins phosphoglycerate kinase (PGK) and alkaline phosphatase (ALP), respectively.

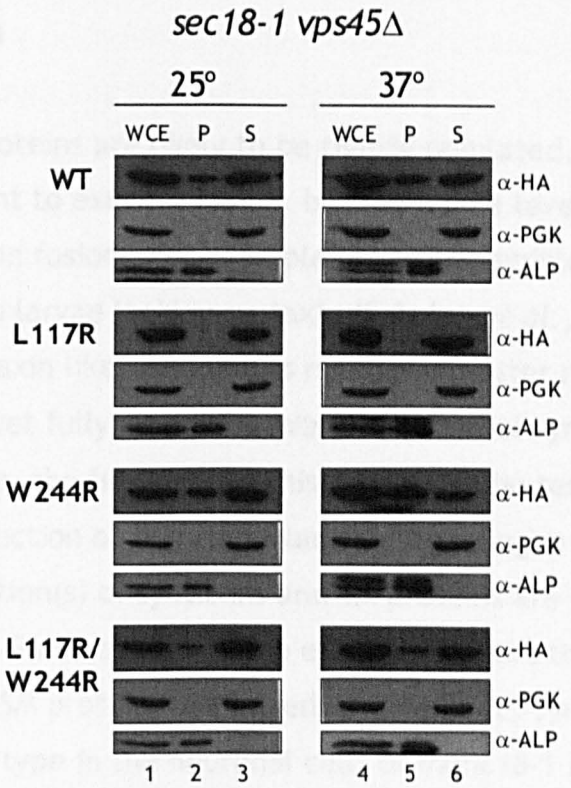

Figure 4.13 The pool of membrane associated Vps45p(L117R/W244R)-HA does not increase upon accumulation of *cis*-complexes. After reaching mid-log phase, *sec18-1 vps45*Δ (LCY006) cells transformed with either pNB706 (*CEN*, driving the production of Vps45p-HA; top row), pNB708 (*CEN*, driving the production of Vps45p(L117R)-HA; second row), pNB707 (*CEN*, driving the production of Vps45p(W244R)-HA; third row), or pNB709 (*CEN*, driving the production of Vps45p(L117R/W244R)-HA; bottom row) were incubated an additional 90 minutes at either the permissive (25°C; left column) or restrictive (37°C; right column) temperatures prior to cell lysis. Differential centrifugation was performed to generate membrane (P; pellet) and cytosolic (S; soluble) fractions from cell lysates (WCE; whole cell extract). Proteins contained within each fraction were resolved by SDS-PAGE and transferred to nitrocellulose membrane. Immunoblot analysis was performed with α-Vps45p antibodies, α-HA antibodies, α-PGK antibodies, and α-ALP antibodies to assess the distributions of endogenous Vps45p, Vps45p-HA, and the cytosolic and membrane marker proteins phosphoglycerate kinase (PGK) and alkaline phosphatase (ALP), respectively.

Chapter Five: Regulation of the protein levels of Tlg2p and Snc2p

5.1 Introduction

The levels of SNARE proteins are likely to be tightly regulated, since a sufficient amount must be present to execute fusion, but too high a level might titrate out other factors involved in fusion. For example, neurotransmitter release is abolished in *Drosophila* larvae lacking syntaxin (Schulze *et al.*, 1995), but their overproduction of syntaxin likewise inhibits neurotransmitter release (Wu *et al.*, 1998). While it is not yet fully clear why overproduction of syntaxin is detrimental in this case, the finding that this defect can be rescued by simultaneous overproduction of Rop (the Munc18-1 homologue in *Drosophila*) indicates that the function(s) of syntaxins and SM proteins are tightly linked *in vivo* (Wu *et al.*, 1998). Some evidence also exists to suggest that the protein levels of syntaxins and SM proteins are linked; for example, syntaxin 1 levels are reduced to 30% of wild type in the neuronal cells of munc18-1 knockout mice (Toonen *et al.*, 2005). While it has not yet been investigated whether this chaperone-like function is a universal feature of all SM proteins, Vps45p and Tlg2p seem to share a similar relationship; Tlg2p is downregulated to undetectable levels in the absence of Vps45p (Bryant and James, 2001). While Tlg2p normally has a half-life of approximately two hours, its half-life is decreased to only 20 minutes in *vps45*Δ cells, despite being initially synthesised to wild-type levels (Bryant and James, 2001). Based on this finding, it has been proposed that one role of Vps45p is to help protect Tlg2p from degradation (Bryant and James, 2001).

In yeast, two major destinations exist at which proteins are degraded: the vacuole and the proteasome. The vacuole is a large, acidified, membrane-bound organelle host to a range of proteases (Klionsky *et al.*, 1990). On the other hand, the 26S proteasome is a multi-enzyme complex, comprised of two 19S regulatory caps and a cylindrical 20S catalytic core, that is found in both the cytosol and the nucleus of eukaryotic cells (Peters *et al.*, 1994; Rivett, 1993; Thrower *et al.*, 2000). Both the vacuolar and the proteasomal systems routinely employ the same molecule, ubiquitin, to target proteins for degradation (Horak,

2003; Urbe, 2005). Ubiquitin is a small (76 kDa) molecule that can be conjugated to other proteins via an amide bond between its C-terminal glycine residue (G76) and the ε-amino group of particular lysine residue(s) in the substrate protein (Pickart, 2004; Weissman, 2001). This conjugation occurs in an E1-E2-E3 cascade, in which E1 is a ubiquitin activating enzyme, E2 is a ubiquitin conjugating enzyme, and E3 is a ubiquitin ligase (Pickart, 2004; Weissman, 2001). The specific manner of conjugation of ubiquitin to the substrate (ubiquitination, alternatively known as ubiquitylation) generally determines whether it is directed to the vacuole or the proteasome (Urbe, 2005). Conjugation of either ubiquitin monomers, or short chains of Lys^{63}-linked ubiquitin, to proteins such as ion/nutrient transporters and signalling receptors targets their internalisation from the plasma membrane and entry into the endocytic pathway, ultimately resulting in their degradation by vacuolar proteases (Hicke, 1999; Hicke, 2001; Rotin *et al.*, 2000). On the other hand, attachment of chains of four Lys^{48}-linked ubiquitin molecules targets proteins for degradation by the proteasome (Peters *et al.*, 1994; Thrower *et al.*, 2000). The capping subunits bind directly to polyubiquitinated proteins and feed them into the proteolytic core (Peters, 1994; Rivett, 1993; Thrower *et al.*, 2000).

By investigating the kinetics of the degradation of Tlg2p in *vps45*Δ strains defective in either vacuolar protease activity or proteasomal activity, it has been demonstrated that the rapid degradation of Tlg2p in *vps45*Δ cells does not occur in *vps45*Δ strains lacking proteasomal activity (Bryant and James, 2001). This result strongly suggests that Tlg2p undergoes proteasomal degradation; however, the mechanism by which Tlg2p is targeted for this degradation is incompletely understood. This chapter presents data that leads to future work with two aims: One, to understand how the levels of Tlg2p are regulated; two, to examine the role played by Vps45p in this process.

5.2 Results

5.2.1 Stabilisation of Tlg2p in vps45Δ *cells by Vps45p and mutant versions thereof*

As discussed above, Vps45p helps stabilise the steady-state protein levels of Tlg2p (Bryant and James, 2001). To investigate the molecular mechanism of this

task, the abilities of various versions of Vps45p-HA to stabilise steady-state levels of Tlg2p were investigated. Figure 5.1 shows the steady-state levels of Tlg2p in wild-type cells (middle panel, lane 1) and *vps45*Δ cells (middle panel, lane 2). Consistent with previous reports (Bryant and James, 2001; Nichols *et al.*, 1998), Tlg2p was downregulated to undetectable levels in *vps45*Δ cells (while the levels of the cytosolic marker protein, phosphoglycerate kinase (PGK), did not change). The introduction of a single-copy plasmid driving the production of a C-terminally HA-tagged version of Vps45p (Vps45p-HA) stabilised the levels of Tlg2p in *vps45*Δ cells to those of wild-type (middle panel, lane 3), indicating that this HA-tagged version of Vps45p can perform the stabilisation function of the wild-type protein.

Despite being produced at approximately one-third the level of wild-type Vps45p-HA (middle panel, lane 4), the dominant negative version of Vps45p (Vps45p(W244R)-HA) was also able to stabilise the levels of Tlg2p in *vps45*Δ cells to those of wild-type (upper panel, lanes 3 and 4). While Vps45p(W244R)-HA was unable to complement the CPY missorting defect of *vps45*Δ cells (Figure 4.1), these data indicate that this failure is not due to an inability to stabilise Tlg2p in *vps45*Δ cells.

The pocket-filled version of Vps45p, Vps45p(L117R)-HA, is produced at similar levels to wild-type Vps45p-HA (upper panel, lanes 3 and 5). However, this amount of Vps45p(L117R)-HA was unable to stabilise the levels of Tlg2p in *vps45*Δ cells to those of wild-type cells. Rather, *vps45*Δ cells producing Vps45p(L117R)-HA contained only about one-fifth of the amount of Tlg2p in wild-type cells (middle panel, lanes 3 and 5). Interestingly, this reduced level of Tlg2p is sufficient to support normal membrane trafficking through the endosomal system, because this strain did not exhibit any defects with respect to the sorting of CPY (Figure 4.1).

The version of Vps45p harbouring both the pocket-filling and dominant negative mutations, Vps45p(L117R/W244R)-HA, was produced at approximately one-third the level of wild-type Vps45p-HA (upper panel, lanes 3 and 6). Like Vps45p(L117R)-HA, the production of Vps45p(L117R/W244R) was unable to effectively stabilise steady-state levels of Tlg2p in *vps45*Δ cells, with these cells containing approximately one-fifth of amount of Tlg2p in wild-type cells.

5.1.2 Steady-state levels of two versions of Tlg2p, unable to interact with Vps45p via the pocket mode, are highly elevated

The observation that Vps45p(L117R)-HA was unable to fully stabilise Tlg2p in *vps45Δ* cells (Figure 5.1) suggested that the pocket mode of interaction with Vps45p protects Tlg2p from degradation. To test this hypothesis, the production of two versions of Tlg2p which were previously demonstrated to be unable to interact with Vps45p via the pocket mode was examined: One version lacked the first N-terminal 36 residues (HA-Tlg2pΔN36), and the second version harboured the F9A/L10A mutations (HA-Tlg2p(F9A/L10A)). When produced recombinantly as fusion proteins, these versions of Tlg2p either did not bind Vps45p ($Tlg2p_{cyto}$ ΔN36-PrA; Figure 3.1) or were strongly impaired in their binding to Vps45p ($Tlg2p_{cyto}$ (F9A/L10A)-PrA; Figure 3.2c). The steady-state levels of each of these versions of Tlg2p in wild-type cells was assessed using immunoblot analysis (Figure 5.2). Compared to the steady-state levels of HA-Tlg2p (lanes 2 and 4), the levels of both HA-Tlg2pΔN36 (lane 3) and HA-Tlg2p(F9A/L10A) (lane 5) were greatly elevated, suggesting that interaction with Vps45p via the pocket mode helps target Tlg2p for its degradation. To reconcile this with the observation that Vps45p(L117R)-HA was unable to fully stabilise Tlg2p in *vps45Δ* cells (Figure 5.1), one explanation is that the truncation of the N-terminal 36 residues of Tlg2p and the F9A/L10A mutations in Tlg2p have had an additional effect, in addition to interfering with the pocket mode interaction with Vps45p. For example, a ubiquitin-conjugating enzyme may interact with this region to conjugate ubiquitin to Tlg2p; the HA-Tlg2pΔN36 and HA-Tlg2p(F9A/L10A) versions of Tlg2p may be inefficient substrates for this enzyme and therefore not be targeted for degradation. As an alternative to this possibility, HA-Tlg2pΔN36 and HA-Tlg2p(F9A/L10A) may be synthesised at increased rates; the elevated levels of these two versions of Tlg2p may be either due to increased synthesis, or a lack of degradation.

5.1.3 Ubiquitination of Tlg2p

The finding that Tlg2p undergoes proteasomal degradation (Bryant and James, 2001) implies that it must somehow be targeted for this degradation; the role of Lys^{48}-linked poly-ubiquitination in targeting substrate proteins to the proteasome

has been well described (Thrower *et al.*, 2000). One goal of future work is to determine whether Tlg2p is ubiquitinated, and if so, to map the sites of ubiquitination. Of the 397 amino acid residues comprising Tlg2p, 29 are lysines and potential ubiquitination sites: K26, K58, K60, K95, K99, K108, K121, K128, K134, K137, K148, K163, K168, K175, K185, K189, K193, K198, K218, K229, K297, K301, K305, K311, K315, K317, K336, K351, and K358. One of these residues, K26, is located in the N-terminal region of Tlg2p that mediates the pocket mode interaction with Vps45p (Figure 3.1). As an initial possibility to explain the overproduction of HA-Tlg2pΔN36 (Figure 5.2), it was hypothesised that a ubiquitination site was present in the truncated region, the removal of which meant that Tlg2p was unable to be ubiquitinated and therefore unable to be directed for degradation. To test this hypothesis, a K26R mutation was introduced into the HA-tagged version of Tlg2p shown in Figure 5.2, and the steady-state levels of HA-Tlg2p and HA-Tlg2p(K26R) in wild-type cells were examined. The data presented in Figure 5.3 indicate that HA-Tlg2p and HA-Tlg2p(K26R) are produced at similar levels, suggesting that if Tlg2p is regulated by ubiquitination, K26 is not the sole ubiquitination site. This result should be interpreted with the caveat that this does not conclusively demonstrate that K26 is not a site of ubiquitination, as the K26R mutation may merely result in the ubiquitination of alternative sites.

To examine the possibility that residue K26 of Tlg2p was shielded from exposure by the insertion of the N-terminal region of Tlg2p into the putative hydrophobic pocket of Vps45p, the production of HA-Tlg2p(K26R) in the absence of Vps45p was investigated. In this experiment, the steady-state levels of HA-Tlg2p and HA-Tlg2p(K26R) in *vps45*Δ cells were examined. The data presented in Figure 5.3 indicate that HA-Tlg2p and HA-Tlg2p(K26R) are still produced at similar levels, even in *vps45*Δ cells, suggesting that interaction with Vps45p does not shield residue K26 of Tlg2p.

5.1.4 Regulation of the protein levels of Snc2p

To investigate the effect of the absence of Vps45p on the steady-state protein levels of Snc2p, whole cell extracts from wild-type and *vps45*Δ cells producing an N-terminally HA-tagged version of Snc2p (HA-Snc2p) were prepared and the levels of HA-Snc2p in these extracts were compared. The data presented in

Figure 5.4 indicate that both Tlg2p and HA-Snc2p are downregulated to undetectable levels in the absence of Vps45p. In contrast to this, the levels of Tlg1p, Vti1p, and the non-SNARE control PGK were similar in both wild-type and *vps45Δ* cells, suggesting that the downregulation of Tlg2p and HA-Snc2p in the absence of Vps45p is specific to these two SNARE proteins.

As an initial step towards characterising the downregulation of Snc2p in *vps45Δ* cells, the same experiment was performed in a strain lacking vacuolar protease activity. The protease encoded by the *PEP4* gene, proteinase A, cleaves vacuolar proteases from their inactive precursors into their mature (i.e. active) forms; hence, *pep4-3* strains are deficient in vacuolar protease activity (Woolford *et al.*, 1986). The data presented in Figure 5.4 show that both Tlg2p and HA-Snc2p are downregulated in *pep4-3 vps45Δ* cells, indicating that this downregulation occurs even in the absence of active vacuolar proteases. This result suggests that Snc2p is degraded by the proteasome; to test this hypothesis, it will be investigated whether the levels of HA-Snc2p are stabilised in *vps45Δ* cells lacking proteasomal activity. If the levels of HA-Snc2p are stabilised in this case, it will be investigated whether Snc2p is ubiquitinated. If so, a further aim would be to map the sites of ubiquitination. Of the 115 amino acid residues comprising Snc2p, 6 of these are lysines and therefore potential sites of ubiquitination: K27, K48, K62, K74, K82, and K90.

Another goal of future work is to understand the role that Vps45p plays in protecting Snc2p from degradation, as suggested by the data presented in Figure 5.4. The interaction between Vps45p/Snc2p is not as well characterised as the Vps45p/Tlg2p interaction; therefore, it is not yet possible to construct versions of Snc2p that are unable to interact with Vps45p and examine their steady-state levels. As one future strategy, error-prone PCR will be used in concert with yeast two-hybrid work to generate versions of Snc2p that are unable to interact with Vps45p. This work will hopefully allow the role of the Vps45/Snc2p interaction to be investigated *in vivo*.

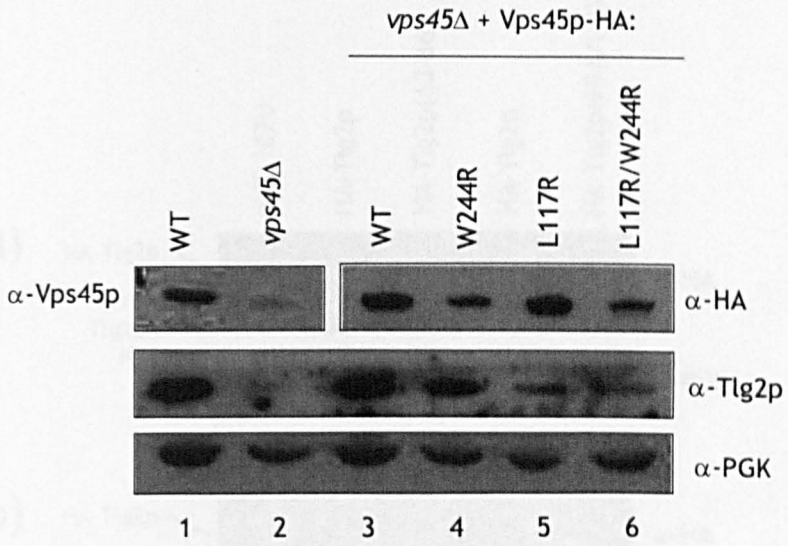

Figure 5.1 Stabilisation of Tlg2p in *vps45*Δ cells by Vps45p-HA (and mutant versions thereof). Proteins contained in whole cell extracts prepared from wild-type (9Dα) cells transformed with YCplac111 (parent vector; lane 1) or *vps45*Δ cells transformed with YCplac111 (parent vector; lane 2), pNB706 (*CEN*, driving the production of Vps45p-HA; lane 3), pNB707 (*CEN*, driving the production of Vps45p(W244R)-HA; lane 4), pNB708 (*CEN*, driving the production of Vps45p(L117R)-HA; lane 5), or pNB709 (*CEN*, driving the production of Vps45p(L117R/W244R)-HA; lane 6) were resolved by SDS-PAGE, transferred to nitrocellulose membrane, and probed with α-HA or α-Vps45p antibodies (upper panel), α-Tlg2p antibodies (middle panel), or α-PGK antibodies (lower panel).

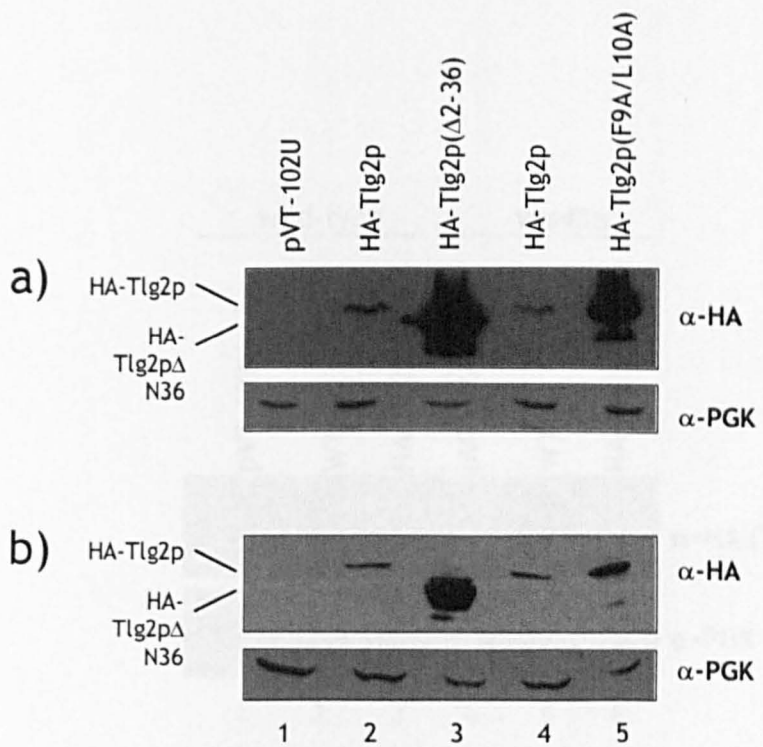

Figure 5.2 The steady-state levels of two versions of Tlg2p, unable to interact with Vps45p via the pocket mode, are highly elevated. a) Whole cell extracts were prepared from wild-type (RPY10) cells harbouring the following plasmids: pVT-102U (parent vector; lane 1), pHA-TLG2 (driving the production of HA-Tlg2p; lane 2), pCOG062 (driving the production of HA-Tlg2pΔN36; lane 3), pHA-TLG2 (driving the production of HA-Tlg2p; lane 4), or pCOG066 (driving the production of HA-Tlg2p(F9A/L10A); lane 5). Proteins contained within whole cell extracts were resolved by SDS-PAGE, transferred to nitrocellulose membrane, and probed with α-HA antibodies (upper panel) and α-PGK antibodies (lower panel). b) Same as (a), except that whole cell extracts were prepared from *vps45Δ* (NOzY2) cells.

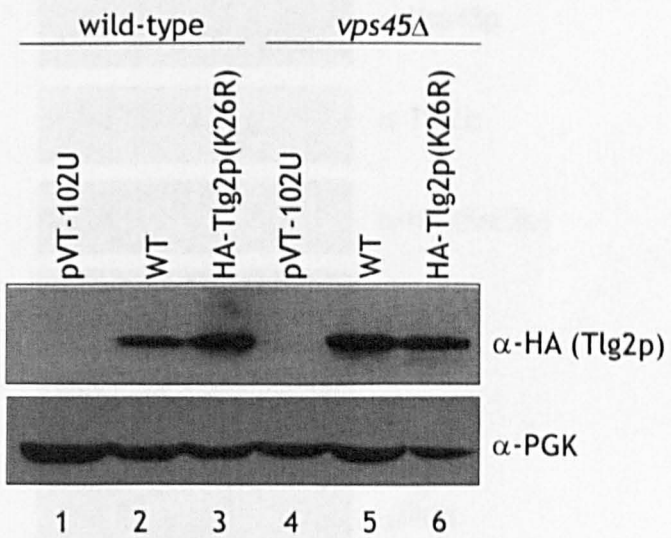

Figure 5.3 The K26R mutation does not affect the steady-state levels of HA-Tlg2p in either wild-type or *vps45*Δ cells. Whole cell extracts were prepared from wild-type (RPY10) or *vps45*Δ (NOzY2) cells harbouring the following plasmids: lanes 1 and 4) pVT-102U (parent vector); lanes 2 and 5) pHA-TLG2 (driving the production of HA-Tlg2p); lanes 3 and 6) pCOG063 (driving the production of HA-Tlg2p(K26R)). Proteins contained within whole cell extracts were resolved by SDS-PAGE, transferred to nitrocellulose membrane, and probed with α-HA (upper panel) or α-PGK (lower panel) antibodies.

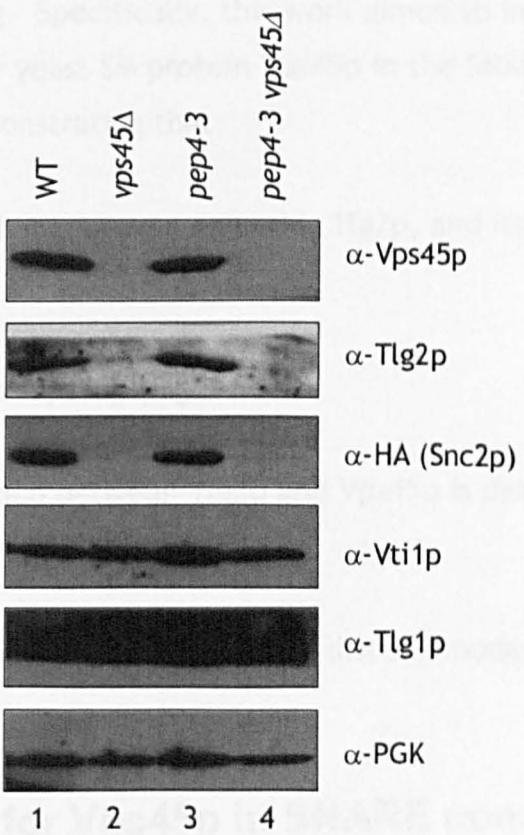

Figure 5.4 Tlg2p and Snc2p are downregulated in *vps45*Δ cells. Whole cell extracts were prepared from wild-type (RPY10), *vps45*Δ, *pep4-3* (9Dα), and *pep4-3 vps45*Δ (LCY008) cells co-transformed with the following plasmids: lane 1, pCOG064 (driving the production of Vps45p-HA) and pCOG054 (driving the production of HA-Snc2p); lanes 2-4, YEplac181 (parent vector) and pCOG054 (driving the production of HA-Snc2p). 1:10 and 1:200 dilutions of whole cell extracts were also created. Proteins contained within the extracts, and dilutions thereof, were resolved by SDS-PAGE and transferred to nitrocellulose membrane. Neat samples of whole cell extracts were probed with α-Vps45p and α-Tlg2p antibodies, 1:10 dilutions of whole cell extracts were probed with α-Vti1p and α-Tlg1p antibodies, and 1:200 dilutions of whole cell extracts were probed with α-HA and α-PGK antibodies.

Chapter Six: Discussion

SM proteins are universally required for membrane fusion, yet a hypothesis describing (a) common function(s) of SM proteins has remained elusive (Jahn, 2000; Toonen and Verhage, 2003). The overall goal of the work presented in this dissertation was to contribute to the current understanding of the role(s) of SM proteins in membrane trafficking. Specifically, this work aimed to investigate the function(s) performed by the yeast SM protein Vps45p in the SNARE cycle. This study was successful in demonstrating that:

1) Vps45p interacts with both its cognate syntaxin, Tlg2p, and its cognate v-SNARE, Snc2p (Figure 3.4)

2) Tlg2p displaces Snc2p from Vps45p (Figure 3.9)

3) The pocket mode interaction between Tlg2p and Vps45p is dispensable for the trafficking of CPY (Figure 4.1), and

4) Vps45p interacts with SNARE complexes via two distinct modes (Figures 4.10 and 4.11).

6.1 A proposed model for Vps45p in SNARE complex assembly

In Figure 6.1, a model describing the role of Vps45p in SNARE complex assembly is presented. In this model, Vps45p initially associates with vesicles destined for the endosomal system via interaction with Snc2p (a). The binding of Vps45p to Snc2p activates Vps45p to adopt its conformation favouring interaction with complexes via the mode distinct from the pocket mode (characterised in Figures 4.10 and 4.11), henceforth referred to as the "second mode". Vesicles laden with Vps45p are transported to target membranes, at which Tlg2p is waiting in a closed (fusion-incompetent) conformation (b). Upon arrival of the vesicle at the target membrane, Vps45p primes Tlg2p by triggering it to undergo a conformational change to an open (fusion-competent) configuration. At the same time, Vps45p releases Snc2p and brings it into close proximity to its cognate SNARE partners. The four SNARE proteins slot into the inner arch of

Vps45p, which acts as a mould to aid their assembly into *trans*-complexes (c). Vps45p associates with these *trans*-complexes via the second mode (N.B. this association is transient). The N-terminal region of Tlg2p soon inserts into the hydrophobic pocket of Vps45p, disrupting the second mode of interaction between Vps45p and *trans*-complexes and allowing the conversion of *trans*- to *cis*-complexes to proceed. Following fusion, Vps45p remains associated with *cis*-complexes via the pocket mode (d). Vps45p maintains its association with monomeric Tlg2p via this mode after *cis*-complexes are disassembled (e). Vps45p eventually dissociates from Tlg2p (f) and localises to the cytosol; Vps45p is now free to re-enter the cycle via its interaction with Snc2p-containing vesicles (a).

6.2 Discussion of model

The finding that Vps45p interacts specifically and directly with both Tlg2p and Snc2p (Figure 3.4) would support a role for SM proteins in ensuring the appropriateness of t- and v-SNARE pairing, as has been previously proposed (Peng and Gallwitz, 2002). Therefore, this model begins by proposing that the association of Vps45p with Snc2p-containing vesicles, followed by the interaction of Vps45p with Tlg2p, provides one layer of regulation to ensure that these vesicles are targeted to the endosomal system rather than to the plasma membrane. Predictions of this model that could be tested are that Vps45p associates with Snc2p *in vivo* prior to complex assembly, and that interfering with the Vps45p/Snc2p interaction would result in the mistargeting of vesicles destined for the endosomal system.

In this model, Vps45p next activates Tlg2p to adopt an open conformation. It is a matter of some controversy whether Tlg2p actually adopts a closed conformation, because NMR studies have not yielded any data to support this idea (Dulubova *et al.*, 2002). It is worth noting that truncated versions of Tlg2p were used in this study; therefore, the full-length version may adopt a closed conformation that was not detectable. Also, although the *in vitro* binding studies presented here (Figure 3.1) did not provide any evidence to suggest that Tlg2p and Vps45p interact in a mode analogous to that of the Munc18-1/syntaxin 1a interaction (i.e. with the syntaxin in its closed conformation), the recombinantly produced proteins used in these experiments lacked any post-

translational modifications which might influence this interaction *in vivo*. It has been demonstrated that Tlg2p can be phosphorylated *in vitro*, and that this phosphorylation inhibits its entry into complexes (Gurunathan *et al.*, 2002). If conformational changes of Tlg2p are regulated by phosphorylation, and if Tlg2p normally adopts an open conformation, it is possible that the recombinantly produced versions of Tlg2p used in these pull-down experiments cannot adopt a closed conformation. A second limitation of these *in vitro* pull-down experiments was that they did not provide any kinetic information about the interactions being studied; therefore, low affinity interactions may not have been uncovered in these experiments.

With no evidence from NMR studies to suggest that Tlg2p adopts a closed conformation (Dulubova *et al.*, 2002), and with no evidence from *in vitro* pull-down experiments to suggest that Tlg2p and Vps45p undertake a mode of interaction analogous to that observed in the Munc18-1/syntaxin 1a crystal structure ((Dulubova *et al.*, 2002), this work), why does this model propose that Tlg2p does adopt a closed conformation? Such a hypothesis provides a satisfying explanation for the finding that the removal of the H_{abc} domain (which would block the accessibility of its SNARE motif from entry into complexes if Tlg2p adopts a closed conformation) eliminates the positive requirement for Vps45p in SNARE complex assembly (Bryant and James, 2001). For this reason, and in light of the caveats to the negative data that have yielded no evidence to suggest that Tlg2p adopts a closed conformation, this model proposes that Vps45p activates Tlg2p to adopt an open conformation.

What is the mechanism by which Vps45p could induce Tlg2p to undergo a conformational change? This action would likely not be executed via the pocket mode interaction, since the pocket-filled mutant Vps45p(L117R) exhibits no observable functional defects (Figure 4.1), implying that this version of Vps45p is still able to facilitate the entry of Tlg2p into complexes. As one possibility for a mechanism, the inner cavity of Vps45p may contact the hinge region between the H_{abc} and SNARE domains of Tlg2p, destabilising the closed conformation (depicted in Figure 6.1b). The importance of the hinge region to the maintenance of the closed conformation has been demonstrated by point mutations in this region that create constitutively open versions of both syntaxin 1a (Dulubova *et al.*, 1999) and Sso1p (Munson *et al.*, 2000). Furthermore, it has

been speculated that a conformational change of Munc18-1 may destabilise the closed conformation of syntaxin 1a, perhaps by displacing the hinge region of syntaxin 1a and making its SNARE motif accessible (Misura *et al.*, 2000).

After activation of Tlg2p, this model proposes that Vps45p continues to play a positive role in fusion by aiding *trans*-complex assembly. Such a role would be consistent with the finding that SM proteins themselves positively influence fusion *in vitro* (Scott *et al.*, 2004). The inner arch of Vps45p is envisioned as a template to catalyse *trans*-complex assembly; helices corresponding to the SNARE motifs of the four SNARE members could slot into the inner cavity of the SM protein in a manner analogous to the four helices of syntaxin 1a in the Munc18-1/syntaxin 1a crystal structure (Misura *et al.*, 2000). If this mechanism is correct, it could help reconcile the discrepancy between the strikingly diverse interactions revealed by the Munc18-1/Sx1a and Sly1p/Sed5p(1-45) crystal structures with the high levels of homology exhibited by SM proteins.

The interaction between Vps45p and *trans*-complexes is hypothesised to be transient; this model proposes that after Tlg2p is primed, its N-terminal region is available for interaction with Vps45p. While Vps45p is bound to *trans*-complexes), the N-terminal region of Tlg2p inserts into the hydrophobic pocket of domain I of Vps45p, triggering a conformational change of Vps45p and aiding its dissociation from *trans*-complexes. The dominant negative version of Vps45p may be impaired in its ability to undergo this conformational change and remain trapped in a non-functional intermediate. As one possibility, the W244R mutation may affect a flexing/bending of the overall arch shape of Vps45p, leaving the mutant protein locked in a more open conformation that more easily accommodates trans-complexes in its inner cavity; this would account for the finding that only versions of Vps45p harbouring this mutation were observed to interact with complexes via the second mode (Figures 4.10 and 4.11).

This model must also account for the removal of the dominant negative effect of Vps45p(W244R) by the L117R mutation (Figure 4.4). Two possibilities would be 1) the pocket mode interaction recruits Vps45p to the site where the dominant negative version of the protein acts, or 2) the pocket mode interaction enhances the effect of the dominant negative version of the protein. The first option is difficult to reconcile with the observation that the pocket filled version of

Vps45p exhibited no observable functional defects, as this version is presumably still able to facilitate the entry of Tlg2p into complexes. Therefore, this model proposes that the pocket mode interaction contributes to a non-productive bridging intermediate between the N-terminal region of Tlg2p, Vps45p, and *trans*-complexes. While associated with *trans*-complexes, Vps45p(W244R) would interact with the N-terminal region of Tlg2p, fail to undergo a conformational change, and accumulate non-productive intermediates; whereas Vps45p(L117R/W244R) would not interact with the N-terminal region of Tlg2p and presumably dissociate rapidly from *trans*-complexes, failing to accumulate the non-productive intermediates. It is admittedly difficult to imagine how Vps45p could undergo both modes of interaction simultaneously, i.e. that the N-terminal region of Tlg2p could insert into the hydrophobic pocket of Vps45p as Vps45p is associated with *trans*-complexes via the second mode. However, this explanation would allow the pocket filled version of Vps45p to activate Tlg2p prior to complex assembly.

In this model, Vps45p remains associated with Tlg2p via the pocket mode during the disassembly of *cis*-complexes, and maintains this interaction afterwards with monomeric Tlg2p (e). This accounts for the finding that the pocket filled version of Vps45p was not associated with membranes (Figure 4.12), which implies that the pocket mode of interaction with Tlg2p mediates the membrane association of Vps45p. Although the pocket filled version of Vps45p might still be able to associate with Snc2p-containing vesicles (a), this pool of membrane-associated Vps45p would likely be too small to be detected in the fractionation experiments presented here.

This model implies that at some stage, Vps45p dissociates from Tlg2p (f) in order to enter its cytosolic pool and associate once more with Snc2p-containing vesicles (a). This model therefore raises the question of how the dissociation of Vps45p from Tlg2p would be orchestrated; one candidate mechanism is phosphorylation. As previously discussed, Tlg2p is phosphorylated *in vitro* (Gurunathan *et al.*, 2002), and preliminary experiments suggest that Tlg2p is also phosphorylated *in vivo* (Scott Shanks, University of Glasgow, unpublished data). The phosphorylation of recombinantly produced Tlg2p inhibits its assembly into complexes (Gurunathan *et al.*, 2002); therefore, it is tempting to speculate that phosphorylation stabilises the closed conformation of Tlg2p.

Perhaps this phosphorylation triggers Tlg2p to adopt its closed conformation, from which Vps45p subsequently dissociates and cycles back off into the cytosol (f). This would allow Vps45p to associate with Snc2p-containing vesicles once again, as depicted at the beginning of the cycle (a). The idea that Tlg2p is regulated by phosphorylation is currently being investigated by others (Scott Shanks), but is beyond the scope of the work presented here.

For simplicity, the model presented in Figure 6.1 does not address the contributions that Rabs, Arfs, coat proteins, and tethering proteins may make to the targeting of Snc2p-containing vesicles to the endosomal system. Physical and genetic interactions were recently demonstrated between Snc2p and Gcs1 Arf-GAP (an Arf-GTPase activating protein), prompting the formulation of a model in which Snc2p-containing vesicles destined for the TGN are sorted to their destination via a combination of coat proteins and their effectors (Robinson *et al.*, 2006). Furthermore, Vps45p interacts with Vac1p (a phosphatidylinositol 3-phosphate binding protein), which in turn interacts with the Rab GTPase Vps21p (Peterson *et al.*, 1999; Tall *et al.*, 1999). These data have suggested a model in which adaptor proteins, such as Vac1p, provide a physical link between vesicles (via interaction with activated Rabs) and target membranes (via interaction with phosphatidylinositol 3-phosphate) (Peterson *et al.*, 1999; Tall *et al.*, 1999). Physical interactions have also been demonstrated between Vac1p and Vps11p, a subunit of the class C VPS complex (Peterson and Emr, 2001); therefore, it has been proposed that this tethering complex may also facilitate the docking of transport vesicles to endosomal membranes (Peterson and Emr, 2001). These studies are reminders of the complexity of the *in vivo* environment and the importance of being aware of the contributions of other factors, outwith those discussed in this dissertation, which influence membrane trafficking.

6.3 Future Work

The work presented in this dissertation suggests some follow-on avenues of exploration. Specific future objectives include:

a) Further analysis of Vps45p/Tlg2p interaction(s)

As discussed in Chapter Three, the *in vitro* pull-down experiments used to investigate the interaction(s) between Vps45p and Tlg2p did not provide any kinetic information. To address this limitation, alternative experimental approaches for studying protein-protein interactions could be utilised. One such approach is Biacore chip technology, through which the rates of complex formation and dissociation can be determined, and the affinity of an interaction can be calculated. Future work is planned in collaboration with Sharon Kelly (University of Glasgow) to investigate whether Vps45p undertakes an additional mode of interaction (i.e. distinct from the pocket mode) with Tlg2p, perhaps one of lower affinity.

b) Characterisation of the Vps45p/Snc2p interaction

Using the same Biacore approach as discussed above, an additional aim is to determine the affinity of the Vps45p/Snc2p interaction. Additional goals include comparison of the affinities of Tlg2p and Snc2p for Vps45p, and of Vps45p and Vps45p(W244R) for Snc2p. As a complementary approach, yeast two-hybrid work aimed at identifying key residues of this interaction is being planned. This strategy will hopefully uncover mutant versions of Vps45p (or Snc2p) that exhibit reduced (or increased) binding to Snc2p (or Vps45p), and will be carried out by Chris MacDonald.

A further objective is to determine what (if any) role the Vps45p/Snc2p interaction plays *in vivo*. A first step would be to determine whether Vps45p associates with monomeric Snc2p, prior to its assembly into complexes (as postulated in the model presented in Figure 6.1). Then, if the yeast two-hybrid work yielded any mutant versions of Vps45p (or Snc2p) that exhibited a reduced (or increased) ability to interact with Snc2p (or Vps45p), the functional consequences of producing these versions of the relevant protein(s) could be examined.

c) Characterisation of the second mode of interaction of Vps45p with SNARE complexes.

The mechanism of the second mode of interaction undertaken by Vps45p with assembled complexes (Figures 4.10 and 4.11) is unknown. Structural studies of Vps45p and Vps45p(W244R) are being planned in collaboration with Mary Munson (University of Massachusetts). One aim of these studies is to investigate whether Vps45p(W244R) adopts a different default conformation than the wild-type version, as discussed in Chapter Four. Structural information about Vps45p(W244R) could also provide insight into the mechanism by which it interacts with complexes.

d) Effect of Vps45p on membrane fusion *in vitro*

The hypothesis that Vps45p acts as a mould to aid the assembly of *trans*-complexes predicts that Vps45p would have a stimulatory effect on membrane fusion *in vitro*, as assessed by the liposome fusion assay. Chris MacDonald and Fiona Brandie are planning to determine the effect of Vps45p on membrane fusion using this assay.

e) Regulation of the protein levels of Tlg2p and Snc2p by Vps45p.

Preliminary data presented in Chapter Five of this dissertation (Figure 5.4), in addition to previous studies (Bryant and James, 2001) suggest that Vps45p helps protect both Tlg2p and Snc2p from proteasomal degradation. As discussed in Chapter Five, immediate aims in this area include 1) determining whether Snc2p is stabilised in *vps45*Δ cells lacking proteasomal activity, 2) investigating whether Tlg2p and Snc2p are substrates for ubiquitination *in vivo*, and 3) if so, identifying their sites of ubiquitination. In addition, a screen aimed to identify versions of Tlg2p that are not downregulated in the absence of Vps45p is currently being constructed by Marion Struthers.

In summary, the work presented in this dissertation has made some contributions toward a unifying hypothesis for SM protein function. However, the extent to which the regulation of membrane trafficking by SM proteins is mechanistically conserved between the different transport pathways will no doubt be the subject of much additional research.

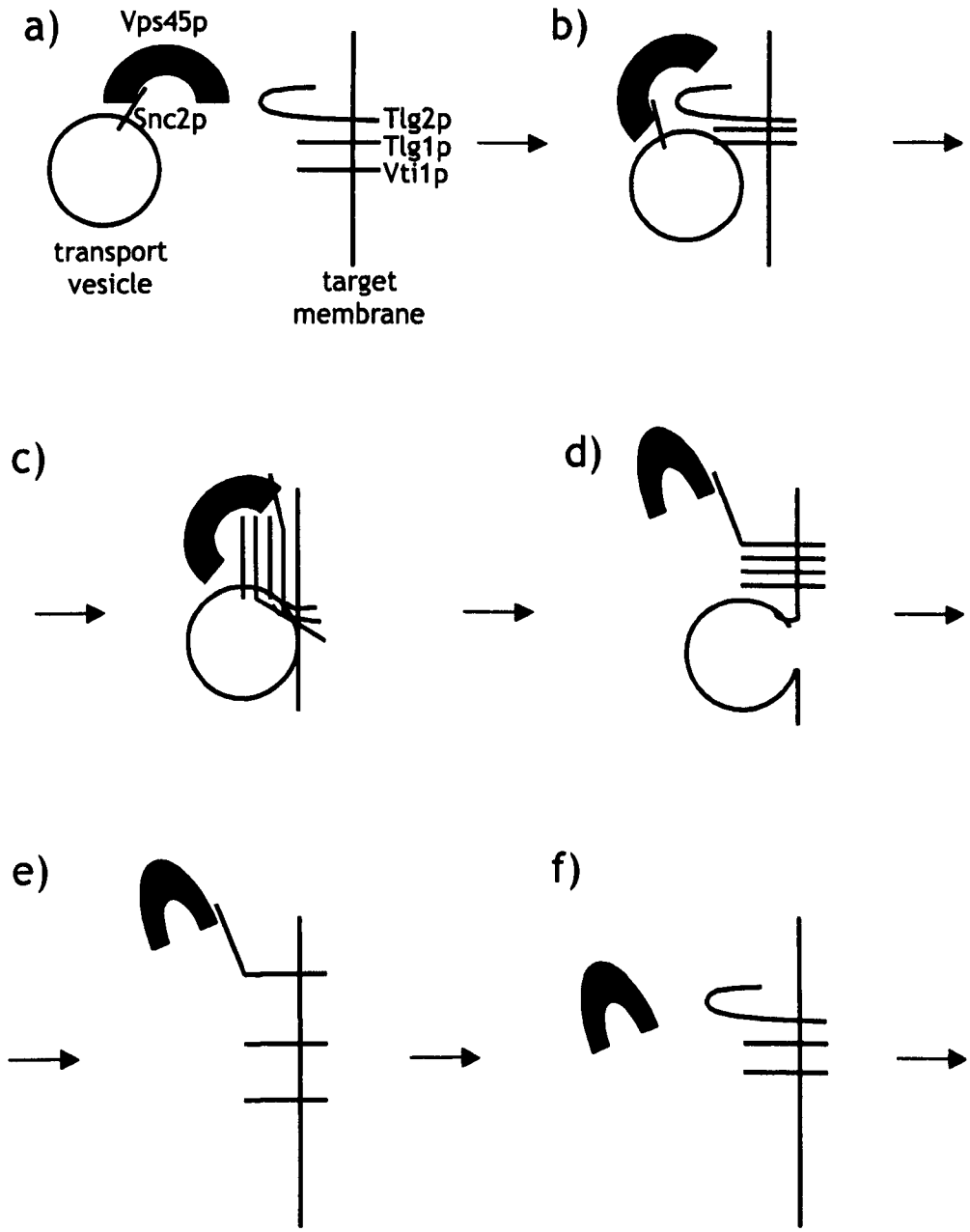

Figure 6.1 A proposed model for Vps45p in SNARE complex assembly. a) Vps45p associates with Snc2p-containing vesicles and is transported to target membranes marked by Tlg2p. b) Upon arrival at the target membrane, Vps45p primes Tlg2p by triggering its conformational change to a more open one. c) The inner cavity of Vps45p acts as a scaffold to facilitate the formation of *trans*-complexes, with which Vps45p associates via the second mode. d) Following the conversion of *trans*-to *cis*-complexes, Vps45p associates with the *cis*-complex via the pocket mode. e) Vps45p remains bound to monomeric Tlg2p via the pocket mode following the disassembly of *cis*-complexes. f) Vps45p eventually dissociates from Tlg2p, entering a cytosolic pool that is once again available to associate with Snc2p-containing vesicles as depicted in step (a).

Bibliography

Aalto, M.K., L. Ruohonen, K. Hosono, and S. Keranen. 1991. Cloning and sequencing of the yeast Saccharomyces cerevisiae SEC1 gene localized on chromosome IV. *Yeast*. 7:643-50.

Abeliovich, H., T. Darsow, and S.D. Emr. 1999. Cytoplasm to vacuole trafficking of aminopeptidase I requires a t-SNARE-Sec1p complex composed of Tlg2p and Vps45p. *Embo J*. 18:6005-16.

Abeliovich, H., E. Grote, P. Novick, and S. Ferro-Novick. 1998. Tlg2p, a yeast syntaxin homolog that resides on the Golgi and endocytic structures. *J Biol Chem*. 273:11719-27.

Antonin, W., I. Dulubova, D. Arac, S. Pabst, J. Plitzner, J. Rizo, and R. Jahn. 2002. The N-terminal domains of syntaxin 7 and vti1b form three-helix bundles that differ in their ability to regulate SNARE complex assembly. *J Biol Chem*. 277:36449-56.

Arac, D., I. Dulubova, J. Pei, I. Huryeva, N.V. Grishin, and J. Rizo. 2005. Three-dimensional structure of the rSly1 N-terminal domain reveals a conformational change induced by binding to syntaxin 5. *J Mol Biol*. 346:589-601.

Baba, M., M. Osumi, S.V. Scott, D.J. Klionsky, and Y. Ohsumi. 1997. Two distinct pathways for targeting proteins from the cytoplasm to the vacuole/lysosome. *J Cell Biol*. 139:1687-95.

Babst, M., D.J. Katzmann, E.J. Estepa-Sabal, T. Meerloo, and S.D. Emr. 2002a. Escrt-III: an endosome-associated heterooligomeric protein complex required for mvb sorting. *Dev Cell*. 3:271-82.

Babst, M., D.J. Katzmann, W.B. Snyder, B. Wendland, and S.D. Emr. 2002b. Endosome-associated complex, ESCRT-II, recruits transport machinery for protein sorting at the multivesicular body. *Dev Cell*. 3:283-9.

Bankaitis, V.A., L.M. Johnson, and S.D. Emr. 1986. Isolation of yeast mutants defective in protein targeting to the vacuole. *Proc Natl Acad Sci U S A*. 83:9075-9.

Banta, L.M., J.S. Robinson, D.J. Klionsky, and S.D. Emr. 1988. Organelle assembly in yeast: characterization of yeast mutants defective in vacuolar biogenesis and protein sorting. *J Cell Biol*. 107:1369-83.

Banta, L.M., T.A. Vida, P.K. Herman, and S.D. Emr. 1990. Characterization of yeast Vps33p, a protein required for vacuolar protein sorting and vacuole biogenesis. *Mol Cell Biol*. 10:4638-49.

Baumert, M., P.R. Maycox, F. Navone, P. De Camilli, and R. Jahn. 1989. Synaptobrevin: an integral membrane protein of 18,000 daltons present in small synaptic vesicles of rat brain. *Embo J*. 8:379-84.

Becherer, K.A., S.E. Rieder, S.D. Emr, and E.W. Jones. 1996. Novel syntaxin homologue, Pep12p, required for the sorting of lumenal hydrolases to the lysosome-like vacuole in yeast. *Mol Biol Cell*. 7:579-94.

Bennett, M.K., N. Calakos, and R.H. Scheller. 1992. Syntaxin: a synaptic protein implicated in docking of synaptic vesicles at presynaptic active zones. *Science*. 257:255-9.

Bennett, M.K., and R.H. Scheller. 1993. The molecular machinery for secretion is conserved from yeast to neurons. *Proc Natl Acad Sci U S A*. 90:2559-63.

Bensen, E.S., G. Costaguta, and G.S. Payne. 2000. Synthetic genetic interactions with temperature-sensitive clathrin in Saccharomyces cerevisiae. Roles for synaptojanin-like Inp53p and dynamin-related Vps1p in clathrin-

dependent protein sorting at the trans-Golgi network. *Genetics*. 154:83-97.

Blachly-Dyson, E., and T.H. Stevens. 1987. Yeast carboxypeptidase Y can be translocated and glycosylated without its amino-terminal signal sequence. *J Cell Biol*. 104:1183-91.

Block, M.R., B.S. Glick, C.A. Wilcox, F.T. Wieland, and J.E. Rothman. 1988. Purification of an N-ethylmaleimide-sensitive protein catalyzing vesicular transport. *Proc Natl Acad Sci U S A*. 85:7852-6.

Bock, J.B., H.T. Matern, A.A. Peden, and R.H. Scheller. 2001. A genomic perspective on membrane compartment organization. *Nature*. 409:839-41.

Bowers, K., and T.H. Stevens. 2005. Protein transport from the late Golgi to the vacuole in the yeast Saccharomyces cerevisiae. *Biochim Biophys Acta*. 1744:438-54.

Bracher, A., and W. Weissenhorn. 2001. Crystal structures of neuronal squid Sec1 implicate inter-domain hinge movement in the release of t-SNAREs. *J Mol Biol*. 306:7-13.

Bracher, A., and W. Weissenhorn. 2002. Structural basis for the Golgi membrane recruitment of Sly1p by Sed5p. *Embo J*. 21:6114-24.

Bracher, A., and W. Weissenhorn. 2004. Crystal structure of the Habc domain of neuronal syntaxin from the squid Loligo pealei reveals conformational plasticity at its C-terminus. *BMC Struct Biol*. 4:6.

Brickner, J.H., J.M. Blanchette, G. Sipos, and R.S. Fuller. 2001. The Tlg SNARE complex is required for TGN homotypic fusion. *J Cell Biol*. 155:969-78.

Bryant, N.J., and D.E. James. 2001. Vps45p stabilizes the syntaxin homologue Tlg2p and positively regulates SNARE complex formation. *Embo J*. 20:3380-8.

Bryant, N.J., and D.E. James. 2003. The Sec1p/Munc18 (SM) protein, Vps45p, cycles on and off membranes during vesicle transport. *J Cell Biol*. 161:691-6.

Bryant, N.J., and T.H. Stevens. 1998. Vacuole biogenesis in Saccharomyces cerevisiae: protein transport pathways to the yeast vacuole. *Microbiol Mol Biol Rev*. 62:230-47.

Burd, C.G., P.A. Mustol, P.V. Schu, and S.D. Emr. 1996. A yeast protein related to a mammalian Ras-binding protein, Vps9p, is required for localization of vacuolar proteins. *Mol Cell Biol*. 16:2369-77.

Burd, C.G., M. Peterson, C.R. Cowles, and S.D. Emr. 1997. A novel Sec18p/NSF-dependent complex required for Golgi-to-endosome transport in yeast. *Mol Biol Cell*. 8:1089-104.

Canaves, J.M., and M. Montal. 1998. Assembly of a ternary complex by the predicted minimal coiled-coil-forming domains of syntaxin, SNAP-25, and synaptobrevin. A circular dichroism study. *J Biol Chem*. 273:34214-21.

Carpp, L.N., L.F. Ciufo, S.G. Shanks, A. Boyd, and N.J. Bryant. 2006. The Sec1p/Munc18 protein Vps45p binds its cognate SNARE proteins via two distinct modes. *J Cell Biol*. 173:927-36.

Carr, C.M., E. Grote, M. Munson, F.M. Hughson, and P.J. Novick. 1999. Sec1p binds to SNARE complexes and concentrates at sites of secretion. *J Cell Biol*. 146:333-44.

Chen, Y.A., and R.H. Scheller. 2001. SNARE-mediated membrane fusion. *Nat Rev Mol Cell Biol*. 2:98-106.

Ciufo, L.F., J.W. Barclay, R.D. Burgoyne, and A. Morgan. 2005. Munc18-1 regulates early and late stages of exocytosis via syntaxin-independent protein interactions. *Mol Biol Cell*. 16:470-82.

Clary, D.O., I.C. Griff, and J.E. Rothman. 1990. SNAPs, a family of NSF attachment proteins involved in intracellular membrane fusion in animals and yeast. *Cell*. 61:709-21.

Coe, J.G., A.C. Lim, J. Xu, and W. Hong. 1999. A role for Tlg1p in the transport of proteins within the Golgi apparatus of Saccharomyces cerevisiae. *Mol Biol Cell*. 10:2407-23.

Cowles, C.R., S.D. Emr, and B.F. Horazdovsky. 1994. Mutations in the VPS45 gene, a SEC1 homologue, result in vacuolar protein sorting defects and accumulation of membrane vesicles. *J Cell Sci*. 107 (Pt 12):3449-59.

Cowles, C.R., W.B. Snyder, C.G. Burd, and S.D. Emr. 1997. Novel Golgi to vacuole delivery pathway in yeast: identification of a sorting determinant and required transport component. *Embo J*. 16:2769-82.

Dascher, C., R. Ossig, D. Gallwitz, and H.D. Schmitt. 1991. Identification and structure of four yeast genes (SLY) that are able to suppress the functional loss of YPT1, a member of the RAS superfamily. *Mol Cell Biol*. 11:872-85.

Deloche, O., and R.W. Schekman. 2002. Vps10p cycles between the TGN and the late endosome via the plasma membrane in clathrin mutants. *Mol Biol Cell*. 13:4296-307.

Deloche, O., B.G. Yeung, G.S. Payne, and R. Schekman. 2001. Vps10p transport from the trans-Golgi network to the endosome is mediated by clathrin-coated vesicles. *Mol Biol Cell*. 12:475-85.

Dresbach, T., M.E. Burns, V. O'Connor, W.M. DeBello, H. Betz, and G.J. Augustine. 1998. A neuronal Sec1 homolog regulates neurotransmitter release at the squid giant synapse. *J Neurosci*. 18:2923-32.

Dulubova, I., S. Sugita, S. Hill, M. Hosaka, I. Fernandez, T.C. Sudhof, and J. Rizo. 1999. A conformational switch in syntaxin during exocytosis: role of munc18. *Embo J*. 18:4372-82.

Dulubova, I., T. Yamaguchi, Y. Gao, S.W. Min, I. Huryeva, T.C. Sudhof, and J. Rizo. 2002. How Tlg2p/syntaxin 16 'snares' Vps45. *Embo J*. 21:3620-31.

Dulubova, I., T. Yamaguchi, Y. Wang, T.C. Sudhof, and J. Rizo. 2001. Vam3p structure reveals conserved and divergent properties of syntaxins. *Nat Struct Biol*. 8:258-64.

Egerton, M., J. Zueco, and A. Boyd. 1993. Molecular characterization of the SEC1 gene of Saccharomyces cerevisiae: subcellular distribution of a protein required for yeast protein secretion. *Yeast*. 9:703-13.

Emr, S.D., I. Schauer, W. Hansen, P. Esmon, and R. Schekman. 1984. Invertase beta-galactosidase hybrid proteins fail to be transported from the endoplasmic reticulum in Saccharomyces cerevisiae. *Mol Cell Biol*. 4:2347-55.

Esmon, P.C., B.E. Esmon, I.E. Schauer, A. Taylor, and R. Schekman. 1987. Structure, assembly, and secretion of octameric invertase. *J Biol Chem*. 262:4387-94.

Fasshauer, D., W.K. Eliason, A.T. Brunger, and R. Jahn. 1998a. Identification of a minimal core of the synaptic SNARE complex sufficient for reversible assembly and disassembly. *Biochemistry*. 37:10354-62.

Fasshauer, D., H. Otto, W.K. Eliason, R. Jahn, and A.T. Brunger. 1997. Structural changes are associated with soluble N-ethylmaleimide-sensitive fusion protein attachment protein receptor complex formation. *J Biol Chem*. 272:28036-41.

Fasshauer, D., R.B. Sutton, A.T. Brunger, and R. Jahn. 1998b. Conserved structural features of the synaptic fusion complex: SNARE proteins reclassified as Q- and R-SNAREs. *Proc Natl Acad Sci U S A*. 95:15781-6.

Fernandez, I., J. Ubach, I. Dulubova, X. Zhang, T.C. Sudhof, and J. Rizo. 1998. Three-dimensional structure of an evolutionarily conserved N-terminal domain of syntaxin 1A. *Cell*. 94:841-9.

Ferro-Novick, S., and R. Jahn. 1994. Vesicle fusion from yeast to man. *Nature*. 370:191-3.

Fiebig, K.M., L.M. Rice, E. Pollock, and A.T. Brunger. 1999. Folding intermediates of SNARE complex assembly. *Nat Struct Biol*. 6:117-23.

Finger, F.P., and P. Novick. 1998. Spatial regulation of exocytosis: lessons from yeast. *J Cell Biol*. 142:609-12.

Finger, F.P., and P. Novick. 2000. Synthetic interactions of the post-Golgi sec mutations of Saccharomyces cerevisiae. *Genetics*. 156:943-51.

Gallwitz, D., and R. Jahn. 2003. The riddle of the Sec1/Munc-18 proteins - new twists added to their interactions with SNAREs. *Trends Biochem Sci*. 28:113-6.

Garcia, E.P., E. Gatti, M. Butler, J. Burton, and P. De Camilli. 1994. A rat brain Sec1 homologue related to Rop and UNC18 interacts with syntaxin. *Proc Natl Acad Sci U S A*. 91:2003-7.

Gietz, R.D., and A. Sugino. 1988. New yeast-Escherichia coli shuttle vectors constructed with in vitro mutagenized yeast genes lacking six-base pair restriction sites. *Gene*. 74:527-34.

Gonzalez, L.C., Jr., W.I. Weis, and R.H. Scheller. 2001. A novel snare N-terminal domain revealed by the crystal structure of Sec22b. *J Biol Chem*. 276:24203-11.

Grabowski, R., and D. Gallwitz. 1997. High-affinity binding of the yeast cis-Golgi t-SNARE, Sed5p, to wild-type and mutant Sly1p, a modulator of transport vesicle docking. *FEBS Lett*. 411:169-72.

Grote, E., C.M. Carr, and P.J. Novick. 2000. Ordering the final events in yeast exocytosis. *J Cell Biol*. 151:439-52.

Gruenberg, J. 2001. The endocytic pathway: a mosaic of domains. *Nat Rev Mol Cell Biol*. 2:721-30.

Gurunathan, S., D. Chapman-Shimshoni, S. Trajkovic, and J.E. Gerst. 2000. Yeast exocytic v-SNAREs confer endocytosis. *Mol Biol Cell*. 11:3629-43.

Gurunathan, S., M. Marash, A. Weinberger, and J.E. Gerst. 2002. t-SNARE phosphorylation regulates endocytosis in yeast. *Mol Biol Cell*. 13:1594-607.

Halachmi, N., and Z. Lev. 1996. The Sec1 family: a novel family of proteins involved in synaptic transmission and general secretion. *J Neurochem*. 66:889-97.

Hama, H., G.G. Tall, and B.F. Horazdovsky. 1999. Vps9p is a guanine nucleotide exchange factor involved in vesicle-mediated vacuolar protein transport. *J Biol Chem*. 274:15284-91.

Hanahan, D. 1983. Studies on transformation of Escherichia coli with plasmids. *J Mol Biol*. 166:557-80.

Hanson, P.I., R. Roth, H. Morisaki, R. Jahn, and J.E. Heuser. 1997. Structure and conformational changes in NSF and its membrane receptor complexes visualized by quick-freeze/deep-etch electron microscopy. *Cell*. 90:523-35.

Harding, T.M., A. Hefner-Gravink, M. Thumm, and D.J. Klionsky. 1996. Genetic and phenotypic overlap between autophagy and the cytoplasm to vacuole protein targeting pathway. *J Biol Chem*. 271:17621-4.

Hardwick, K.G., and H.R. Pelham. 1992. SED5 encodes a 39-kD integral membrane protein required for vesicular transport between the ER and the Golgi complex. *J Cell Biol*. 119:513-21.

Harrison, S.D., K. Broadie, J. van de Goor, and G.M. Rubin. 1994. Mutations in the Drosophila Rop gene suggest a function in general secretion and synaptic transmission. *Neuron*. 13:555-66.

Hasilik, A., and W. Tanner. 1978. Biosynthesis of the vacuolar yeast glycoprotein carboxypeptidase Y. Conversion of precursor into the enzyme. *Eur J Biochem*. 85:599-608.

Hata, Y., C.A. Slaughter, and T.C. Sudhof. 1993. Synaptic vesicle fusion complex contains unc-18 homologue bound to syntaxin. *Nature*. 366:347-51.

Hayashi, T., H. McMahon, S. Yamasaki, T. Binz, Y. Hata, T.C. Sudhof, and H. Niemann. 1994. Synaptic vesicle membrane fusion complex: action of clostridial neurotoxins on assembly. *Embo J*. 13:5051-61.

Herman, P.K., and S.D. Emr. 1990. Characterization of VPS34, a gene required for vacuolar protein sorting and vacuole segregation in Saccharomyces cerevisiae. *Mol Cell Biol*. 10:6742-54.

Herman, P.K., J.H. Stack, J.A. DeModena, and S.D. Emr. 1991. A novel protein kinase homolog essential for protein sorting to the yeast lysosome-like vacuole. *Cell*. 64:425-37.

Hess, D.T., T.M. Slater, M.C. Wilson, and J.H. Skene. 1992. The 25 kDa synaptosomal-associated protein SNAP-25 is the major methionine-rich polypeptide in rapid axonal transport and a major substrate for palmitoylation in adult CNS. *J Neurosci*. 12:4634-41.

Hicke, L. 1999. Gettin' down with ubiquitin: turning off cell-surface receptors, transporters and channels. *Trends Cell Biol*. 9:107-12.

Hicke, L. 2001. Protein regulation by monoubiquitin. *Nat Rev Mol Cell Biol*. 2:195-201.

Horak, J. 2003. The role of ubiquitin in down-regulation and intracellular sorting of membrane proteins: insights from yeast. *Biochim Biophys Acta*. 1614:139-55.

Horazdovsky, B.F., G.R. Busch, and S.D. Emr. 1994. VPS21 encodes a rab5-like GTP binding protein that is required for the sorting of yeast vacuolar proteins. *Embo J*. 13:1297-309.

Horazdovsky, B.F., C.R. Cowles, P. Mustol, M. Holmes, and S.D. Emr. 1996. A novel RING finger protein, Vps8p, functionally interacts with the small GTPase, Vps21p, to facilitate soluble vacuolar protein localization. *J Biol Chem*. 271:33607-15.

Horazdovsky, B.F., and S.D. Emr. 1993. The VPS16 gene product associates with a sedimentable protein complex and is essential for vacuolar protein sorting in yeast. *J Biol Chem*. 268:4953-62.

Horsnell, W.G., G.J. Steel, and A. Morgan. 2002. Analysis of NSF mutants reveals residues involved in SNAP binding and ATPase stimulation. *Biochemistry*. 41:5230-5.

Hosono, R., S. Hekimi, Y. Kamiya, T. Sassa, S. Murakami, K. Nishiwaki, J. Miwa, A. Taketo, and K.I. Kodaira. 1992. The unc-18 gene encodes a novel protein affecting the kinetics of acetylcholine metabolism in the nematode Caenorhabditis elegans. *J Neurochem*. 58:1517-25.

Hurley, J.H., and S.D. Emr. 2006. The ESCRT complexes: structure and mechanism of a membrane-trafficking network. *Annu Rev Biophys Biomol Struct*. 35:277-98.

Ito, H., Y. Fukuda, K. Murata, and A. Kimura. 1983. Transformation of intact yeast cells treated with alkali cations. *J Bacteriol*. 153:163-8.

Jagadish, M.N., C.S. Fernandez, D.R. Hewish, S.L. Macaulay, K.H. Gough, J. Grusovin, A. Verkuylen, L. Cosgrove, A. Alafaci, M.J. Frenkel, and C.W. Ward. 1996. Insulin-responsive tissues contain the core complex protein

SNAP-25 (synaptosomal-associated protein 25) A and B isoforms in addition to syntaxin 4 and synaptobrevins 1 and 2. *Biochem J.* 317 (Pt 3):945-54.

Jagadish, M.N., J.T. Tellam, S.L. Macaulay, K.H. Gough, D.E. James, and C.W. Ward. 1997. Novel isoform of syntaxin 1 is expressed in mammalian cells. *Biochem J.* 321 (Pt 1):151-6.

Jahn, R. 2000. Sec1/Munc18 proteins: mediators of membrane fusion moving to center stage. *Neuron.* 27:201-4.

Jahn, R., and T.C. Sudhof. 1999. Membrane fusion and exocytosis. *Annu Rev Biochem.* 68:863-911.

Johnson, L.M., V.A. Bankaitis, and S.D. Emr. 1987. Distinct sequence determinants direct intracellular sorting and modification of a yeast vacuolar protease. *Cell.* 48:875-85.

Jones, E.W. 1977. Proteinase mutants of Saccharomyces cerevisiae. *Genetics.* 85:23-33.

Katzmann, D.J., M. Babst, and S.D. Emr. 2001. Ubiquitin-dependent sorting into the multivesicular body pathway requires the function of a conserved endosomal protein sorting complex, ESCRT-I. *Cell.* 106:145-55.

Kawasaki, M., K. Nakayama, and S. Wakatsuki. 2005. Membrane recruitment of effector proteins by Arf and Rab GTPases. *Curr Opin Struct Biol.* 15:681-9.

Kee, Y., R.C. Lin, S.C. Hsu, and R.H. Scheller. 1995. Distinct domains of syntaxin are required for synaptic vesicle fusion complex formation and dissociation. *Neuron.* 14:991-8.

Klionsky, D.J., and S.D. Emr. 1989. Membrane protein sorting: biosynthesis, transport and processing of yeast vacuolar alkaline phosphatase. *Embo J.* 8:2241-50.

Klionsky, D.J., and S.D. Emr. 2000. Autophagy as a regulated pathway of cellular degradation. *Science.* 290:1717-21.

Klionsky, D.J., P.K. Herman, and S.D. Emr. 1990. The fungal vacuole: composition, function, and biogenesis. *Microbiol Rev.* 54:266-92.

Laemmli, U.K. 1970. Cleavage of structural proteins during the assembly of the head of bacteriophage T4. *Nature.* 227:680-5.

LaGrassa, T.J., and C. Ungermann. 2005. The vacuolar kinase Yck3 maintains organelle fragmentation by regulating the HOPS tethering complex. *J Cell Biol.* 168:401-14.

Lerman, J.C., J. Robblee, R. Fairman, and F.M. Hughson. 2000. Structural analysis of the neuronal SNARE protein syntaxin-1A. *Biochemistry.* 39:8470-9.

Lin, R.C., and R.H. Scheller. 1997. Structural organization of the synaptic exocytosis core complex. *Neuron.* 19:1087-94.

Lin, R.C., and R.H. Scheller. 2000. Mechanisms of synaptic vesicle exocytosis. *Annu Rev Cell Dev Biol.* 16:19-49.

Lipschutz, J.H., and K.E. Mostov. 2002. Exocytosis: the many masters of the exocyst. *Curr Biol.* 12:R212-4.

Marcusson, E.G., B.F. Horazdovsky, J.L. Cereghino, E. Gharakhanian, and S.D. Emr. 1994. The sorting receptor for yeast vacuolar carboxypeptidase Y is encoded by the VPS10 gene. *Cell.* 77:579-86.

Mayer, A., W. Wickner, and A. Haas. 1996. Sec18p (NSF)-driven release of Sec17p (alpha-SNAP) can precede docking and fusion of yeast vacuoles. *Cell.* 85:83-94.

McNew, J.A., F. Parlati, R. Fukuda, R.J. Johnston, K. Paz, F. Paumet, T.H. Sollner, and J.E. Rothman. 2000. Compartmental specificity of cellular membrane fusion encoded in SNARE proteins. *Nature.* 407:153-9.

Misura, K.M., J.B. Bock, L.C. Gonzalez, Jr., R.H. Scheller, and W.I. Weis. 2002. Three-dimensional structure of the amino-terminal domain of syntaxin 6, a SNAP-25 C homolog. *Proc Natl Acad Sci U S A*. 99:9184-9.

Misura, K.M., R.H. Scheller, and W.I. Weis. 2000. Three-dimensional structure of the neuronal-Sec1-syntaxin 1a complex. *Nature*. 404:355-62.

Munson, M., X. Chen, A.E. Cocina, S.M. Schultz, and F.M. Hughson. 2000. Interactions within the yeast t-SNARE Sso1p that control SNARE complex assembly. *Nat Struct Biol*. 7:894-902.

Nichols, B.J., J.C. Holthuis, and H.R. Pelham. 1998. The Sec1p homologue Vps45p binds to the syntaxin Tlg2p. *Eur J Cell Biol*. 77:263-8.

Nicholson, K.L., M. Munson, R.B. Miller, T.J. Filip, R. Fairman, and F.M. Hughson. 1998. Regulation of SNARE complex assembly by an N-terminal domain of the t-SNARE Sso1p. *Nat Struct Biol*. 5:793-802.

Nickel, W., T. Weber, J.A. McNew, F. Parlati, T.H. Sollner, and J.E. Rothman. 1999. Content mixing and membrane integrity during membrane fusion driven by pairing of isolated v-SNAREs and t-SNAREs. *Proc Natl Acad Sci U S A*. 96:12571-6.

Nilsson, B., T. Moks, B. Jansson, L. Abrahmsen, A. Elmblad, E. Holmgren, C. Henrichson, T.A. Jones, and M. Uhlen. 1987. A synthetic IgG-binding domain based on staphylococcal protein A. *Protein Eng*. 1:107-13.

Noda, T., and Y. Ohsumi. 1998. Tor, a phosphatidylinositol kinase homologue, controls autophagy in yeast. *J Biol Chem*. 273:3963-6.

Nothwehr, S.F., N.J. Bryant, and T.H. Stevens. 1996. The newly identified yeast GRD genes are required for retention of late-Golgi membrane proteins. *Mol Cell Biol*. 16:2700-7.

Novick, P., S. Ferro, and R. Schekman. 1981. Order of events in the yeast secretory pathway. *Cell*. 25:461-9.

Novick, P., C. Field, and R. Schekman. 1980. Identification of 23 complementation groups required for post-translational events in the yeast secretory pathway. *Cell*. 21:205-15.

Novick, P., and R. Schekman. 1979. Secretion and cell-surface growth are blocked in a temperature-sensitive mutant of Saccharomyces cerevisiae. *Proc Natl Acad Sci U S A*. 76:1858-62.

Ossig, R., C. Dascher, H.H. Trepte, H.D. Schmitt, and D. Gallwitz. 1991. The yeast SLY gene products, suppressors of defects in the essential GTP-binding Ypt1 protein, may act in endoplasmic reticulum-to-Golgi transport. *Mol Cell Biol*. 11:2980-93.

Oyler, G.A., G.A. Higgins, R.A. Hart, E. Battenberg, M. Billingsley, F.E. Bloom, and M.C. Wilson. 1989. The identification of a novel synaptosomal-associated protein, SNAP-25, differentially expressed by neuronal subpopulations. *J Cell Biol*. 109:3039-52.

Panek, H.R., E. Conibear, J.D. Bryan, R.T. Colvin, C.D. Goshorn, and L.C. Robinson. 2000. Identification of Rgp1p, a novel Golgi recycling factor, as a protein required for efficient localization of yeast casein kinase 1 to the plasma membrane. *J Cell Sci*. 113 Pt 24:4545-55.

Parlati, F., J.A. McNew, R. Fukuda, R. Miller, T.H. Sollner, and J.E. Rothman. 2000. Topological restriction of SNARE-dependent membrane fusion. *Nature*. 407:194-8.

Parlati, F., O. Varlamov, K. Paz, J.A. McNew, D. Hurtado, T.H. Sollner, and J.E. Rothman. 2002. Distinct SNARE complexes mediating membrane fusion in Golgi transport based on combinatorial specificity. *Proc Natl Acad Sci U S A*. 99:5424-9.

Parlati, F., T. Weber, J.A. McNew, B. Westermann, T.H. Sollner, and J.E. Rothman. 1999. Rapid and efficient fusion of phospholipid vesicles by the

alpha-helical core of a SNARE complex in the absence of an N-terminal regulatory domain. *Proc Natl Acad Sci U S A.* 96:12565-70.

Paumet, F., B. Brugger, F. Parlati, J.A. McNew, T.H. Sollner, and J.E. Rothman. 2001. A t-SNARE of the endocytic pathway must be activated for fusion. *J Cell Biol.* 155:961-8.

Pelham, H.R. 1999. SNAREs and the secretory pathway-lessons from yeast. *Exp Cell Res.* 247:1-8.

Pelham, H.R. 2002. Insights from yeast endosomes. *Curr Opin Cell Biol.* 14:454-62.

Peng, R., and D. Gallwitz. 2002. Sly1 protein bound to Golgi syntaxin Sed5p allows assembly and contributes to specificity of SNARE fusion complexes. *J Cell Biol.* 157:645-55.

Peng, R., and D. Gallwitz. 2004. Multiple SNARE interactions of an SM protein: Sed5p/Sly1p binding is dispensable for transport. *Embo J.* 23:3939-49.

Peters, J.M. 1994. Proteasomes: protein degradation machines of the cell. *Trends Biochem Sci.* 19:377-82.

Peters, J.M., W.W. Franke, and J.A. Kleinschmidt. 1994. Distinct 19 S and 20 S subcomplexes of the 26 S proteasome and their distribution in the nucleus and the cytoplasm. *J Biol Chem.* 269:7709-18.

Peterson, M.R., C.G. Burd, and S.D. Emr. 1999. Vac1p coordinates Rab and phosphatidylinositol 3-kinase signaling in Vps45p-dependent vesicle docking/fusion at the endosome. *Curr Biol.* 9:159-62.

Peterson, M.R., and S.D. Emr. 2001. The class C Vps complex functions at multiple stages of the vacuolar transport pathway. *Traffic.* 2:476-86.

Pevsner, J. 1996. The role of Sec1p-related proteins in vesicle trafficking in the nerve terminal. *J Neurosci Res.* 45:89-95.

Pevsner, J., S.C. Hsu, J.E. Braun, N. Calakos, A.E. Ting, M.K. Bennett, and R.H. Scheller. 1994a. Specificity and regulation of a synaptic vesicle docking complex. *Neuron.* 13:353-61.

Pevsner, J., S.C. Hsu, and R.H. Scheller. 1994b. n-Sec1: a neural-specific syntaxin-binding protein. *Proc Natl Acad Sci U S A.* 91:1445-9.

Pfeffer, S.R. 1999. Transport-vesicle targeting: tethers before SNAREs. *Nat Cell Biol.* 1:E17-22.

Pickart, C.M. 2004. Back to the future with ubiquitin. *Cell.* 116:181-90.

Piper, R.C., N.J. Bryant, and T.H. Stevens. 1997. The membrane protein alkaline phosphatase is delivered to the vacuole by a route that is distinct from the VPS-dependent pathway. *J Cell Biol.* 138:531-45.

Piper, R.C., E.A. Whitters, and T.H. Stevens. 1994. Yeast Vps45p is a Sec1p-like protein required for the consumption of vacuole-targeted, post-Golgi transport vesicles. *Eur J Cell Biol.* 65:305-18.

Poirier, M.A., J.C. Hao, P.N. Malkus, C. Chan, M.F. Moore, D.S. King, and M.K. Bennett. 1998. Protease resistance of syntaxin.SNAP-25.VAMP complexes. Implications for assembly and structure. *J Biol Chem.* 273:11370-7.

Price, A., D. Seals, W. Wickner, and C. Ungermann. 2000. The docking stage of yeast vacuole fusion requires the transfer of proteins from a cis-SNARE complex to a Rab/Ypt protein. *J Cell Biol.* 148:1231-8.

Protopopov, V., B. Govindan, P. Novick, and J.E. Gerst. 1993. Homologs of the synaptobrevin/VAMP family of synaptic vesicle proteins function on the late secretory pathway in S. cerevisiae. *Cell.* 74:855-61.

Raymond, C.K., I. Howald-Stevenson, C.A. Vater, and T.H. Stevens. 1992. Morphological classification of the yeast vacuolar protein sorting mutants: evidence for a prevacuolar compartment in class E vps mutants. *Mol Biol Cell.* 3:1389-402.

Raymond, C.K., P.J. O'Hara, G. Eichinger, J.H. Rothman, and T.H. Stevens. 1990. Molecular analysis of the yeast VPS3 gene and the role of its product in vacuolar protein sorting and vacuolar segregation during the cell cycle. *J Cell Biol.* 111:877-92.

Rayner, J.C., and S. Munro. 1998. Identification of the MNN2 and MNN5 mannosyltransferases required for forming and extending the mannose branches of the outer chain mannans of Saccharomyces cerevisiae. *J Biol Chem.* 273:26836-43.

Riento, K., M. Kauppi, S. Keranen, and V.M. Olkkonen. 2000. Munc18-2, a functional partner of syntaxin 3, controls apical membrane trafficking in epithelial cells. *J Biol Chem.* 275:13476-83.

Rivett, A.J. 1993. Proteasomes: multicatalytic proteinase complexes. *Biochem J.* 291 (Pt 1):1-10.

Rizo, J., and T.C. Sudhof. 2002. Snares and Munc18 in synaptic vesicle fusion. *Nat Rev Neurosci.* 3:641-53.

Robinson, J.S., D.J. Klionsky, L.M. Banta, and S.D. Emr. 1988. Protein sorting in Saccharomyces cerevisiae: isolation of mutants defective in the delivery and processing of multiple vacuolar hydrolases. *Mol Cell Biol.* 8:4936-48.

Robinson, M., P.P. Poon, C. Schindler, L.E. Murray, R. Kama, G. Gabriely, R.A. Singer, A. Spang, G.C. Johnston, and J.E. Gerst. 2006. The Gcs1 Arf-GAP mediates Snc1,2 v-SNARE retrieval to the Golgi in yeast. *Mol Biol Cell.* 17:1845-58.

Roeder, A.D., and J.M. Shaw. 1996. Vacuole partitioning during meiotic division in yeast. *Genetics.* 144:445-58.

Rothman, J.E. 1994. Mechanisms of intracellular protein transport. *Nature.* 372:55-63.

Rothman, J.H., I. Howald, and T.H. Stevens. 1989. Characterization of genes required for protein sorting and vacuolar function in the yeast Saccharomyces cerevisiae. *Embo J.* 8:2057-65.

Rothman, J.H., and T.H. Stevens. 1986. Protein sorting in yeast: mutants defective in vacuole biogenesis mislocalize vacuolar proteins into the late secretory pathway. *Cell.* 47:1041-51.

Rotin, D., O. Staub, and R. Haguenauer-Tsapis. 2000. Ubiquitination and endocytosis of plasma membrane proteins: role of Nedd4/Rsp5p family of ubiquitin-protein ligases. *J Membr Biol.* 176:1-17.

Sambrook, J., E. F. Fritsch, *et al.* 1989. Molecular Cloning: A Laboratory Manual. Cold Spring Harbor, NY, Cold Spring Harbor Laboratory Press.

Sato, T.K., P. Rehling, M.R. Peterson, and S.D. Emr. 2000. Class C Vps protein complex regulates vacuolar SNARE pairing and is required for vesicle docking/fusion. *Mol Cell.* 6:661-71.

Schmid, S.L. 1997. Clathrin-coated vesicle formation and protein sorting: an integrated process. *Annu Rev Biochem.* 66:511-48.

Schmitt, H.D., M. Puzicha, and D. Gallwitz. 1988. Study of a temperature-sensitive mutant of the ras-related YPT1 gene product in yeast suggests a role in the regulation of intracellular calcium. *Cell.* 53:635-47.

Schu, P.V., K. Takegawa, M.J. Fry, J.H. Stack, M.D. Waterfield, and S.D. Emr. 1993. Phosphatidylinositol 3-kinase encoded by yeast VPS34 gene essential for protein sorting. *Science.* 260:88-91.

Schulze, K.L., J.T. Littleton, A. Salzberg, N. Halachmi, M. Stern, Z. Lev, and H.J. Bellen. 1994. rop, a Drosophila homolog of yeast Sec1 and vertebrate n-Sec1/Munc-18 proteins, is a negative regulator of neurotransmitter release in vivo. *Neuron.* 13:1099-108.

Schulze, K.L., K. Broadie, M.S. Perin, and H.J. Bellen. 1995. Genetic and electrophysiological studies of Drosophila syntaxin-1A demonstrate its role in nonneuronal secretion and neurotransmission. *Cell*. 80:311-20.

Schutz, D., F. Zilly, T. Lang, R. Jahn, and D. Bruns. 2005. A dual function for Munc-18 in exocytosis of PC12 cells. *Eur J Neurosci*. 21:2419-32.

Scopes, R.K. 1975. 3-phosphoglycerate kinase of baker's yeast. *Methods Enzymol*. 42:134-8.

Scott, B.L., J.S. Van Komen, H. Irshad, S. Liu, K.A. Wilson, and J.A. McNew. 2004. Sec1p directly stimulates SNARE-mediated membrane fusion in vitro. *J Cell Biol*. 167:75-85.

Seaman, M.N., E.G. Marcusson, J.L. Cereghino, and S.D. Emr. 1997. Endosome to Golgi retrieval of the vacuolar protein sorting receptor, Vps10p, requires the function of the VPS29, VPS30, and VPS35 gene products. *J Cell Biol*. 137:79-92.

Segev, N., J. Mulholland, and D. Botstein. 1988. The yeast GTP-binding YPT1 protein and a mammalian counterpart are associated with the secretion machinery. *Cell*. 52:915-24.

Seron, K., V. Tieaho, C. Prescianotto-Baschong, T. Aust, M.O. Blondel, P. Guillaud, G. Devilliers, O.W. Rossanese, B.S. Glick, H. Riezman, S. Keranen, and R. Haguenauer-Tsapis. 1998. A yeast t-SNARE involved in endocytosis. *Mol Biol Cell*. 9:2873-89.

Shaw, J.D., K.B. Cummings, G. Huyer, S. Michaelis, and B. Wendland. 2001. Yeast as a model system for studying endocytosis. *Exp Cell Res*. 271:1-9.

Sherman, F., Fink, G.R. and Hicks, J. 1986. Methods in Yeast Genetics. Cold Spring Harbor Laboratory Press, Cold Spring Harbor, NY, pp. 146-153.

Sikorski, R.S., and P. Hieter. 1989. A system of shuttle vectors and yeast host strains designed for efficient manipulation of DNA in Saccharomyces cerevisiae. *Genetics*. 122:19-27.

Sollner, T., M.K. Bennett, S.W. Whiteheart, R.H. Scheller, and J.E. Rothman. 1993a. A protein assembly-disassembly pathway in vitro that may correspond to sequential steps of synaptic vesicle docking, activation, and fusion. *Cell*. 75:409-18.

Sollner, T., S.W. Whiteheart, M. Brunner, H. Erdjument-Bromage, S. Geromanos, P. Tempst, and J.E. Rothman. 1993b. SNAP receptors implicated in vesicle targeting and fusion. *Nature*. 362:318-24.

Stevens, T., B. Esmon, and R. Schekman. 1982. Early stages in the yeast secretory pathway are required for transport of carboxypeptidase Y to the vacuole. *Cell*. 30:439-48.

Struck, D.K., D. Hoekstra, and R.E. Pagano. 1981. Use of resonance energy transfer to monitor membrane fusion. *Biochemistry*. 20:4093-9.

Sutton, R.B., D. Fasshauer, R. Jahn, and A.T. Brunger. 1998. Crystal structure of a SNARE complex involved in synaptic exocytosis at 2.4 A resolution. *Nature*. 395:347-53.

Tall, G.G., H. Hama, D.B. DeWald, and B.F. Horazdovsky. 1999. The phosphatidylinositol 3-phosphate binding protein Vac1p interacts with a Rab GTPase and a Sec1p homologue to facilitate vesicle-mediated vacuolar protein sorting. *Mol Biol Cell*. 10:1873-89.

Tang, B.L., D.Y. Low, and W. Hong. 1998. Syntaxin 11: a member of the syntaxin family without a carboxyl terminal transmembrane domain. *Biochem Biophys Res Commun*. 245:627-32.

Thrower, J.S., L. Hoffman, M. Rechsteiner, and C.M. Pickart. 2000. Recognition of the polyubiquitin proteolytic signal. *Embo J*. 19:94-102.

Thurmond, D.C., B.P. Ceresa, S. Okada, J.S. Elmendorf, K. Coker, and J.E. Pessin. 1998. Regulation of insulin-stimulated GLUT4 translocation by Munc18c in 3T3L1 adipocytes. *J Biol Chem.* 273:33876-83.

Thurmond, D.C., M. Kanzaki, A.H. Khan, and J.E. Pessin. 2000. Munc18c function is required for insulin-stimulated plasma membrane fusion of GLUT4 and insulin-responsive amino peptidase storage vesicles. *Mol Cell Biol.* 20:379-88.

Toonen, R.F., K.J. de Vries, R. Zalm, T.C. Sudhof, and M. Verhage. 2005. Munc18-1 stabilizes syntaxin 1, but is not essential for syntaxin 1 targeting and SNARE complex formation. *J Neurochem.* 93:1393-400.

Toonen, R.F., and M. Verhage. 2003. Vesicle trafficking: pleasure and pain from SM genes. *Trends Cell Biol.* 13:177-86.

Trimble, R.B., F. Maley, and F.K. Chu. 1983. GlycoProtein biosynthesis in yeast. protein conformation affects processing of high mannose oligosaccharides on carboxypeptidase Y and invertase. *J Biol Chem.* 258:2562-7.

Trimble, W.S., D.M. Cowan, and R.H. Scheller. 1988. VAMP-1: a synaptic vesicle-associated integral membrane protein. *Proc Natl Acad Sci U S A.* 85:4538-42.

Ungar, D., and F.M. Hughson. 2003. SNARE protein structure and function. *Annu Rev Cell Dev Biol.* 19:493-517.

Ungermann, C., and D. Langosch. 2005. Functions of SNAREs in intracellular membrane fusion and lipid bilayer mixing. *J Cell Sci.* 118:3819-28.

Ungermann, C., K. Sato, and W. Wickner. 1998. Defining the functions of trans-SNARE pairs. *Nature.* 396:543-8.

Urbanowski, J.L., and R.C. Piper. 2001. Ubiquitin sorts proteins into the intralumenal degradative compartment of the late-endosome/vacuole. *Traffic.* 2:622-30.

Urbe, S. 2005. Ubiquitin and endocytic protein sorting. *Essays Biochem.* 41:81-98.

Valdivia, R.H., D. Baggott, J.S. Chuang, and R.W. Schekman. 2002. The yeast clathrin adaptor protein complex 1 is required for the efficient retention of a subset of late Golgi membrane proteins. *Dev Cell.* 2:283-94.

Valls, L.A., C.P. Hunter, J.H. Rothman, and T.H. Stevens. 1987. Protein sorting in yeast: the localization determinant of yeast vacuolar carboxypeptidase Y resides in the propeptide. *Cell.* 48:887-97.

Verhage, M., A.S. Maia, J.J. Plomp, A.B. Brussaard, J.H. Heeroma, H. Vermeer, R.F. Toonen, R.E. Hammer, T.K. van den Berg, M. Missler, H.J. Geuze, and T.C. Sudhof. 2000. Synaptic assembly of the brain in the absence of neurotransmitter secretion. *Science.* 287:864-9.

Vernet, T., D. Dignard, and D.Y. Thomas. 1987. A family of yeast expression vectors containing the phage f1 intergenic region. *Gene.* 52:225-33.

Vida, T.A., G. Huyer, and S.D. Emr. 1993. Yeast vacuolar proenzymes are sorted in the late Golgi complex and transported to the vacuole via a prevacuolar endosome-like compartment. *J Cell Biol.* 121:1245-56.

Voets, T., R.F. Toonen, E.C. Brian, H. de Wit, T. Moser, J. Rettig, T.C. Sudhof, E. Neher, and M. Verhage. 2001. Munc18-1 promotes large dense-core vesicle docking. *Neuron.* 31:581-91.

Wada, Y., and Y. Anraku. 1992. Genes for directing vacuolar morphogenesis in Saccharomyces cerevisiae. II. VAM7, a gene for regulating morphogenic assembly of the vacuoles. *J Biol Chem.* 267:18671-5.

Wada, Y., K. Kitamoto, T. Kanbe, K. Tanaka, and Y. Anraku. 1990. The SLP1 gene of Saccharomyces cerevisiae is essential for vacuolar morphogenesis and function. *Mol Cell Biol.* 10:2214-23.

Webb, G.C., M. Hoedt, L.J. Poole, and E.W. Jones. 1997. Genetic interactions between a pep7 mutation and the PEP12 and VPS45 genes: evidence for a novel SNARE component in transport between the Saccharomyces cerevisiae Golgi complex and endosome. *Genetics*. 147:467-78.

Weber, T., B.V. Zemelman, J.A. McNew, B. Westermann, M. Gmachl, F. Parlati, T.H. Sollner, and J.E. Rothman. 1998. SNAREpins: minimal machinery for membrane fusion. *Cell*. 92:759-72.

Weimbs, T., S.H. Low, S.J. Chapin, K.E. Mostov, P. Bucher, and K. Hofmann. 1997. A conserved domain is present in different families of vesicular fusion proteins: a new superfamily. *Proc Natl Acad Sci U S A*. 94:3046-51.

Weimbs, T., K. Mostov, S.H. Low, and K. Hofmann. 1998. A model for structural similarity between different SNARE complexes based on sequence relationships. *Trends Cell Biol*. 8:260-2.

Weimer, R.M., and J.E. Richmond. 2005. Synaptic vesicle docking: a putative role for the Munc18/Sec1 protein family. *Curr Top Dev Biol*. 65:83-113.

Weisman, L.S., and W. Wickner. 1992. Molecular characterization of VAC1, a gene required for vacuole inheritance and vacuole protein sorting. *J Biol Chem*. 267:618-23.

Weissman, A.M. 2001. Themes and variations on ubiquitylation. *Nat Rev Mol Cell Biol*. 2:169-78.

Whyte, J.R., and S. Munro. 2002. Vesicle tethering complexes in membrane traffic. *J Cell Sci*. 115:2627-37.

Williams, A.L., S. Ehm, N.C. Jacobson, D. Xu, and J.C. Hay. 2004. rsly1 binding to syntaxin 5 is required for endoplasmic reticulum-to-Golgi transport but does not promote SNARE motif accessibility. *Mol Biol Cell*. 15:162-75.

Woolford, C.A., L.B. Daniels, F.J. Park, E.W. Jones, J.N. Van Arsdell, and M.A. Innis. 1986. The PEP4 gene encodes an aspartyl protease implicated in the posttranslational regulation of Saccharomyces cerevisiae vacuolar hydrolases. *Mol Cell Biol*. 6:2500-10.

Wu, M.N., J.T. Littleton, M.A. Bhat, A. Prokop, and H.J. Bellen. 1998. ROP, the Drosophila Sec1 homolog, interacts with syntaxin and regulates neurotransmitter release in a dosage-dependent manner. *Embo J*. 17:127-39.

Yamaguchi, T., I. Dulubova, S.W. Min, X. Chen, J. Rizo, and T.C. Sudhof. 2002. Sly1 binds to Golgi and ER syntaxins via a conserved N-terminal peptide motif. *Dev Cell*. 2:295-305.

Yang, B., M. Steegmaier, L.C. Gonzalez, Jr., and R.H. Scheller. 2000. nSec1 binds a closed conformation of syntaxin1A. *J Cell Biol*. 148:247-52.

Yasukawa, T., C. Kanei-Ishii, T. Maekawa, J. Fujimoto, T. Yamamoto, and S. Ishii. 1995. Increase of solubility of foreign proteins in Escherichia coli by coproduction of the bacterial thioredoxin. *J Biol Chem*. 270:25328-31.

Zerial, M., and H. McBride. 2001. Rab proteins as membrane organizers. *Nat Rev Mol Cell Biol*. 2:107-17.

Vitae

Lindsay Nicole Carpp was born on July 5, 1979 in Cleveland, Ohio to Christopher Paul Carpp and Carol Ann Carpp. She has two younger brothers, Jason Christopher Carpp and Jonathan Gregory Carpp, and two younger sisters, Laura Madeline Carpp and Grace Aaliyah Carpp. After graduating in 1997 from Urbandale High School in Urbandale, Iowa, she enrolled at Iowa State University in Ames, Iowa to study biochemistry and philosophy. In the summer of 1999, she participated in the Howard Hughes Undergraduate Summer Research Program at the University of Iowa under the supervision of Dr. Robert E. Malone, in the Department of Genetics. In the summer of 2000, she participated in the Stanford Summer Research Program under the supervision of Dr. Suzanne Pfeffer, in the Department of Biochemistry. In the third year of her undergraduate degree, she undertook a research project in Dr. Steven Rodermel's group, in the Department of Botany. She participated in an exchange program between Iowa State University and the University of Glasgow in the fourth year of her undergraduate degree, and spent the year studying philosophy at the University of Glasgow. After returning to Iowa in 2001 and completing her fifth year at Iowa State University, she was conferred a Bachelor of Arts (Philosophy) and a Bachelor of Science (Biochemistry) in the spring of 2002.

She entered the Wellcome Trust Four Year PhD Programme (Molecular Functions in Disease) at the University of Glasgow in the fall of 2002 and undertook two initial rotations, during the M.Res phase of this programme, in the laboratories of Dr. Kathryn Ayscough and Dr. Maggie Harnett. Her third rotation was in the laboratory of Dr. Nia Bryant, where she subsequently stayed for the PhD phase of the programme.

Following her time in Glasgow, she hopes to undertake a Master of Teaching programme at the University of Sydney and work towards her goal of becoming a secondary school biology and chemistry teacher.